Electronic Supplementary Material (ESI) for ChemComm.

Visible-Light Driven Acetoxylation and Dioxygenation of Indoles via Electron Donor-Acceptor Complexes

Aditya Paul, Arunava Sengupta, and Somnath Yadav*

Department of Chemistry and Chemical Biology, Indian Institute of Technology (ISM) Dhanbad, 826004, Jharkhand, India.

Table of Contents

1. General procedure: All the commercially available starting materials and reagents were used without further purification. Anhydrous solvents were prepared following the reported procedures. TLC was performed on pre-coated aluminum plates of silica gel 60 F_{254}. The photocatalytic reactions were performed in a borosilicate glass tube of internal diameter 1.2 cm by irradiation with blue LED strips (8 W; manufacturer: Lumens, Korea; wavelength range: 420-560 nm, λ_{max}: 450 nm, intensity: 63.33 Wm^{-2}) without using any filters. The reaction tube was placed at a distance of 10 cm from the light source. Visualization of the TLC plates were performed under UV irradiation using 254 nm wavelength or the plates were strained using vanillin stain solution followed by heating with a heat-gun. All synthesised compounds were purified by column chromatography on silica gel (Merck, 100-200 mesh or 230-400 mesh) using mixtures of ethyl acetate and petroleum ether as eluent. The products were characterised by standard spectroscopic techniques. All the photochemical reactions were performed with a blue LED strip having wavelength $\lambda = 455$ (±15) nm. Absorption spectral data were collected using Shimadzu RF-1600. Shimadzu RF-6000 Fluorescence Spectrometer was used to record all the emission spectra. All the emission spectral data were collected using a quartz cuvette of 1.0 cm length with data interval of 1.0, scan speed of 6000 and spectral bandwidth of 5.0 for both excitation and emission and all the data were processed using Lab solution Rf software. NMR spectra were recorded at room temperature on a Bruker 400 (400 MHz for ^{1}H, 100 MHz for ^{13}C, 377 MHz for ^{19}F) NMR spectrometer. The chemical shifts were recorded relative to $CDCl_3$ as internal standards. The following calibrations were used: $CDCl_3$ δ = 7.26 ppm and 77.16 ppm. Abbreviations used for signal multiplicity: ^{1}H - NMR: s = singlet, d = doublet, t = triplet, dd = doublet of doublets, dt = doublet of triplets, and m = multiplet. Coupling constants (*J*) are reported in Hertz (Hz). High-resolution mass spectra (HRMS) were obtained with Waters XEVO G2-XS QTOF. Single-crystal X-Ray diffraction data were recorded on a Supernova Rigaku Oxford diffractometer. IR spectroscopy was performed on a Perkin Elmer instrument in the solid state.

2. Procedure for the synthesis of the *N*-benzylindole-DAIB EDA complex:

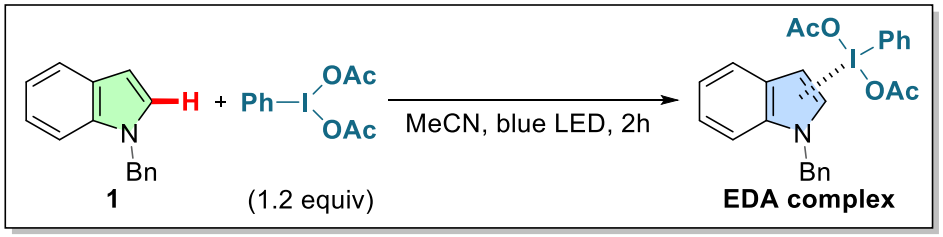

A Schlenk-tube equipped with a stir-bar was charged with **1a** (0.132 g, 0.5 mmol, 1.0 equiv.) and MeCN (2.0 mL). The solution was stirred at room temperature and diacetoxyiodobenzene (DAIB) (0.193 g, 0.24 mmol, 1.2 equiv.) was added to the reaction mixture. The mixture was stirred for 2 h. Then, the resulting solution was evaporated to dryness under reduced pressure to afford *N*-benzylindole-DAIB EDA complex as solid product. The formation of EDA complex was further confirmed using UV-Visible and Fluorescence spectroscopy.

3. UV-Vis experiment for the conformation of EDA-complex:

The UV-Visible spectroscopic experiments were performed using a quartz cuvette of 1.0 cm path length. Initially, UV spectra of the starting materials i.e., *N*-benzylindole (**1a**), *N*-methylindole (**1b**) and diacetoxyiodobenzene (**DAIB**) were recorded individually at concentrations of 2×10^{-3} (M) in dichloromethane (DCM). From the absorption plots, it was observed that *N*-benzylindole (**1a**) and diacetoxyiodobenzene did not show any absorption band at the visible region. Later, the 1:1 (i.e., **1a** and **DAIB**) binary mixture of these starting materials were mixed and the UV-Vis spectrum was recorded after 2 hours of mixing at the identical concentration as previous. This time the mixture of **1a** and **DAIB** showed a bathochromic shift with a hump at around ~408 nm with respect to starting materials. The bathochromic shoulder suggests the formation of EDA complex between **1a** and **DAIB** (Fig. S1). On the other hand, with **1b** and **DAIB** the same experiment was performed and a broad new peak at ~400-440 nm was observed. The comparative plot (Fig. S1) between **1a** and **1b** led us to believe that the spectroscopic experiments can be better performed with **1a**.

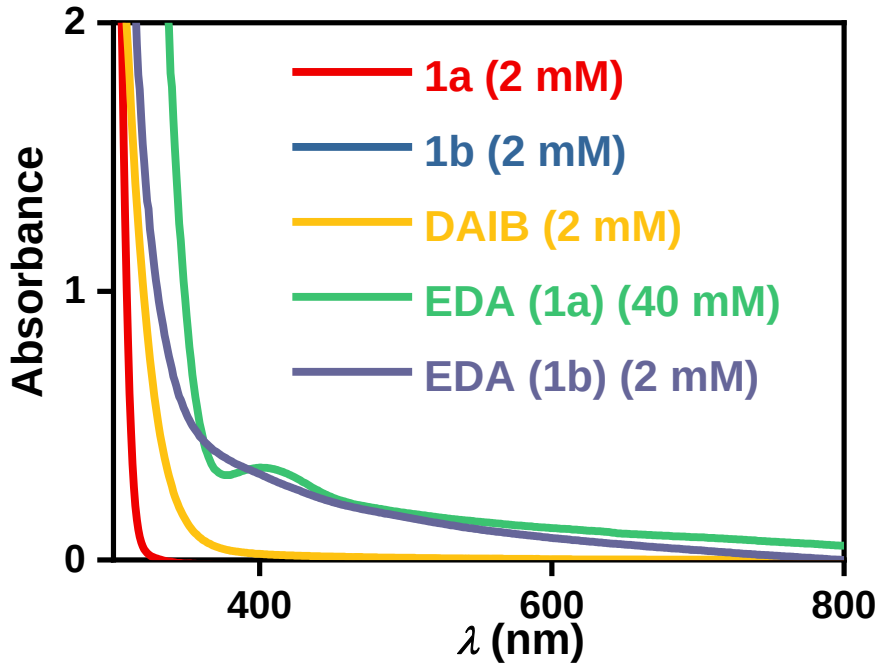

Figure S1. Absorption spectra of **1a**, **1b**, **DAIB** and **EDA** complex obtained from 1a and 1b, respectively, in dichloromethane solvent.

4. Fluorescence experiments

4.1. Determination of Stoichiometric ratio of the starting materials for the formation of EDA complex:

To determine the stoichiometry of the starting materials **1a** and **DAIB** for the formation of EDA complex, a Job's plot (Fig. 2c in manuscript) was performed. For this purpose, we measured the emission spectra of nine sets of isolated EDA complexes prepared from different molar ratios of **1a** and **DAIB** in DCM. All the EDA complexes (0.02 M) were excited at 445 nm and the emission spectra were recorded from 455 to 800 nm (Fig. S2). The maximum fluorescence intensities at λem ~500 nm for all the solutions were plotted against mole fraction of DAIB. The graph shows that the formation of EDA complex is best obtained at the ~50% mole fraction of DAIB, indicating the combination of a 1:1 molar ratio of **1a** and DAIB is the optimum choice for the reaction to happen.

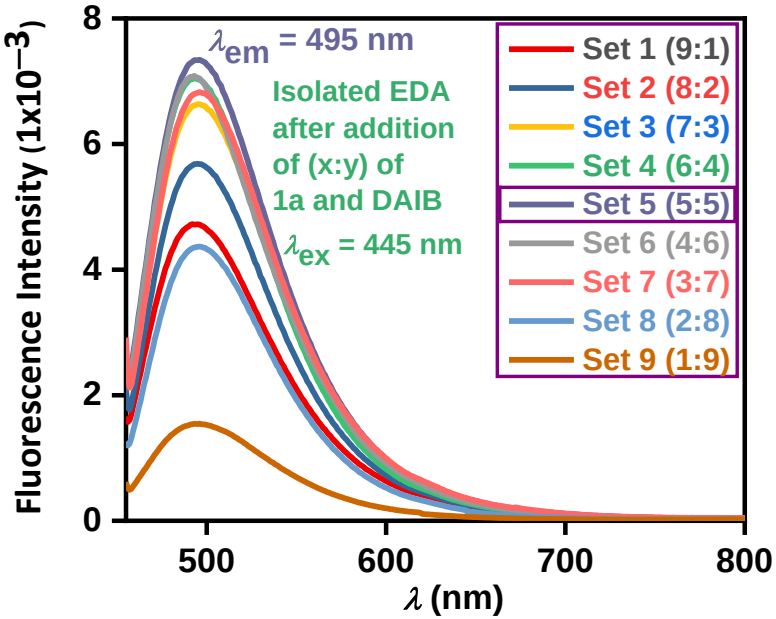

Figure S2. Job's plot for the formation of EDA adducts (with isolated EDA using x:y ratio *N*-benzylindole and DAIB). Maximum fluorescence intensity at (5:5) ratio of *N*-benzylindole and DAIB.

4.2. Time dependent emission study for the formation of EDA complex:

Fluorescence spectra of a 1:1 (V/V) mixture of *N*-benzylated indole **1a** and DAIB (3.0×10^{-3} M) in dichloromethane (DCM) were collected as a function of time to determine the exact time for the formation of EDA-complex. The solutions for the fluorescence experiments were prepared by making a stock solution from a 1:1 mixture of *N*-benzylindole (6.0×10^{-3} M) and DAIB (6.0×10^{-3} M) in DCM. Initially, we measured the absorption of all the starting materials in DCM. The characteristic absorption spectral transitions were observed at 282 nm for the *N*-benzylindole and an absorption shoulder between 400-455 nm for the EDA-complex at the same condition. Then 3.5 mL aliquots of the stock solution were collected in the cuvette and measured the emission spectra for 2 hours. The solution was excited at 282 and 445 nm with fixed time intervals and the emission intensities were recorded from 292 nm to 800 nm and 455 to 800 nm, respectively. Characteristic emission transitions for *N*-benzylindoles were observed at 325, 630 (sh) and 670 nm in the initial stages of the reaction.

Time-dependent change in the fluorescence spectra can be further observed as all the emissions at 325, 630 and 670 nm decayed (Fig. S3) gradually with time. The decaying of the characteristic emission spectra of **1a** with time was due to the concomitant formation of EDA complex (Fig. S4). The formation of the EDA-complex was further corroborated with the generation of a new distinguishable emission at 505 nm when excited at 445 nm (Fig. 2d in manuscript). The gradual increase in the emission spectra at 505 nm signifies EDA complex's gradual formation (Fig. S4).

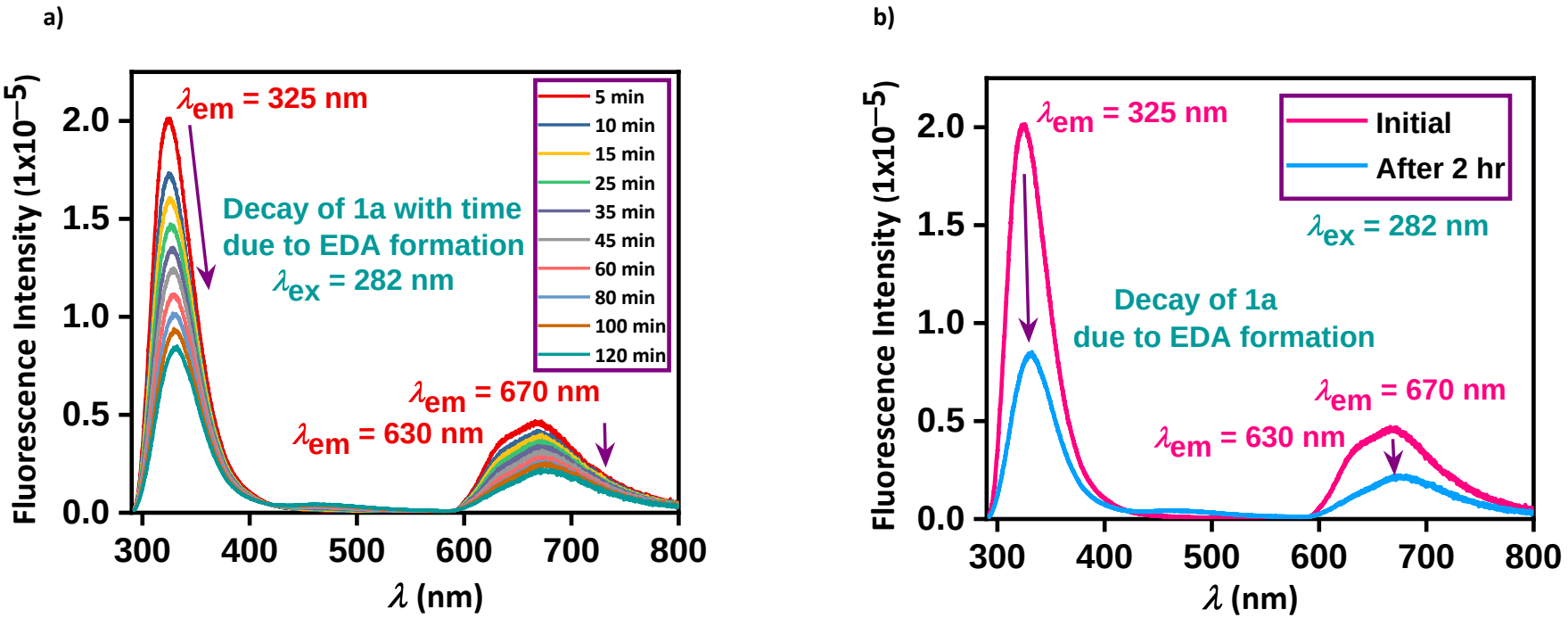

Figure S3. (*a*) Change in emission spectra with time after the addition of DAIB (1:1 v/v) to **1a** in CH_2Cl_2 at excitation at 282 nm. (*b*) Decay of characterised emissions at 325, 630 and 670 nm with time for *N*-benzylindole.

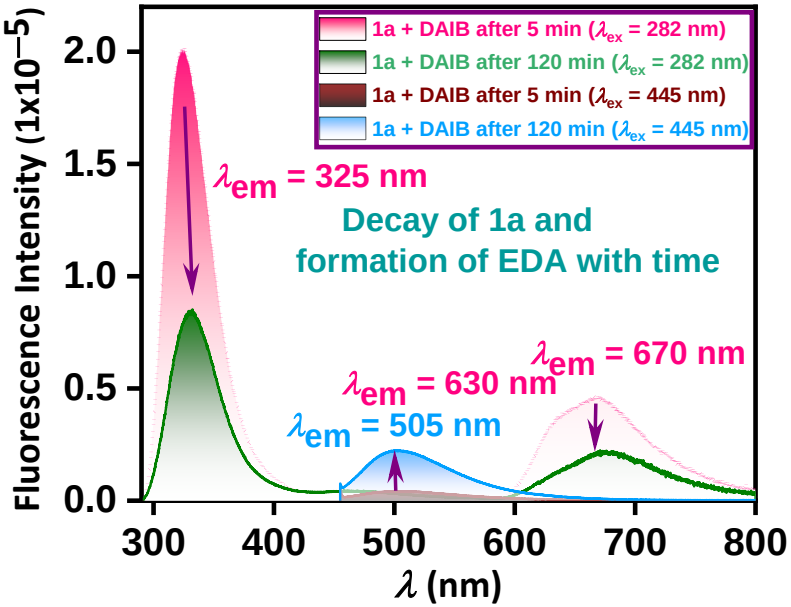

Figure S4. Fluorescence spectra of **1a** after addition of DAIB (1:1) at different excitation (282 nm and 445 nm).

5. NMR titration

A solution of DAIB solution (3×10^{-2} M) was prepared in $CDCl_3$ (20 mg in 6.0 mL). From the mother solution, 0.6 mL solution was taken into an NMR tube and 2.0 equiv. *N*-benzylindole **1a** was added as solid until the solution get saturate (20.0 equiv.) with **1a**. The chemical shift of the **1a** was recorded in presence of TMS as the internal standard. A prominent change in the chemical shift signal for the benzylic protons (appeared at δ = 5.21 ppm at 1:0 **1a**:DAIB, designated as H_a in Fig. S5) along with a marginal change in chemical shift for the proton at C2 position of **1a** (appeared at δ = 6.52 ppm at 1:0 **1a**:DAIB, designated as H_b) were observed upon increasing the amount of the **1a** up to 1.0 equiv and 20.0 equiv. (Fig. S6) respectively..

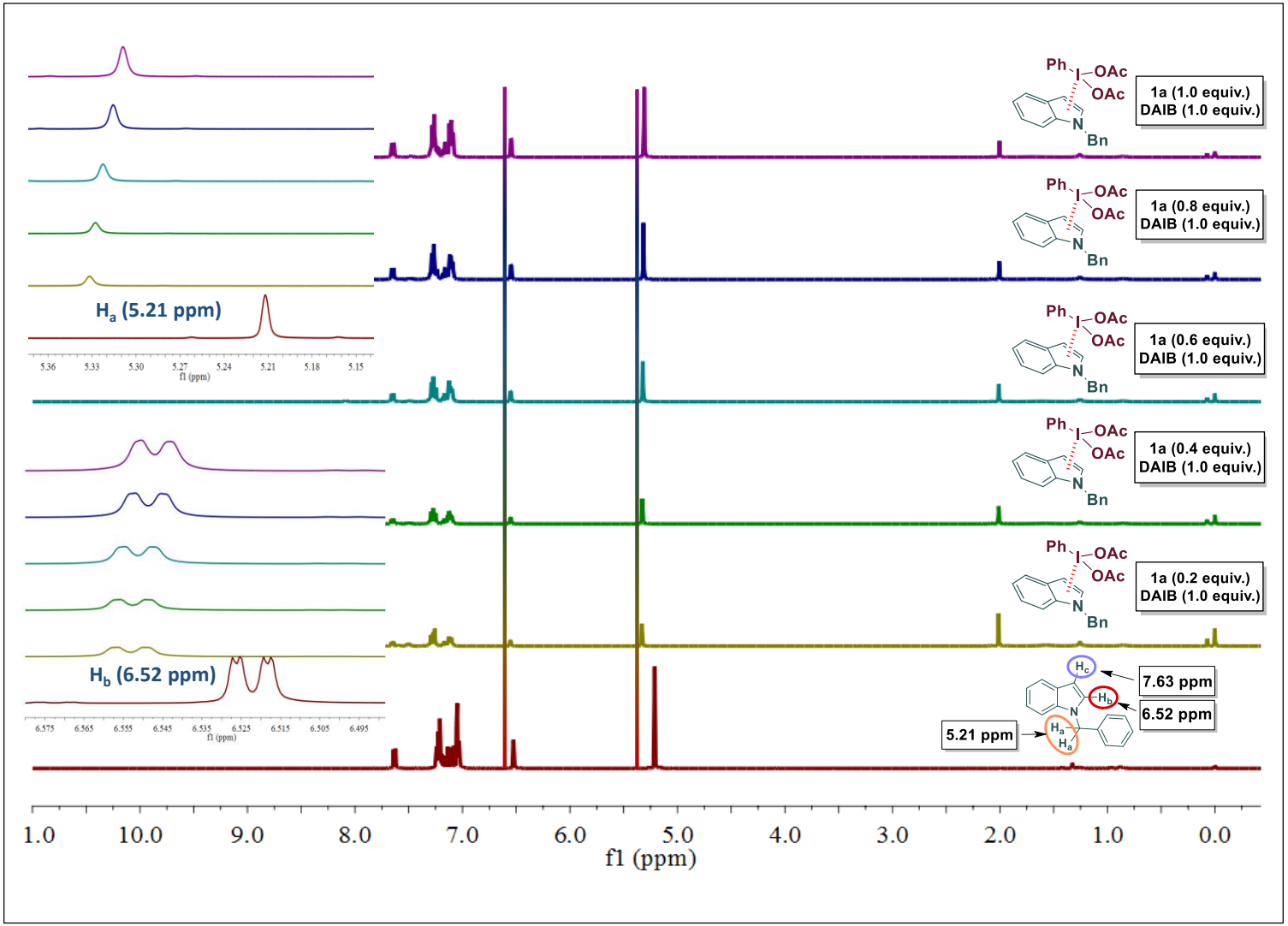

Figure S5. ^{1}H NMR spectra of the titration between DAIB and increasing the proportion of *N*-benzylindole **1a** until 1.0 equiv**.**

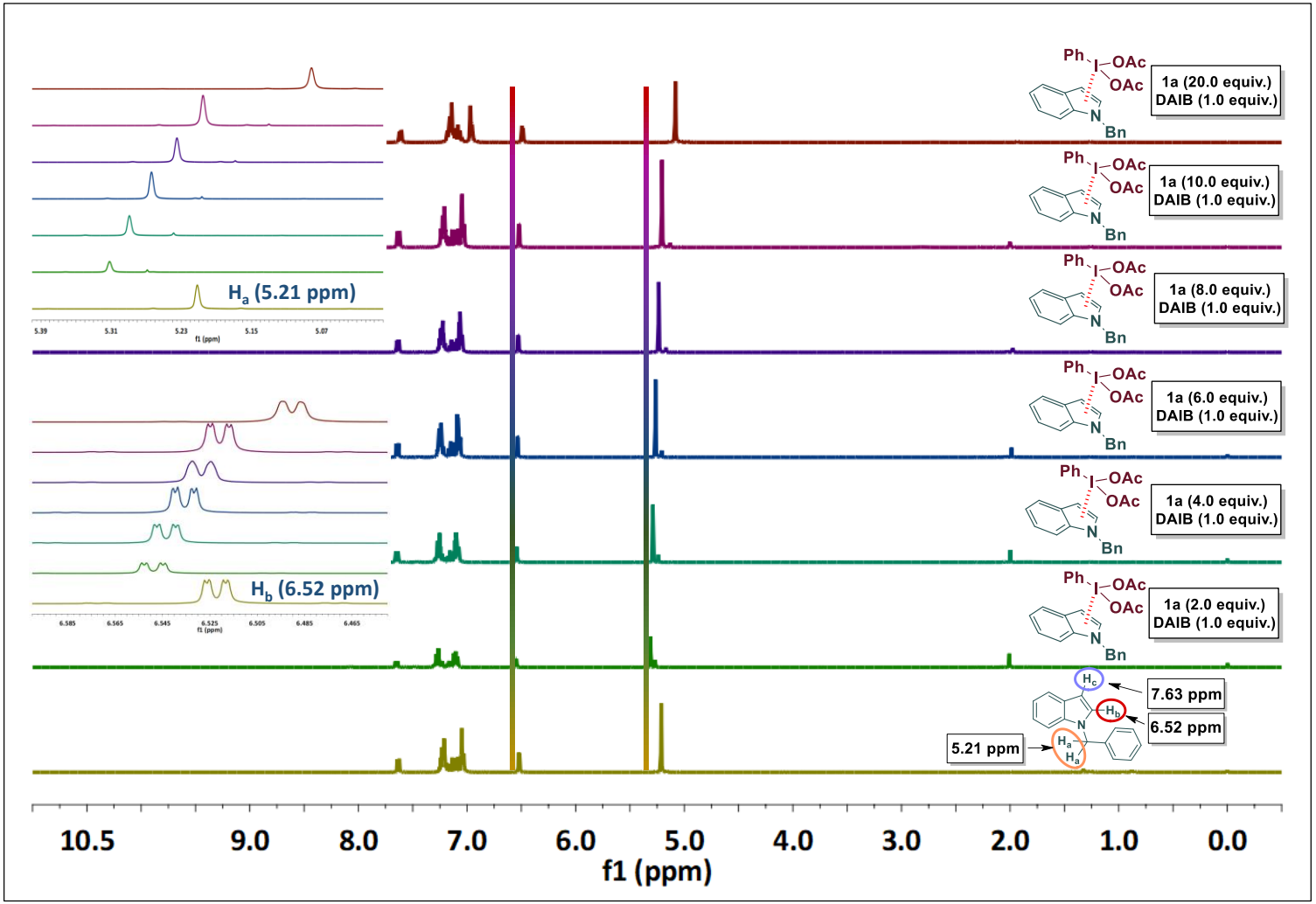

Figure S6. 1H NMR spectra of the titration between DAIB and increasing the proportion of *N*-benzylindole **1a** until 20.0 equiv**.**

6. General procedure for the synthesis of C3-acetoxyindole:

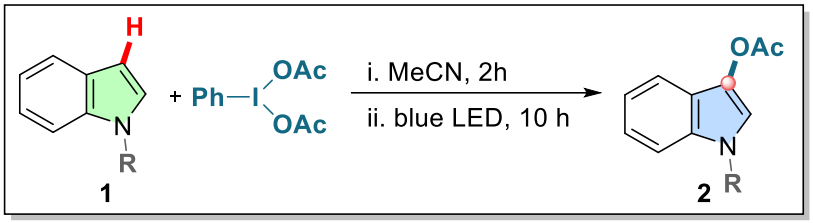

A Schlenk-tube equipped with a stir-bar was charged with **1** (0.2 mmol, 1.0 equiv.) and MeCN (2.0 mL). The solution was stirred at room temperature and diacetoxyiodobenzene (DAIB) (0.24 mmol, 1.2 equiv.) was added to the reaction mixture. The mixture was stirred for 2 h. Then, the solution was irradiated with a blue LED (λ_{max} = 450 nm) lamp for 10 h. Then the reaction mixture was quenched with water and extracted with ethyl acetate (2 × 10 mL). The combined organic layer was dried over anhydrous Na_2SO_4 and concentrated to afford a residue. The residue was subject to flash column chromatography on silica gel using petroleum ether/EtOAc (v/v) as eluent to give the pure products.

7. Rection with other substituted hypervalent iodine reagents:

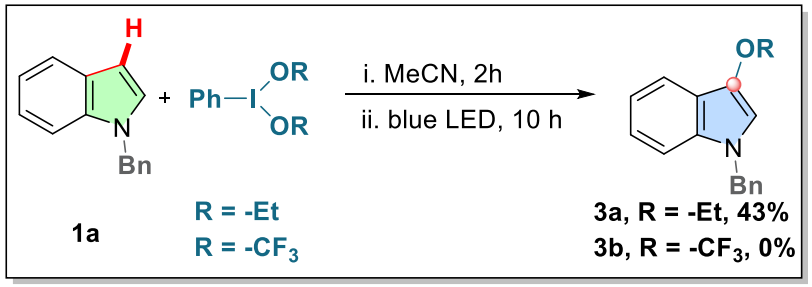

A Schlenk-tube equipped with a stir-bar was charged with **1a** (0.2 mmol, 1.0 equiv.) and MeCN (2.0 mL). The solution was stirred at room temperature and substituted hypervalent iodine reagents (0.24 mmol, 1.2 equiv.) was added to the reaction mixture. The overall reaction mixture was initially stirred for 2 h at room temperature and then a period of 10 h under the irradiated with a blue LED (λ_{max} = 450 nm). Then the reaction mixture was quenched with water and extracted with ethyl acetate (2 × 10 mL). The combined organic layer was dried over anhydrous Na_2SO_4 and concentrated to afford a crude mixture. The crude

mixture was subject to flash column chromatography on silica gel using petroleum ether/EtOAc (v/v) as eluent to furnish the pure desire products. With $PhI(OEt)_2$.43% of the desire product **4** was achieved. However no such desire C-3 substituted product **4'** was found to form with $PhI(OTf)_2$.

8. General procedure for the synthesis of isatin:

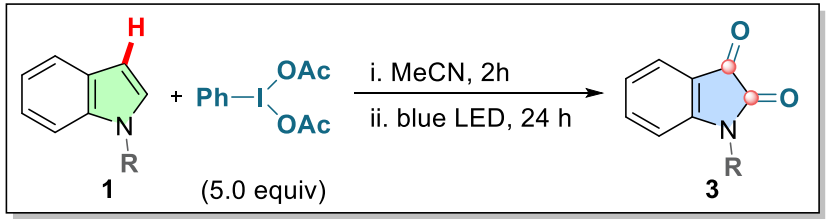

A Schlenk-tube equipped with a stir-bar was charged with **1** (0.2 mmol) and MeCN (2.0 mL). The solution was stirred at room temperature and diacetoxyiodobenzene (DAIB) (1.0 mmol, 5.0 equiv.) was added in the reaction mixture. The mixture was stirred for 2 h. Then, the solution was irradiated with a blue LED (λ_{max} = 450 nm) lamp for 24 h. Then the reaction mixture was quenched with water and extracted with ethyl acetate (2 × 10 mL). The combined organic layer was dried over anhydrous Na_2SO_4 and concentrated to afford the residue. The residue was subject to flash column chromatography on silica gel using petroleum ether/EtOAc (v/v) as eluent to give the pure products.

9. Control Experiments

9.1. Radical trapping experiments using radical scavengers:

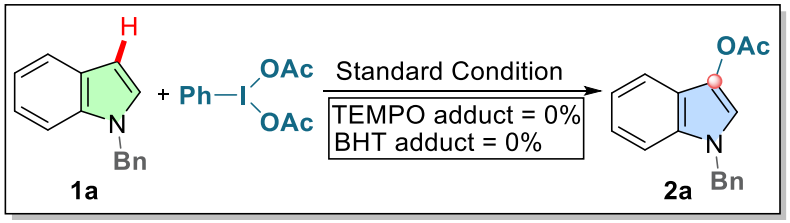

Two oven dried Screw cap vessels were equipped with a magnetic bar and charged with **1a** (0.2 mmol, 1.0 equiv.), $PhI(OAc)_2$ (1.2 equiv.) and 1.0 mL MeCN was added into the reaction vessels. Two radical scavengers i.e., TEMPO and BHT (2.0 equiv.) were added separately in these two reaction vessels and overall reaction mixtures were stirred for 12 hours at room temperature under the irradiation of blue LED. No such desire radical adducts were found to form during the course of the reaction.

9.2. Reaction of DAIB with 3-substitutedindole:

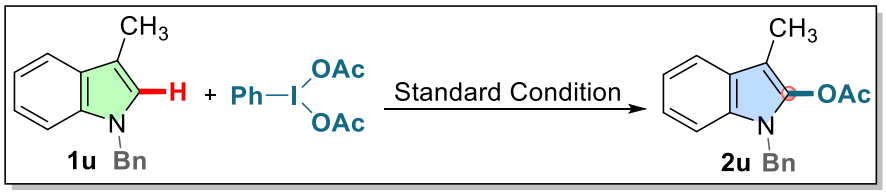

A Schlenk-tube equipped with a stir-bar was charged with **1u** (0.2 mmol, 1.0 equiv.) and MeCN (2.0 mL). The solution was stirred at room temperature and diacetoxyiodobenzene (DAIB) (0.24 mmol, 1.2 equiv.) was added to the reaction mixture. The mixture was stirred for 2 h. Then, the solution was irradiated with a blue LED (λ_{max} = 450 nm) lamp for 10 h. TLC analysis suggested that no conversion of the starting material into any of the product was observed. The reaction mixture was quenched with water and extracted with ethyl acetate (2 × 10 mL). The combined organic layer was dried over anhydrous Na_2SO_4 and concentrated to afford a residue. The residue was subject to flash column chromatography on silica gel using petroleum ether/EtOAc (v/v) as eluent. Almost all the starting material was obtained after purification.

10. Computational study

10.1 Computational details

Gaussian 09 program package[1] has been used to perform all the DFT (density functional theory) and TD-DFT (time-dependent density functional theory) calculations with B3LYP[2] functional (spin-unrestricted for triplet states and spin restricted for singlet states). All the molecules were modelled using Gauss view 6.0[3] and optimized to their energy minima geometries. The absence of negative frequencies of the corresponding minima confirmed the localization of the stable states of molecules on the potential energy surface (PES). B3LYP functional with the 6-31G(d,p) basis set[4] was used for carbon, nitrogen, oxygen and

hydrogen atoms, whereas the Stutgart-Dresden fully relativistic multielectron pseudopotential SDD basis set[5] was used on iodine atoms for a more relativistic effect. In the overall calculations, the effect of solvation (acetonitrile, dielectric constant e = 37.5) was taken into consideration by performing self-consistent reaction field (SCRF)[6] (model IEF-PCM)[7] calculations. The energies were corrected with the thermal corrections to the Gibbs free energy obtained from the frequency calculations on the optimized geometries. TD-DFT calculations (nstates =30) were performed using the same solvent SCRF approach (acetonitrile as solvent). TD-DFT-derived electronic emission spectra were plotted using GaussSum.[8] Corresponding orbitals and spin-density plots were drawn using Chemcraft[9] visualization program.

10.2. DFT-results

DFT calculations were used to assign the correct reaction mechanism and the feasibility of the electron donor-acceptor (EDA) complex formation. Among all the three possible mechanisms, the EDA complex formation is typical. So primarily, the focus has been given to proving the existence of that. A slight change in the absorption spectral feature was observed as a new broad shoulder peak was obtained at ~410 nm. As the absorption change was not distinguishable enough, the EDA complex formation was monitored with time using the emission spectroscopic method instead. A new emission peak is generated at 505 nm when a 1:1 mixture of **1a** and DAIB is excited at ~445 nm after 2hr of mixing. This indicated a possibility of the formation of EDA complex. The possible geometry of the EDA was thus modelled and optimized (Fig. 1 and S7(a)). The energy-minimized stable, optimized geometry shows the EDA's possible singlet ground state with T-stacking instead of π–π stacking. The HOMO molecular orbital is predominately indole based and the LUMO is DAIB-based ($\Delta E_{\text{HOMO-LUMO}}$ = 3.01 eV, *i.e.*, 24277 cm^{-1} or 415 nm) (Fig. 2(f)). The experimentally found electronic transition at ~410 nm can thus correlate to the theoretically calculated electronic transition at 415 nm, which can be assigned mainly due to HOMO (indole as the electron donor) to LUMO (DAIB as the electron acceptor) electron transfer. Further TD-DFT calculations were performed for the emission transitions from triplet excited state to singlet ground state and it was found that the experimentally found 505 nm emission peak can be accurately correlated to the theoretically found emission peak at 504 nm (2.45 eV, *i.e.*, 19761 cm^{-1}) (Fig. S7(b)). Thus, the formation of EDA is evident as both the emission spectroscopic experimental result and the theoretical calculations based on the proposed EDA model match perfectly.

The triplet excited state of the EDA was exposed for a prolonged time in the presence of blue light and as a result, a triplet diradical species **A** is proposed to form as an intermediate. The **A** was modelled, optimised (Fig. S8(a)) and an animation (See ESI Movie-1) for the formation of such species from EDA is

portrayed. The spin density plot of **A** (Fig. S8(b)) revealed that one unpaired electron is delocalized throughout the five-member ring of the indole and one acetate anion. In contrast, the other unpaired electron resides mainly in PhIOAc moiety. The molecular orbital diagram also depicts the same as the α-HOMO (111α) was found to be DAIB centred and α-HOMO-1 (110α) is indole cantered (Fig. S9).

Further, intermediate species **A** will generate intermediate **B** producing the product. Following this proposed mechanism, **B** was modelled and optimized (Fig. S10(a)). The initial proposed **B** is converted to the product during optimization, where the acetate anion takes up the H^+ from the intermediate. The process was portrayed using animation (see ESI Movie-2).

The other two alternate mechanisms (Fig. S11) were also explored, but for both the proposed mechanisms, intermediate **B′** cannot be found using DFT calculations.

All the relevant molecules were modelled and geometry optimised figures are represented from Fig. S12-S21 and their DFT-optimized cartesian coordinates are tabulated from Table S1-S10.

(*a*)

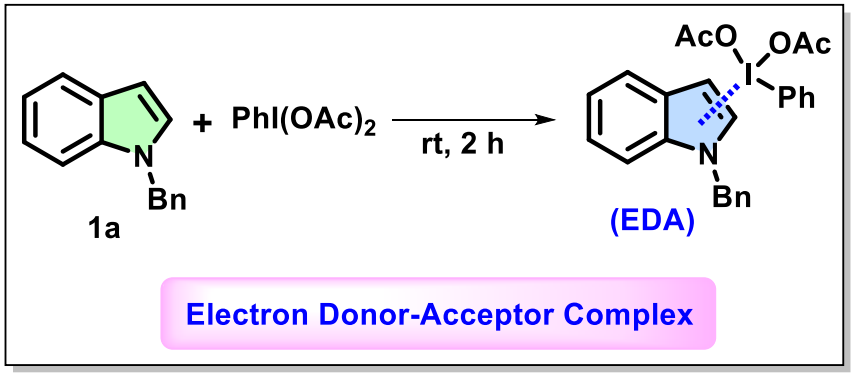

(*b*)

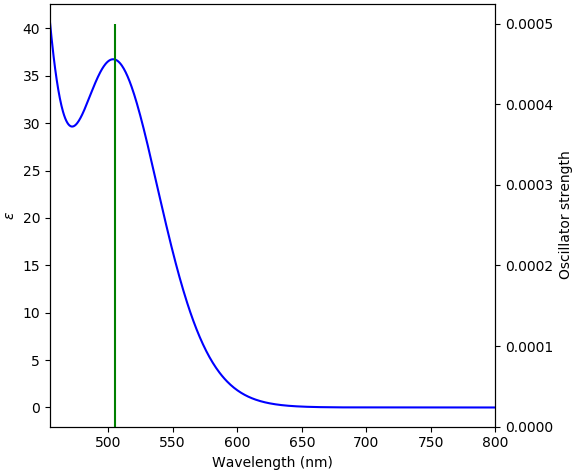

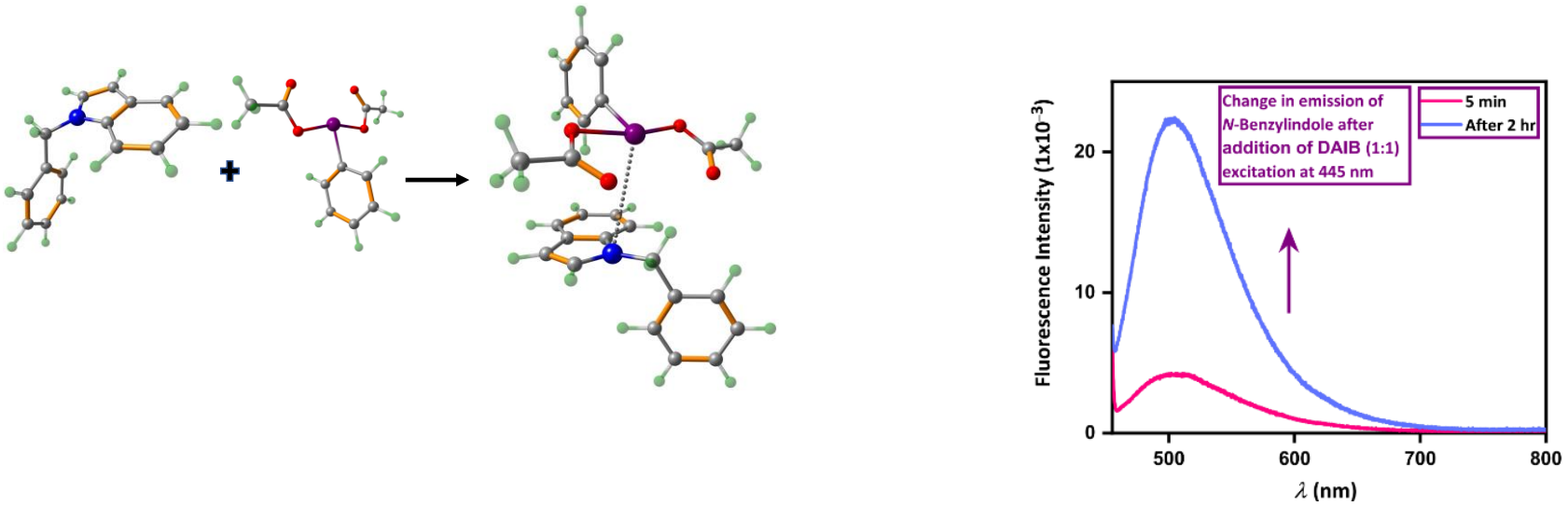

Figure S7. (a) Preparation of EDA complex between *N*-benzylindole (**1a**) and DAIB under room temperature and DFT optimized geometries of **1a**, **DAIB** and **EDA**. (b) Comparison between experimental and theoretical fluorescence spectrum at 505 nm (corresponding to 2.45 eV emission between triplet excited LUMO to singlet HOMO ground state).

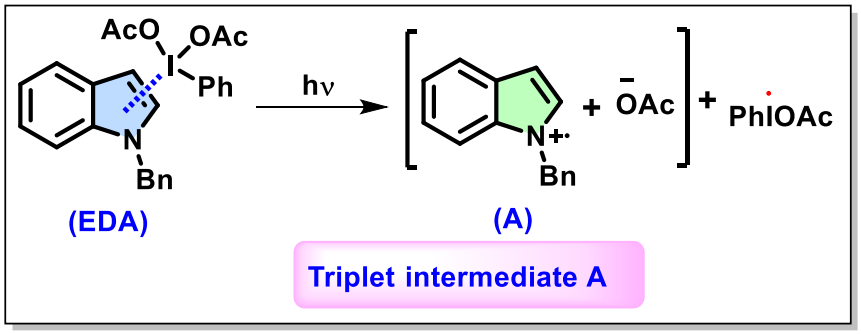

(*a*)

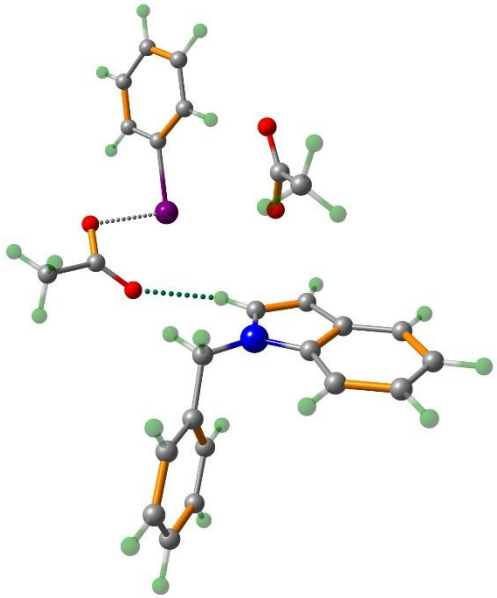

(*b*)

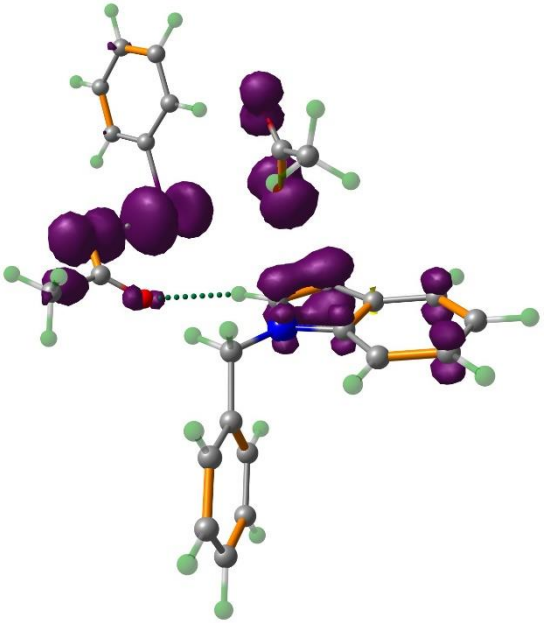

Figure S8. (*a*) optimized geometry of the triplet diradical intermediate **A** and (*b*) spin density plot of the triplet intermediate **A**.

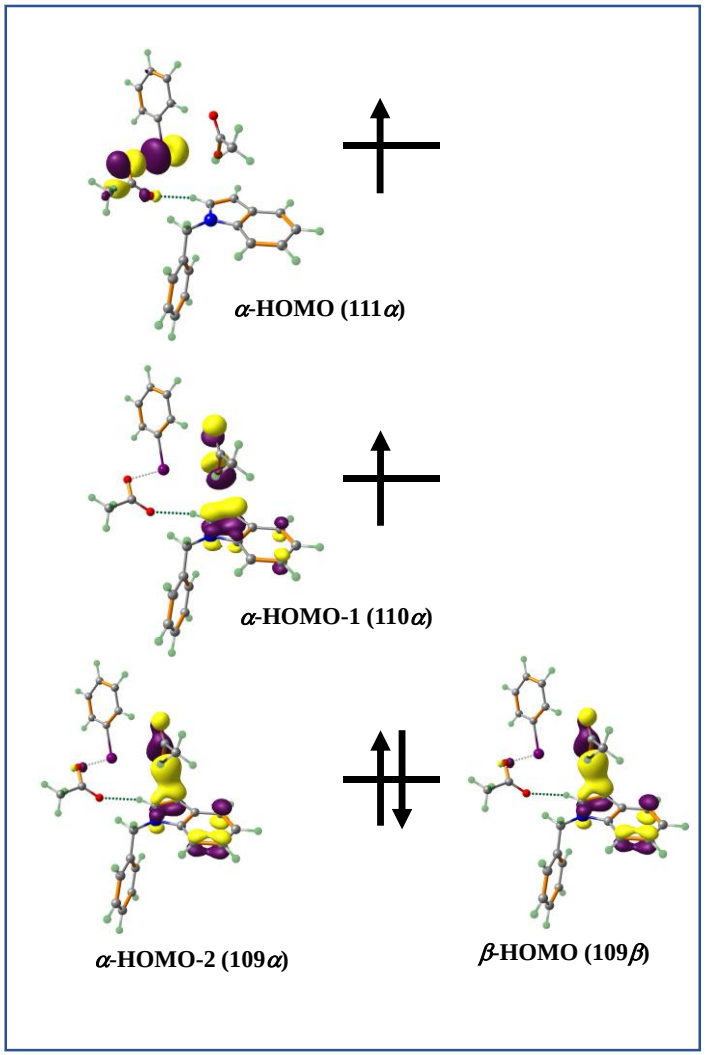

Figure S9. Molecular orbital diagrams of intermediate **A**.

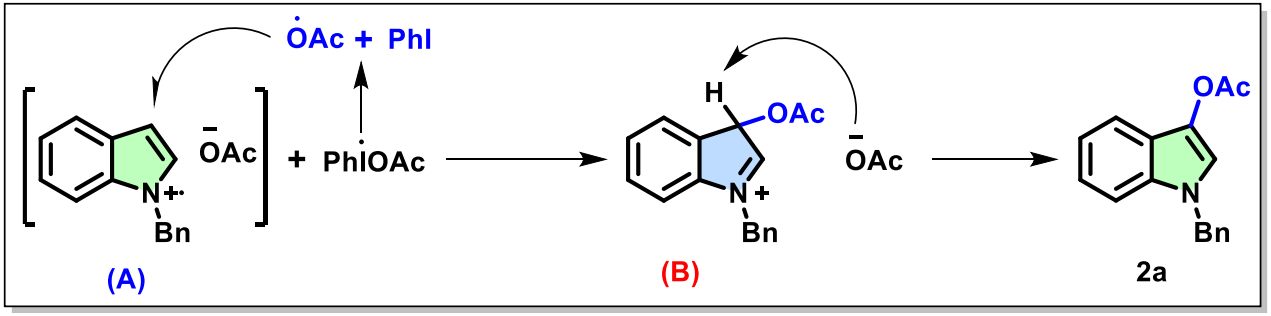

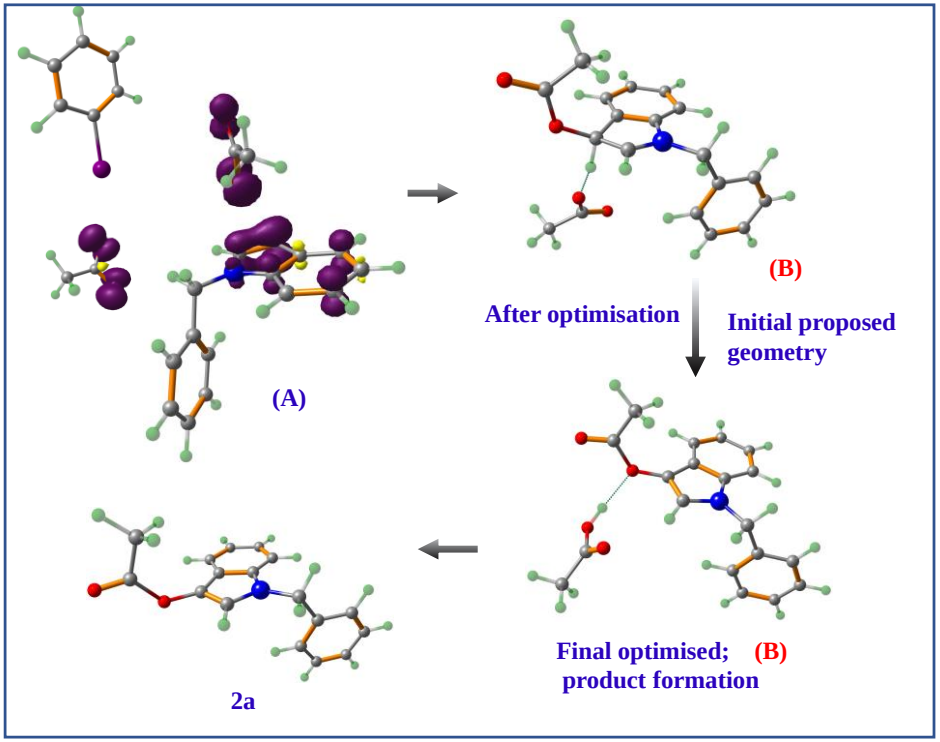

Figure S10. Product formation through an intermediate **B**.

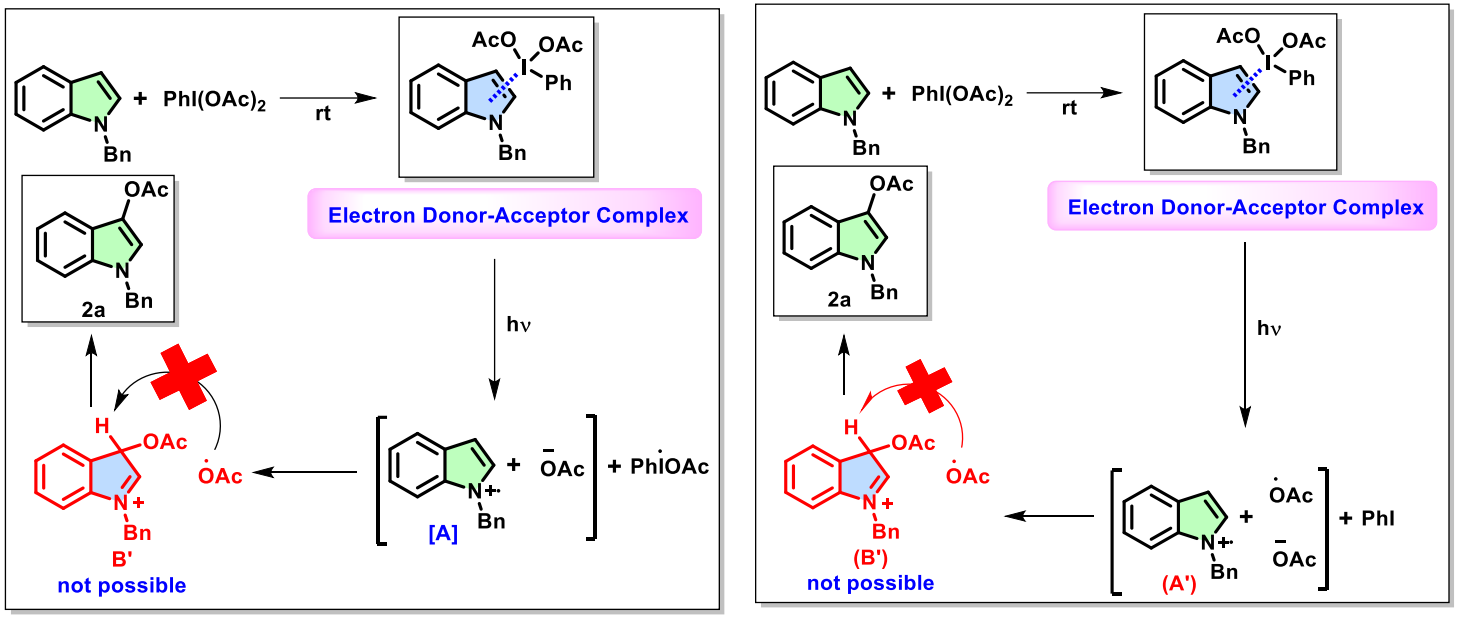

Figure S11. The other two mechanisms are not possible as proposed intermediate **B′** is not possible as the combination of multiplicity 2 and 172 electrons is impossible.

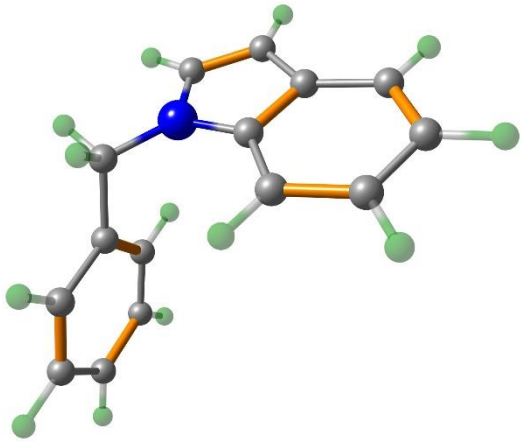

Figure S12. DFT-optimized geometry of **1a**.

Table S1. DFT-optimized cartesian coordinates of **1a**.

Zero-point correction= 0.239407 (Hartree/Particle)
Thermal correction to Energy= 0.251539
Thermal correction to Enthalpy= 0.252483
Thermal correction to Gibbs Free Energy= 0.199072
Sum of electronic and zero-point Energies= -633.967234
Sum of electronic and thermal Energies= -633.955102
Sum of electronic and thermal Enthalpies= -633.954158
Sum of electronic and thermal Free Energies= -634.007569

C15NH13

N	8.379090000	5.925696000	14.950289000
C	10.112242000	6.183126000	13.519504000
C	8.821153000	5.740468000	13.651038000
C	9.405054000	6.498094000	15.681881000
C	10.515575000	6.677576000	14.805880000
C	7.058455000	4.353714000	16.384651000

C	7.063946000	5.563010000	15.460928000
H	6.428455000	5.373501000	14.589780000
H	6.632951000	6.425215000	15.980808000
C	7.827412000	3.218418000	16.097753000
H	8.469682000	3.211868000	15.221709000
C	9.449661000	6.878195000	17.029672000
H	8.601255000	6.727098000	17.689114000
C	11.693039000	7.258363000	15.312037000
H	12.553412000	7.406897000	14.665092000
C	11.738948000	7.638832000	16.647956000
H	12.643334000	8.087784000	17.048463000
C	10.628083000	7.450408000	17.497825000
H	10.694521000	7.755512000	18.538030000
C	7.779865000	2.101487000	16.932329000
H	8.383509000	1.229081000	16.699369000
C	6.959125000	2.102968000	18.063609000
H	6.923494000	1.233430000	18.713174000
C	6.242998000	4.349536000	17.522217000
H	5.646557000	5.227255000	17.758784000
C	6.189773000	3.230127000	18.356258000
H	5.553796000	3.243430000	19.236574000
H	8.157648000	5.304642000	12.917031000
H	10.701043000	6.164406000	12.613310000

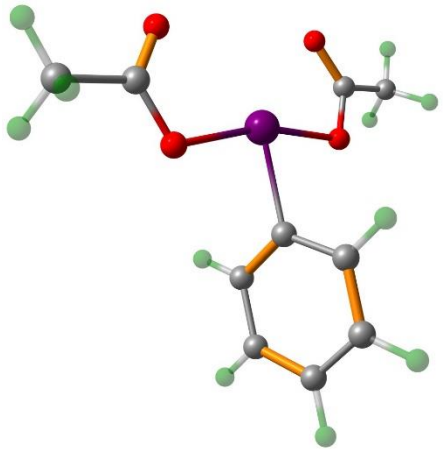

Figure S13. DFT-optimized geometry of DAIB.

Table S2. DFT-optimized cartesian coordinates for DAIB.

Zero-point correction= 0.192324 (Hartree/Particle)
Thermal correction to Energy= 0.209556
Thermal correction to Enthalpy= 0.210501
Thermal correction to Gibbs Free Energy= 0.143056
Sum of electronic and zero-point Energies= -699.759163
Sum of electronic and thermal Energies= -699.741930
Sum of electronic and thermal Enthalpies= -699.740986
Sum of electronic and thermal Free Energies= -699.808431

C10H11O4I

C	0.000869000	-4.318753000	-0.000277000
C	-0.376996000	-3.623994000	-1.151318000
C	-0.378231000	-2.226512000	-1.162735000
C	0.000236000	-1.560585000	-0.000143000
C	0.379003000	-2.226451000	1.162386000
C	0.378411000	-3.623933000	1.150832000

H	0.001119000	-5.404166000	-0.000330000
H	-0.669443000	-4.163401000	-2.046621000
H	-0.667234000	-1.684038000	-2.055350000
H	0.667750000	-1.683930000	2.055057000
H	0.671103000	-4.163294000	2.046083000
I	-0.000228000	0.588299000	-0.000058000
O	2.206565000	0.299185000	-0.230085000
O	-2.206848000	0.298219000	0.230466000
C	2.751765000	1.490502000	-0.281883000
C	-2.752586000	1.489288000	0.282244000
O	2.094064000	2.532499000	-0.207417000
O	-2.095366000	2.531583000	0.207706000
C	4.258679000	1.471717000	-0.447151000
C	-4.259471000	1.469817000	0.447718000
H	-4.518283000	0.987282000	1.394546000
H	-4.648317000	2.487977000	0.435244000
H	-4.715226000	0.885675000	-0.356074000
H	4.714591000	0.887794000	0.356711000
H	4.517846000	0.989291000	-1.393938000
H	4.647053000	2.490057000	-0.434636000

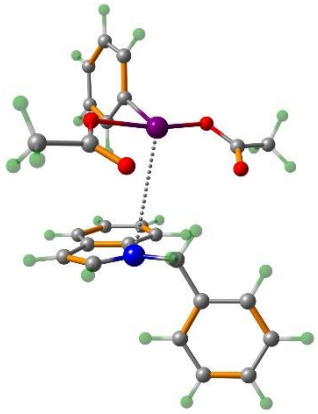

Figure S14. DFT-optimized geometry of EDA complex.

Table S3. DFT-optimized cartesian coordinates for EDA complex (Singlet ground state).

C25NH24O4I

N	6.177813000	2.391106000	5.466368000
C	6.978907000	4.448253000	4.961640000
C	6.974819000	3.121849000	4.603342000
C	5.653090000	3.256103000	6.410235000
C	6.134555000	4.567227000	6.117230000
C	6.736541000	0.125242000	6.392615000
C	5.945608000	0.954394000	5.389926000
H	6.191548000	0.649454000	4.366992000
H	4.876258000	0.757391000	5.513934000
C	7.960561000	0.558436000	6.917253000
H	8.347482000	1.536271000	6.645065000
C	4.796354000	3.001462000	7.490663000
H	4.449385000	1.997279000	7.712796000
C	5.731699000	5.639574000	6.935932000
H	6.088770000	6.646693000	6.736462000
C	4.877098000	5.390679000	8.006150000
H	4.567234000	6.209422000	8.649850000
C	4.414269000	4.083674000	8.279894000
H	3.753946000	3.918235000	9.126379000
C	8.681572000	-0.253260000	7.798236000
H	9.628147000	0.098039000	8.199971000
C	8.188123000	-1.508477000	8.164304000
H	8.748714000	-2.138196000	8.849497000
C	6.241318000	-1.130640000	6.772396000
H	5.283240000	-1.467305000	6.382840000
C	6.963831000	-1.944810000	7.648338000
H	6.566815000	-2.915379000	7.933316000
H	7.470740000	2.621964000	3.782784000
H	7.514623000	5.241201000	4.458576000
C	0.048484000	6.756590000	4.699326000
C	1.239942000	6.485448000	5.377013000

C	1.922369000	5.284737000	5.156066000
C	1.377280000	4.379110000	4.249799000
C	0.192156000	4.621515000	3.560373000
C	-0.473921000	5.828574000	3.794008000
H	-0.474345000	7.691826000	4.876650000
H	1.648102000	7.204134000	6.081106000
H	2.845924000	5.075050000	5.685011000
H	-0.209990000	3.898255000	2.859910000
H	-1.399831000	6.037541000	3.266477000
I	2.424708000	2.536809000	3.918729000
O	3.388748000	3.715499000	2.284000000
O	1.107701000	1.835107000	5.601770000
C	4.352543000	2.996935000	1.749953000
C	1.533631000	0.670730000	6.032539000
O	4.620991000	1.852453000	2.121240000
O	2.518268000	0.095656000	5.559186000
C	5.111242000	3.713877000	0.649774000
C	0.697270000	0.087102000	7.156057000
H	-0.288470000	-0.185989000	6.765938000
H	1.188621000	-0.799381000	7.558544000
H	0.546174000	0.831386000	7.942370000
H	4.416041000	4.185940000	-0.049009000
H	5.721164000	4.505080000	1.097698000
H	5.756464000	3.006348000	0.127690000

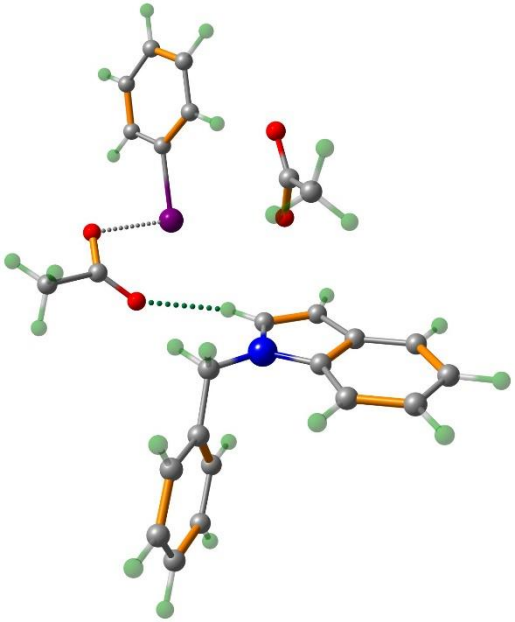

Figure S15. DFT-optimized geometry of triplet diradical species **A**.

Table S4. DFT-optimized cartesian coordinates of triplet diradical species **A**.

Zero-point correction= 0.428908 (Hartree/Particle)
Thermal correction to Energy= 0.460963
Thermal correction to Enthalpy= 0.461907
Thermal correction to Gibbs Free Energy= 0.352242
Sum of electronic and zero-point Energies= -1333.726097
Sum of electronic and thermal Energies= -1333.694042
Sum of electronic and thermal Enthalpies= -1333.693098
Sum of electronic and thermal Free Energies= -1333.802763

C25NH24O4I

N	6.099933000	2.378350000	5.947347000

C	6.264079000	3.171868000	3.835529000
C	5.489675000	2.424439000	4.731175000
C	7.292952000	3.108988000	5.882539000
C	7.416407000	3.614894000	4.557258000
C	6.410323000	0.548176000	7.623697000
C	5.562044000	1.710026000	7.132263000
H	4.560515000	1.360986000	6.858200000
H	5.451982000	2.451646000	7.932687000
C	6.967498000	-0.375299000	6.728592000
H	6.827924000	-0.240965000	5.659538000
C	8.246785000	3.359407000	6.866712000
H	8.153142000	2.956951000	7.869534000
C	8.535380000	4.399498000	4.223242000
H	8.647027000	4.798646000	3.219221000
C	9.491122000	4.657840000	5.203491000
H	10.359805000	5.263112000	4.962651000
C	9.347466000	4.144867000	6.507391000
H	10.109147000	4.359145000	7.251191000
C	7.704964000	-1.463096000	7.200457000
H	8.133450000	-2.169044000	6.494634000
C	7.890707000	-1.646127000	8.574654000
H	8.464818000	-2.492603000	8.940256000
C	6.604422000	0.360655000	8.998071000
H	6.181017000	1.072634000	9.703458000
C	7.336300000	-0.731788000	9.473661000
H	7.477653000	-0.862598000	10.542856000
H	4.536565000	1.935142000	4.585000000
H	6.029235000	3.337861000	2.796477000
C	-2.311712000	5.300941000	2.325798000
C	-2.559517000	3.949512000	2.062751000
C	-1.543609000	3.003883000	2.224395000
C	-0.286899000	3.441777000	2.650617000
C	-0.012544000	4.783265000	2.924378000
C	-1.045998000	5.711406000	2.753193000
H	-3.105531000	6.031355000	2.198426000

H	-3.542388000	3.625341000	1.732948000
H	-1.731321000	1.954627000	2.025544000
H	0.966528000	5.115972000	3.261320000
H	-0.847539000	6.758605000	2.961261000
I	1.281371000	2.011167000	2.894671000
O	4.074857000	4.515642000	3.756542000
O	0.499585000	1.269668000	5.327577000
C	3.742486000	5.547776000	4.459837000
C	1.535806000	0.889819000	6.003221000
O	2.698538000	6.164211000	4.181965000
O	2.708107000	0.841188000	5.609774000
C	4.628378000	5.957635000	5.619096000
C	1.172959000	0.492655000	7.442014000
H	1.717123000	-0.419823000	7.697995000
H	1.504176000	1.295741000	8.108599000
H	0.099805000	0.345949000	7.569770000
H	4.470428000	5.266159000	6.454439000
H	5.685203000	5.911947000	5.343679000
H	4.363703000	6.966181000	5.943610000

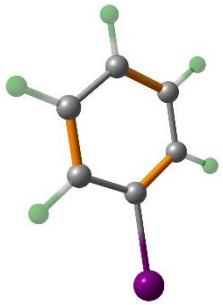

Figure S16. DFT-Optimized geometry of PhI

Table S5. DFT-optimized cartesian coordinates of PhI.

Zero-point correction= 0.090083 (Hartree/Particle)
Thermal correction to Energy= 0.095999
Thermal correction to Enthalpy= 0.096943
Thermal correction to Gibbs Free Energy= 0.058279
Sum of electronic and zero-point Energies= -242.974436
Sum of electronic and thermal Energies= -242.968521
Sum of electronic and thermal Enthalpies= -242.967577
Sum of electronic and thermal Free Energies= -243.006240

C6H5I

C	0.000400000	-4.276206000	-0.001306000
C	-0.205773000	-3.576502000	-1.191739000
C	-0.207761000	-2.178047000	-1.200912000
C	0.000134000	-1.501741000	-0.000291000
C	0.208158000	-2.178890000	1.199831000
C	0.206439000	-3.577335000	1.189639000
H	0.000503000	-5.361805000	-0.001701000
H	-0.366561000	-4.113311000	-2.121882000
H	-0.368516000	-1.637686000	-2.126736000
H	0.368810000	-1.639174000	2.126047000
H	0.367329000	-4.114789000	2.119392000
I	-0.000076000	0.662447000	0.000531000

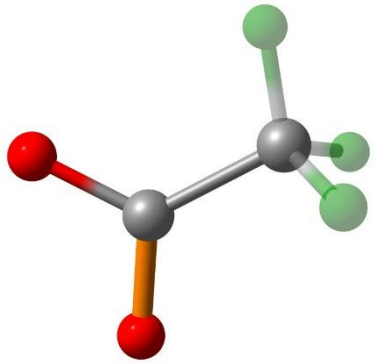

Figure S17. DFT-optimized geometry of doublet acetate radical.

Table S6. DFT-optimized cartesian coordinates of doublet acetate radical.

Zero-point correction= 0.047730 (Hartree/Particle)
Thermal correction to Energy= 0.051406
Thermal correction to Enthalpy= 0.052350
Thermal correction to Gibbs Free Energy= 0.021170
Sum of electronic and zero-point Energies= -228.373720
Sum of electronic and thermal Energies= -228.370043
Sum of electronic and thermal Enthalpies= -228.369099
Sum of electronic and thermal Free Energies= -228.400280

C2H3O2

O	5.742315000	5.776046000	3.035629000
C	5.720880000	6.871079000	3.670403000
O	5.168172000	7.772606000	2.978379000
C	6.273163000	7.064324000	5.039180000
H	5.782551000	6.372131000	5.729358000
H	7.342683000	6.834869000	5.033446000
H	6.115602000	8.092907000	5.367705000

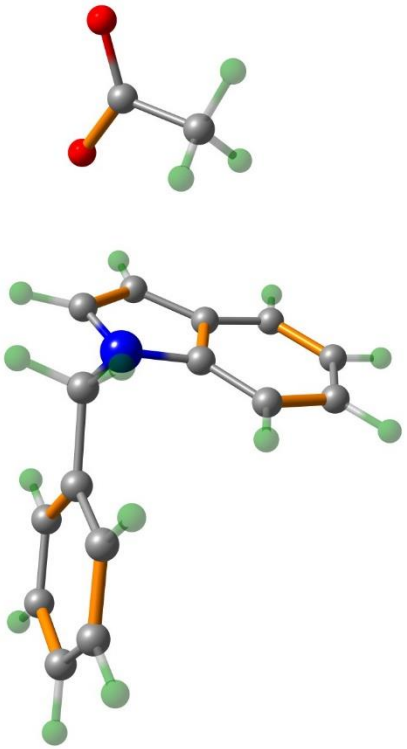

Figure S18. DFT-optimized geometry of fraction of A. Indole-acetate radical.

Table S7. DFT-optimized cartesian coordiantes of fraction of A. indole acetate radical species.

Zero-point correction=	0.289188 (Hartree/Particle)
Thermal correction to Energy=	0.307560
Thermal correction to Enthalpy=	0.308505
Thermal correction to Gibbs Free Energy=	0.237633
Sum of electronic and zero-point Energies=	-862.351419
Sum of electronic and thermal Energies=	-862.333046
Sum of electronic and thermal Enthalpies=	-862.332102

Sum of electronic and thermal Free Energies= -862.402974

C17NH16O2

N	6.077809000	3.096130000	5.487276000
C	7.504823000	3.692139000	3.836523000
C	6.196746000	3.298480000	4.151804000
C	7.315205000	3.360463000	6.092523000
C	8.226152000	3.736422000	5.064990000
C	4.935643000	1.288501000	6.781754000
C	4.857557000	2.683208000	6.184225000
H	4.047996000	2.744015000	5.451506000
H	4.637854000	3.416163000	6.966098000
C	5.397373000	0.203337000	6.025126000
H	5.739611000	0.360685000	5.006090000
C	7.687796000	3.298657000	7.431047000
H	6.992208000	3.001600000	8.207473000
C	9.552602000	4.061150000	5.405954000
H	10.262099000	4.351539000	4.637435000
C	9.931399000	4.002326000	6.742866000
H	10.949844000	4.248612000	7.025258000
C	9.011659000	3.626917000	7.739905000
H	9.335504000	3.588454000	8.775115000
C	5.425354000	-1.078562000	6.573779000
H	5.787296000	-1.911428000	5.978378000
C	4.987145000	-1.292018000	7.883812000
H	5.009419000	-2.290532000	8.309797000
C	4.501563000	1.068340000	8.093695000
H	4.143396000	1.904171000	8.689148000
C	4.523649000	-0.216292000	8.642204000
H	4.184804000	-0.372680000	9.661902000
H	5.359552000	3.138822000	3.490604000
H	7.875282000	3.884482000	2.842684000
O	5.954251000	5.622191000	2.990260000
C	5.794715000	6.742045000	3.615232000
O	5.317409000	7.722243000	3.018672000

C	6.200099000	6.818116000	5.074497000
H	5.640328000	6.083683000	5.661374000
H	7.262105000	6.581477000	5.185616000
H	6.004064000	7.819003000	5.463274000

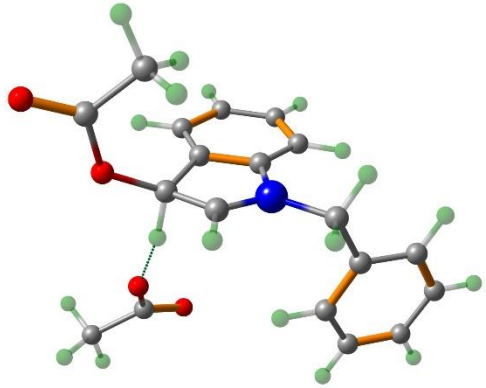

Figure S19. DFT-optimized geometry of initial proposed intermediated **B**.

Table S8. DFT-optimized cartesian coordinates of initial proposed intermediate **B**.

C19NH19O4

N	5.752745000	2.753297000	5.894012000
C	6.177015000	3.669738000	3.848251000
C	5.336843000	2.773609000	4.652390000
C	6.743904000	3.762999000	6.103265000
C	6.953819000	4.419954000	4.883310000
C	6.375636000	0.846129000	7.369881000
C	5.290345000	1.809710000	6.933864000
H	4.434610000	1.282410000	6.506202000
H	4.931512000	2.405976000	7.775685000
C	7.137061000	0.142123000	6.428038000
H	6.991778000	0.315006000	5.365119000
C	7.413603000	4.099452000	7.274230000
H	7.262123000	3.560796000	8.201764000
C	7.866057000	5.466798000	4.809960000

H	8.050279000	5.980799000	3.872832000
C	8.527971000	5.843954000	5.982561000
H	9.231476000	6.669624000	5.955727000
C	8.310750000	5.166788000	7.191280000
H	8.851985000	5.471814000	8.080456000
C	8.103091000	-0.770970000	6.849605000
H	8.693397000	-1.306464000	6.112574000
C	8.311785000	-0.994714000	8.213263000
H	9.064384000	-1.706281000	8.538717000
C	6.594528000	0.626616000	8.734429000
H	6.012937000	1.175857000	9.469862000
C	7.555904000	-0.295079000	9.154819000
H	7.717030000	-0.458324000	10.215890000
H	4.582736000	2.085224000	4.291655000
O	5.627972000	4.322049000	2.713195000
O	9.890946000	1.499052000	3.496775000
C	4.613307000	5.244669000	2.779905000
C	9.120993000	1.720026000	2.544040000
O	4.275603000	5.754059000	1.737281000
O	7.921933000	2.143809000	2.621481000
C	3.949927000	5.515072000	4.106995000
C	9.653957000	1.590868000	1.110754000
H	8.876176000	1.233587000	0.432648000
H	9.973136000	2.576150000	0.754200000
H	10.515062000	0.920169000	1.083555000
H	3.391183000	4.638862000	4.450029000
H	4.677415000	5.781658000	4.876764000
H	3.249507000	6.337419000	3.968698000
H	6.951583000	2.916173000	3.376401000

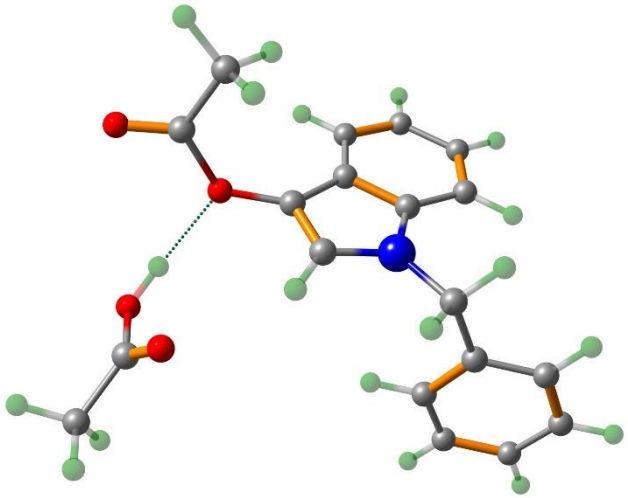

Figure S20. DFT-Optimized geometry of final product **2a+AcOH**.

Table S9. DFT-optimized cartesian coordiantes of final product **2a+AcOH**.

Zero-point correction= 0.343853 (Hartree/Particle)
Thermal correction to Energy= 0.367198
Thermal correction to Enthalpy= 0.368142
Thermal correction to Gibbs Free Energy= 0.284582
Sum of electronic and zero-point Energies= -1090.844312
Sum of electronic and thermal Energies= -1090.820967
Sum of electronic and thermal Enthalpies= -1090.820023
Sum of electronic and thermal Free Energies= -1090.903584

C19NH19O4

N	6.056246000	2.624644000	6.056755000
C	6.662979000	4.111894000	4.498634000
C	6.147909000	2.857148000	4.699108000
C	6.527517000	3.737915000	6.732979000

C	6.929116000	4.708988000	5.771001000
C	6.653413000	0.532471000	7.295818000
C	5.567061000	1.393693000	6.670789000
H	5.046866000	0.837592000	5.884917000
H	4.816250000	1.650126000	7.424900000
C	7.852535000	0.275158000	6.618309000
H	8.030027000	0.725763000	5.645743000
C	6.635952000	3.979717000	8.108936000
H	6.338480000	3.233943000	8.838282000
C	7.451308000	5.941261000	6.202459000
H	7.770917000	6.688078000	5.481908000
C	7.556062000	6.177805000	7.566761000
H	7.959233000	7.122808000	7.917925000
C	7.150875000	5.207650000	8.508815000
H	7.247399000	5.422589000	9.568648000
C	8.822895000	-0.550328000	7.186300000
H	9.748861000	-0.739768000	6.651266000
C	8.605638000	-1.133282000	8.438058000
H	9.361989000	-1.775364000	8.879427000
C	6.444945000	-0.051181000	8.550489000
H	5.520091000	0.145063000	9.087158000
C	7.413494000	-0.882503000	9.118687000
H	7.237730000	-1.326435000	10.094115000
H	5.863297000	2.115422000	3.967930000
O	6.968029000	4.654762000	3.250419000
O	6.726717000	1.668455000	1.667237000
C	6.108376000	5.525973000	2.601868000
C	7.793121000	1.942446000	1.143615000
O	6.445559000	5.902935000	1.506263000
O	8.453133000	3.089390000	1.371362000
C	4.844302000	5.916092000	3.316513000
C	8.527212000	1.055186000	0.170963000
H	8.641272000	1.570330000	-0.787340000
H	9.531359000	0.840054000	0.547437000
H	7.976981000	0.126201000	0.028099000

H	4.240543000	5.031371000	3.534992000
H	5.071407000	6.399929000	4.269998000
H	4.286606000	6.598906000	2.677538000
H	7.930303000	3.637567000	1.997278000

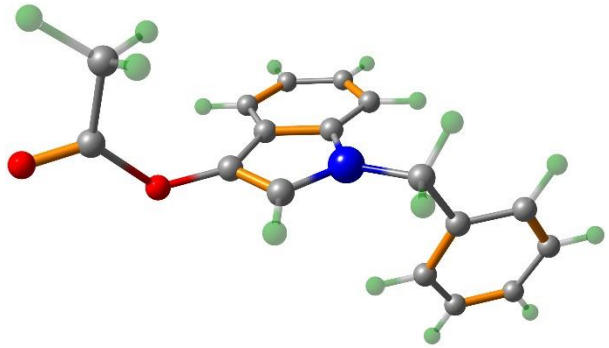

Figure 21. DFT-optimized geometry of **2a**.

Table S10. DFT-optimized cartesian coordinates of **2a**.

Zero-point correction= 0.280998 (Hartree/Particle)
Thermal correction to Energy= 0.297872
Thermal correction to Enthalpy= 0.298816
Thermal correction to Gibbs Free Energy= 0.233371
Sum of electronic and zero-point Energies= -861.800035
Sum of electronic and thermal Energies= -861.783161
Sum of electronic and thermal Enthalpies= -861.782217
Sum of electronic and thermal Free Energies= -861.847663

C17NH15O2

N	5.708236000	2.647601000	6.031417000
C	6.036851000	3.601363000	4.027298000
C	5.398906000	2.581114000	4.685247000
C	6.562416000	3.717270000	6.237684000

C	6.798038000	4.348077000	4.982797000
C	6.273405000	0.794219000	7.618359000
C	5.217156000	1.733858000	7.057043000
H	4.404161000	1.159508000	6.602053000
H	4.772042000	2.317993000	7.869255000
C	7.230153000	0.196246000	6.788426000
H	7.248025000	0.434724000	5.728835000
C	7.149913000	4.190541000	7.418909000
H	6.975683000	3.701990000	8.371658000
C	7.642023000	5.470649000	4.915430000
H	7.836913000	5.956966000	3.964293000
C	8.221866000	5.937871000	6.087401000
H	8.877794000	6.802546000	6.054480000
C	7.976667000	5.304307000	7.325232000
H	8.447027000	5.692510000	8.223548000
C	8.164532000	-0.695991000	7.315205000
H	8.902942000	-1.150503000	6.661177000
C	8.151875000	-1.005076000	8.678049000
H	8.880254000	-1.698949000	9.086928000
C	6.270009000	0.483983000	8.983248000
H	5.535864000	0.947530000	9.637597000
C	7.201122000	-0.413440000	9.511213000
H	7.187240000	-0.642376000	10.572738000
H	4.745782000	1.812064000	4.299936000
O	6.029196000	3.806138000	2.653433000
C	5.135104000	4.667170000	2.064064000
O	5.207231000	4.806568000	0.864883000
C	4.136676000	5.363161000	2.953527000
H	3.514899000	4.634817000	3.480377000
H	4.646636000	5.963777000	3.711631000
H	3.512003000	6.003793000	2.332868000

10.3 Reference

1. M. J. Frisch, G. W. Trucks, H. B. Schlegel, G. E. Scuseria, M. A. Robb, J. R. Cheeseman, G. Scalmani, V. Barone, B. Mennucci, G. A. Petersson, H. Nakatsuji, M. Caricato, X. Li, H. P. Hratchian, A. F. Izmaylov, J. Bloino, G. Zheng, J. L. Sonnenberg, M. Hada, M. Ehara, K. Toyota, R. Fukuda, J. Hasegawa, M. Ishida, T. Nakajima, Y. Honda, O. Kitao, H. Nakai, T. Vreven, J. A. Jr. Montgomery, J. E Peralta, M. O. Bearpark, J. J. Heyd, E. Brothers, K. N. Kudin, V. N. Staroverov, R. Kobayashi, J. Normand, K. Raghavachari, A. Rendell, J. C. Burant, S. S. Iyengar, J. Tomasi, M. Cossi, N. Rega, N. J. Millam, J. E. Klene, J. B. Knox, V. Cross, C. Bakken, J. Adamo, M. Jaramillo, R. Gomperts, R. E. Stratmann, O. Yazyev, A. J. Austin, R. Cammi, C. Pomelli, J. W. Ochterski, R. L. Martin, K. Morokuma, V. G. Zakrzewski, G. A. Voth, P. Salvador, J. J. Dannenberg, S. Dapprich, A. D. Daniels, Ö. Farkas, J. B. Foresman, J. V. Ortiz, J. Cioslowski and D. J. Fox, Gaussian 09, revision B.01; Gaussian, Inc.: Wallingford, CT 2010.

2. (*a*) A. D. Becke, *J. Chem. Phys.*, 1993, **98**, 5648-5652; (*b*) C. Lee, W. Yang and R. G. Parr, *Phys. Rev. B: Condens. Matter*, 1988, **37**, 785-789; (*c*) P. J. Stevens, F. J. Devlin, C. F. Chabalowski, and M. J. Frisch, *J. Phys. Chem.*, 1994, **98**, 11623-11627.
3. D. Roy, T. A. Keith, J. M. Millam, GaussView, Version 6, Semichem Inc., Shawnee Mission, KS, 2016.
4. (a) G. A. Petersson, A. Bennett, T. G. Tensfeldt, M. A. Al-Laham, W. A. Shirley, and J. Mantzaris, *J. Chem. Phys.*, 1988, **89**, 2193-2218; (b) G. A. Petersson and M. A. Al-Laham, *J. Chem. Phys.*, 1991, **94**, 6081-6090.
5. H. Stroll, B. Metz and M. Dolg, *J. Comput. Chem*., 2002, **23**, 767-778.
6. (*a*) S. R. Edinger, C. Cortis, P. S. Shenkin and R. A. Friesner, *J. Phys. Chem. B*, 1997, **101**, 1190-1197; (b) M. Fridrichs, R. Zhou, S. R. Edinger and R. A. Friesner, *J. Chem. Phys B*, 1999, **103**, 3057-3061; (*c*) B. Marten, K. Kim, C. Cortis, R. A. Friesner, R. B. Murphy, M. N. Ringnalda, D. Stikoff and B. Honig, *J. Phys. Chem.*, 1996, **100**, 11775-11788.
7. M. Cossi, V. Barone, R. Cammi and J. Tomasi, *Chem Phys, Lett.*, 1996, **255**, 327-335.
8. N. M. O'Boyle, A. L. Tenderholt, K. M. Langner, *J. Comput. Chem.*, 2008, **29**, 839-845.
9. G. A. Zhurko, Chemcraft - graphical program for visualization of quantum chemistry computations. Ivanovo, Russia, 2005. *https://chemcraftprog.com*.

11. NMR

11.1 NMR data

1. 1-benzyl-1*H*-indol-3-yl acetate (2a)[1]

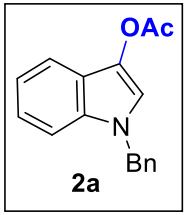

Reaction condition: The reaction was carried out with 0.041 g (0.2 mM) of **1a** and 0.077 g DAIB, under the irradiation of 8W blue LED for 12 h.

Yield: 65%, 34 mg

R_f: 0.5; EtOAc/Petroleum ether = 1/19

MP: 140-142 °C

Nature: Brown solid

^{1}H NMR (400 MHz, $CDCl_3$): δ (ppm) 7.58 (td, J = 7.8 Hz, 1.0 Hz, 1H), 7.34 (s, 1H), 7.32-7.27 (m, 4H), 7.20 (dt, J = 7.5 Hz, 1.6 Hz, 1H), 7.15-7.11 (m, 3H), 5.28 (s, 2H), 2.36 (s, 3H).

^{13}C{^{1}H} NMR (100 MHz, $CDCl_3$): δ (ppm) 168.7, 137.4, 133.5, 129.9, 128.9, 127.8, 127.0, 122.7, 120.6, 119.7, 117.8, 117.4, 109.8, 50.2, 21.1.

IR (ATR) υ (cm^{-1}): 1765, 1378, 1465, 1182, 658, 569.

2. 1-methyl-1*H*-indol-3-yl acetate (2b)

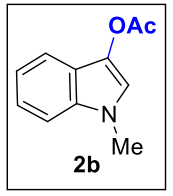

Reaction condition: The reaction was carried out with 0.026 g (0.2 mM) of **1b** and 0.077 g DAIB, under the irradiation of 8W blue LED for 12 h.

Yield: 61%, 24 mg

R_f: 0.5; EtOAc/Petroleum ether = 1/19

Nature: Yellow oil

^{1}H NMR (400 MHz, $CDCl_3$): δ (ppm) 7.55 (dd, J = 7.2 Hz, 0.8 Hz, 1H), 7.30 (d, J = 8.0 Hz, 1H), 7.29-7.23 (m, 2H), 7.15-7.11 (m, 1H), 3.75 (s, 3H), 2.36 (s, 3H).

^{13}C{^{1}H} NMR (100 MHz, $CDCl_3$): δ (ppm) 168.9, 133.8, 129.2, 122.4, 120.2, 119.4, 118.0, 117.6, 109.4, 32.9, 21.1.

IR (ATR) υ (cm^{-1}): 1741, 1360, 651, 580.

HRMS (ESI) *m/z* calcd for $[M+H]^+$ $C_{11}H_{12}NO_2^+$ 190.0863, found 190.0791.

---

3. 1-allyl-1*H*-indol-3-yl acetate (2c)

Reaction condition: The reaction was carried out with 0.023 g (0.2 mM) of **1c** and 0.077 g **DAIB**, under the irradiation of 8W blue LED for 12 h.

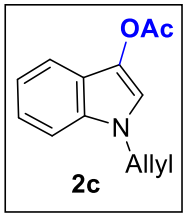

2c

Yield: 52%, 22 mg

R_f: 0.4; EtOAc/Petroleum ether = 1/19

Nature: colourless oil

^{1}H NMR (400 MHz, $CDCl_3$): δ (ppm) 7.56 (td, J = 8.2 Hz, 0.4 Hz, 1H), 7.29 (d, J = 6.0 Hz, 2H), 7.22 (dt, J = 7.6 Hz, 1.2 Hz, 1H), 7.14-7.10 (m, 1H), 6.03-5.94 (m, 1H), 5.23-5.19 (s, 1H), 5.15-5.10 (m, 1H), 4.69 (td, J = 5.6 Hz, 1.6 Hz, 2H), 2.36 (s, 3H).

^{13}C{^{1}H} NMR (100 MHz, $CDCl_3$): δ (ppm) 186.8, 133.34, 133.28, 129.7, 122.5, 120.5, 119.6, 117.8, 117.7, 117.0, 109.7, 49.0, 21.1.

IR (ATR) υ (cm^{-1}): 1745, 260, 891, 563, 541.

HRMS (ESI) *m/z* calcd for $[M+H]^+$ $C_{13}H_{14}NO_2^+$ 216.1019, found 238.0859.

---

4. 1-phenyl-1*H*-indol-3-yl acetate (2d)[1]

Reaction condition: The reaction was carried out with 0.039 g (0.2 mM) of **1d** and 0.077 g **DAIB**, under the irradiation of 8W blue LED for 12 h.

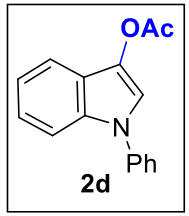

Yield: 59%, 30 mg

R_f: 0.5; EtOAc/Petroleum ether = 1/19

Nature: pale yellow oil

^{1}H NMR (400 MHz, $CDCl_3$): δ (ppm) 7.63-7.50 (m, 7H), 7.36 (d, J = 4.4 Hz, 1H), 7.25-7.17 (m, 2H), 2.40 (s, 3H).

^{13}C{^{1}H} NMR (100 MHz, $CDCl_3$): δ (ppm) 168.6, 139.6, 137.6, 133.0, 129.7, 126.6, 124.5, 123.4, 121.4, 120.5, 118.0, 117.1, 110.7, 21.2.

IR (ATR) υ (cm^{-1}): 1761, 1278, 886, 771, 608, 532.

5. 1-pivaloyl-1*H*-indol-3-yl acetate (2e)

Reaction condition: The reaction was carried out with 0.040 g (0.2 mM) of **1e** and 0.077 g **DAIB**, under the irradiation of 8W blue LED for 12 h.

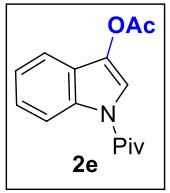

Yield: 41%, 21 mg

R_f: 0.8; EtOAc/Petroleum ether = 1/49

Nature: colourless liquid.

^{1}H NMR (400 MHz, $CDCl_3$): δ (ppm) 8.53 (d, J = 8.4 Hz, 1H), 8.07 (s, 1H), 7.53 (d, J = 7.6 Hz, 1H), 7.39 (t, J =7.8 Hz, 1H), 7.30 (t, J = 7.4 Hz, 1H), 2.39 (s, 3H), 1.52 (s, 9H).

^{13}C{^{1}H} NMR (100 MHz, $CDCl_3$): δ (ppm) 177.3, 168.1, 134.13, 134.09, 126.3, 123.8, 122.8, 117.6, 117.2, 114.2, 41.3, 28.7, 21.2.

IR (ATR) υ (cm^{-1}): 1758, 1722, 1227, 873, 713, 662, 569.

HRMS (ESI) *m/z* calcd for $[M+H]^+$ $C_{15}H_{18}NO_3^+$ 260.1281, found 260.1219.

6. 1-pivaloyl-1*H*-indol-2-yl acetate (2e')

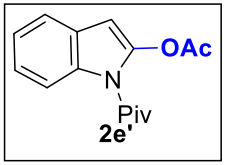

Reaction condition: The reaction was carried out with 0.040 g (0.2 mM) of **1e** and 0.077 g **DAIB**, under the irradiation of 8W blue LED for 12 h.

Yield: 12%, 6 mg

R_f: 0.5; EtOAc/Petroleum ether = 1/19

Nature: colourless liquid

^{1}H NMR (400 MHz, $CDCl_3$): δ (ppm) 8.37 (d, J = 8.8 Hz, 1H), 7.74 (dd, J = 7.6 Hz, 1.2 Hz, 1H), 7.67-7.63 (m, 1H), 7.25-7.21 (m, 1H), 6.55 (s, 1H), 2.31 (s, 3H), 1.38 (s, 9H).

^{13}C{^{1}H} NMR (100 MHz, $CDCl_3$): δ (ppm) 192.5, 177.7, 169.1, 155.3, 137.7, 124.8, 124.4, 122.0, 119.8, 79.9, 41.9, 28.2, 21.0.

IR (ATR) υ (cm^{-1}): 1762, 1741, 1243, 1168, 1083, 762, 507.

HRMS (ESI) *m/z* calcd for $[M]^+$ $C_{15}H_1NO_3$ 260.1281, found 259.1184.

7. methyl 3-acetoxy-1-benzyl-1*H*-indole-4-carboxylate (2f)

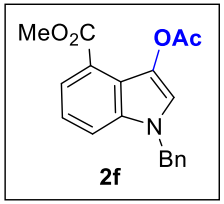

Reaction condition: The reaction was carried out with 0.053 g (0.2 mM) of **1f** and 0.077 g **DAIB**, under the irradiation of 8W blue LED for 12 h.

Yield: 48%, 30 mg

R_f: 0.25; EtOAc/Petroleum ether = 1/9

Nature: Pale yellow solid

MP: 186–188 °C

^{1}H NMR (400 MHz, $CDCl_3$): δ (ppm) 7.77 (d, J = 7.6 Hz, 1H), 7.44 (d, J = 8.0 Hz, 1H), 7.32-7.27 (m, 3H), 7.19 (d, J = 7.6 Hz, 1H), 7.16 (s, 1H), 7.10 (d, J = 6.4 Hz, 2H), 5.26 (s, 2H), 3.92 (s, 3H), 2.38 (s, 3H).

^{13}C{^{1}H} NMR (400 MHz, $CDCl_3$): δ (ppm) 170.5, 167.4, 136.6, 135.2, 129.2, 128.9, 128.0, 126.9, 123.8, 122.9, 121.4, 121.1, 119.1, 114.5, 52.1, 50.2, 21.0.

IR (ATR) υ (cm^{-1}): 3208, 2921, 1751, 1706, 1442, 982, 752.

HRMS (ESI) *m/z* calcd for $[M+H]^+$ $C_{19}H_{18}NO_4^+$ 324.1230, found 324.1025.

---

8. 1-benzyl-4-(benzyloxy)-1*H*-indol-3-yl acetate (2g)

Reaction condition: The reaction was carried out with 0.062 g (0.2 mM) of **1g** and 0.077 g **DAIB**, under the irradiation of 8W blue LED for 12 h.

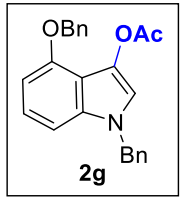

2g

Yield: 55%, 41 mg

R_f: 0.25; EtOAc/Petroleum ether = 1/19

Nature: Greenish solid

MP: 185–187 °C

^{1}H NMR (400 MHz, $CDCl_3$): δ (ppm) 7.51 (d, J = 7.2 Hz, 2H), 7.42-7.38 (m, 2H), 7.36-7.27 (m, 4H), 7.13-7.06 (m, 3H), 6.94 (s, 1H), 6.88 (d, J = 8.4 Hz, 1H), 6.57 (d, J = 8.0 Hz, 1H), 5.23 (s, 2H), 5.10 (s, 2H), 1.95 (s, 3H).

^{13}C{^{1}H} NMR (100 MHz, $CDCl_3$): δ (ppm) 170.2, 152.7, 137.3 (2C, overlap), 136.0, 128.9, 128.6, 128.3, 128.1, 127.8, 127.0, 123.6, 116.6, 111.8, 103.6, 101.1, 70.3, 50.4, 20.6.

IR (ATR) υ (cm^{-1}): 2806, 1758, 1453, 1266, 1168, 676, 543.

HRMS (ESI) *m/z* calcd for $[M+H]^+$ $C_{24}H_{22}NO_3^+$ 372.1594, found 372.1624.

---

9. 1-benzyl-4-cyano-1*H*-indol-3-yl acetate (2h)

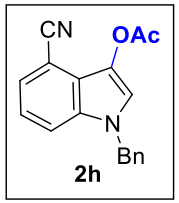

2h

Reaction condition: The reaction was carried out with 0.046 g (0.2 mM) of **1h** and 0.077 g **DAIB**, under the irradiation of 8W blue LED for 12 h.

Yield: 56%, 32 mg

R_f: 0.3; EtOAc/Petroleum ether = 1/13

Nature: Yellow solid

MP: 171–173 °C

^{1}H NMR (400 MHz, $CDCl_3$): δ (ppm) 7.46 (dd, J = 11.6 Hz, 8.4 Hz, 2H), 7.38 (s, 1H), 7.34-7.29 (m, 3H), 7.19 (dd, J = 8.0 Hz, 7.6 Hz, 1H), 7.11 (d, J = 6.0 Hz, 2H), 5.29 (s, 2H), 2.42 (s, 3H).

^{13}C{^{1}H} NMR (100 MHz, $CDCl_3$): δ (ppm) 169.4, 136.2, 133.5, 129.1, 128.6, 128.2, 126.9, 126.2, 122.2, 120.8, 118.2, 114.8, 101.2, 50.5, 20.7.

IR (ATR) υ (cm^{-1}): 2256, 1748, 1228, 857, 732, 665, 556.

HRMS (ESI) *m/z* calcd for $[M+ Na]^+$ $C_{18}H_1N_2O_2Na^+$ 313.0947, found 313.0958.

10. 1-benzyl-5-methoxy-1*H*-indol-3-yl acetate (2i)[1]

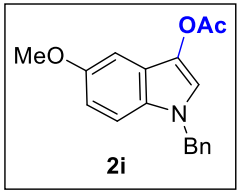

2i

Reaction condition: The reaction was carried out with 0.047 g (0.2 mM) of **1i** and 0.077 g **DAIB**, under the irradiation of 8W blue LED for 12 h.

Yield: 68%, 40 mg

R_f: 0.3; EtOAc/Petroleum ether = 1/19

Nature: Off-white solid

MP: 160–162 °C

^{1}H NMR (400 MHz, $CDCl_3$): δ (ppm) 7.32-7.26 (m, 4H), 7.14 (d, J = 8.8 Hz, 2H), 7.11 (s, 1H), 6.99 (d, J = 2.4 Hz, 1H), 6.85 (dd, J = 8.8 Hz, 2.4 Hz, 1H), 5.23 (s, 2H), 3.86 (s, 3H), 2.36 (s, 3H).

^{13}C{^{1}H} NMR (100 MHz, $CDCl_3$): δ (ppm) 168.7, 154.3, 137.4, 129.6, 129.0, 128.9, 127.8, 126.9, 120.7, 118.1, 113.4, 110.9, 99.0, 55.9, 50.4, 21.1.

IR (ATR) υ (cm^{-1}): 3205, 2915, 1745, 908, 825, 766.

---

11. 1-benzyl-5-nitro-1*H*-indol-3-yl acetate (2j)

Reaction condition: The reaction was carried out with 0.050 g (0.2 mM) of **1j** and 0.077 g **DAIB**, under the irradiation of 8W blue LED for 12 h.

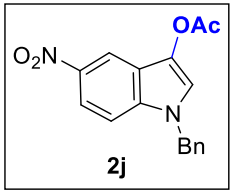

2j

Yield: 53%, 33 mg

R_f: 0.3; EtOAc/Petroleum ether = 1/9

Nature: Yellow solid

MP: 168–170 °C

^{1}H NMR (400 MHz, $CDCl_3$): δ (ppm) 8.57 (d, J = 2.4 Hz, 1H), 8.08 (dd, J = 9.2 Hz, 2.4 Hz, 1H), 7.51 (s, 1H), 7.33-7.28 (m, 4H), 7.13 (d, J = 8.0 Hz, 2H), 5.31 (s, 2H), 2.38 (s, 3H).

^{13}C{^{1}H} NMR (100 MHz, $CDCl_3$): δ (ppm) 168.2, 141.7, 136.0, 135.7, 131.5, 129.2, 128.4, 127.0, 120.4, 120.0, 118.2, 115.6, 110.0, 50.8, 21.0.

IR (ATR) υ (cm^{-1}): 1753, 1558, 1286, 636, 587.

HRMS (ESI) *m/z* calcd for $[M+H]^+$ $C_{17}H_{15}N_2O_4^+$ 311.1026, found 311.1038.

---

12. 1-benzyl-5-bromo-1*H*-indol-3-yl acetate (2k)[1]

Reaction condition: The reaction was carried out with 0.057 g (0.2 mM) of **1k** and 0.077 g **DAIB**, under the irradiation of 8W blue LED for 12 h.

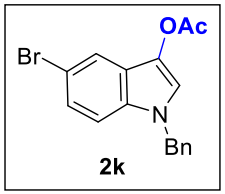

2k

Yield: 56%, 38 mg

R_f: 0.5; EtOAc/Petroleum ether = 1/19

Nature: Yellow solid

MP: 175–177 °C

^{1}H NMR (400 MHz, $CDCl_3$): δ (ppm) 7.71 (d, J = 1.6 Hz, 1H), 7.34 (s, 1H), 7.30-7.26 (m, 3H), 7.24 (d, J = 2.0 Hz, 1H), 7.12-7.09 (m, 3H), 5.24 (s, 2H), 2.34 (s, 3H).

^{13}C{^{1}H} NMR (100 MHz, $CDCl_3$): δ (ppm) 168.5, 136.8, 132.1, 129.1, 129.0, 128.0, 126.9, 125.6, 122.1, 120.5, 118.7, 113.1, 111.4, 50.5, 21.0.

IR (ATR) υ (cm^{-1}): 1737, 1248, 1162, 678, 555.

13. 1-benzyl-5-iodo-1*H*-indol-3-yl acetate (2l)

Reaction condition: The reaction was carried out with 0.067 g (0.2 mM) of **1l** and 0.077 g **DAIB**, under the irradiation of 8W blue LED for 12 h.

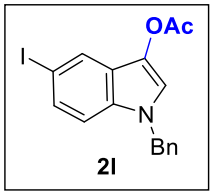

2l

Yield: 58%, 45 mg

R_f: 0.5; EtOAc/Petroleum ether = 1/19

Nature: White solid

MP: 191–193 °C

^{1}H NMR (400 MHz, $CDCl_3$): δ (ppm) 7.92 (d, *J* = 0.8 Hz, 1H), 7.42 (dd, *J* = 8.4 Hz, 1.2 Hz, 1H), 7.30 (d, *J* = 9.6 Hz, 4H), 7.09 (d, *J* = 6.8 Hz, 2H), 7.02 (d, *J* = 8.4 Hz, 1H), 5.23 (s, 2H), 2.34 (s, 3H).

^{13}C{^{1}H} NMR (100 MHz, $CDCl_3$): δ (ppm) 168.5, 136.8, 132.5, 131.0, 129.0, 128.7, 128.0, 126.9, 126.7, 122.9, 118.3, 111.9, 83.1, 50.4, 21.1.

IR (ATR) υ (cm^{-1}): 1751, 1257, 808, 712, 665, 558.

HRMS (ESI) *m/z* calcd for $[M+H]^+$ $C_{17}H_{15}INO_2^+$ 392.0147, found 392.0163.

---

14. 1-benzyl-6-bromo-1*H*-indol-3-yl acetate (2m)

Reaction condition: The reaction was carried out with 0.057 g (0.2 mM) of **1m** and 0.077 g **DAIB**, under the irradiation of 8W blue LED for 12 h.

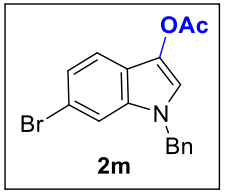

2m

Yield: 48%, 33 mg

R_f: 0.5; EtOAc/Petroleum ether = 1/19

Nature: White solid

MP: 171–174 °C

^{1}H NMR (400 MHz, $CDCl_3$): δ (ppm) 7.45 (d, *J* = 8.8 Hz, 2H), 7.32-7.28 (m, 4H), 7.24 (d, *J* = 8.4 Hz, 1H), 7.12 (d, *J* = 6.4 Hz, 2H), 5.21 (s, 2H), 2.35 (s, 3H).

^{13}C{^{1}H} NMR (400 MHz, $CDCl_3$): δ (ppm) 168.4, 136.7, 134.1, 129.9, 129.0, 128.0, 126.9, 123.1, 119.4, 119.2, 117.9, 116.5, 112.8, 50.3, 21.0.

IR (ATR) υ (cm^{-1}): 1737, 1248, 1162, 678, 555

HRMS (ESI) *m/z* calcd for $[M+H]^+$ $C_{17}H_{15}BrNO_2^+$ 344.0281, found 342.0128.

---

15. 1-benzyl-6-fluro-1*H*-indol-3-yl acetate (2n)

Reaction condition: The reaction was carried out with 0.045 mg (0.2 mM) of **1n** and 0.077 g **DAIB**, under the irradiation of 8W blue LED for 12 h.

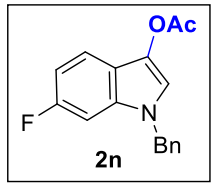

Yield: 37%, 21 mg

R_f: 0.5; EtOAc/Petroleum ether = 1/19

Nature: Off-white solid

MP: 168–170 °C

^{1}H NMR (400 MHz, $CDCl_3$): δ (ppm) 7.48 (dd, J = 8.8 Hz, 5.2 Hz, 1H), 7.33–7.27 (m, 4H), 7.12 (d, J = 6.4 Hz, 2H), 6.93–6.86 (m, 2H), 5.21 (s, 2H), 2.34 (s, 3H).

^{13}C{^{1}H} NMR (400 MHz, $CDCl_3$): δ (ppm) 168.6, 136.8, 129.0, 128.0, 127.0, 118.9, 118.2, 117.7, 117.3, 108.9, 108.6, 96.4, 96.2, 50.5, 21.2.

^{19}F NMR (373 MHz, $CDCl_3$): δ (ppm) -119.5.

IR (ATR) υ (cm^{-1}): 3218, 2895, 1752, 1440, 1186, 642, 558.

HRMS (ESI) *m/z* calcd for $[M]^+$ $C_{17}H_{14}FNO_2^+$ 248.1081, found 283.1067.

16. methyl 3-acetoxy-1-benzyl-1*H*-indole-6-carboxylate (2o)

Reaction condition: The reaction was carried out with 0.053 g (0.2 mM) of **1o** and 0.077 g **DAIB**, under the irradiation of 8W blue LED for 12 h.

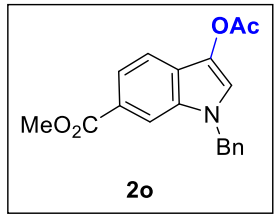

Yield: 45%, 29 mg

R_f: 0.25; EtOAc/Petroleum ether = 1/9

Nature: Pale-yellow solid

MP: 182–185 °C

^{1}H NMR (400 MHz, $CDCl_3$): δ (ppm) 8.10 (s, 1H), 7.86 (dd, J = 8.4 Hz, 0.8 Hz, 1H), 7.61 (d, J = 8.4 Hz, 1H), 7.49 (s, 1H), 7.33-7.27 (m, 3H), 7.13 (d, J = 6.4 Hz, 2H), 5.31 (s, 2H), 3.92 (s, 3H), 2.35 (s, 3H).

^{13}C{^{1}H} NMR (100 MHz, $CDCl_3$): δ (ppm) 168.4, 167.9, 136.8, 132.7, 129.9, 128.9, 128.0, 126.9, 124.4, 123.5, 120.7, 120.6, 117.5, 112.2, 52.1, 50.1, 21.0.

IR (ATR) υ (cm^{-1}): 3216, 1765, 1714, 1226, 969, 562.

HRMS (ESI) ***m/z*** calcd for $[M+H]^+$ $C_{19}H_{18}NO_4^+$ 324.1230, found 324.1357.

---

17. 1-benzyl-7-(bromo)-1*H*-indol-3-yl acetate (2p)

Reaction condition: The reaction was carried out with 0.057 g (0.2 mM) of **1p** and 0.077 g **DAIB**, under the irradiation of 8W blue LED for 12 h.

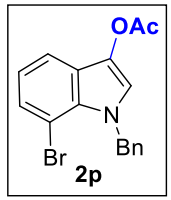

Yield: 55%, 38 mg

R_f: 0.5; EtOAc/Petroleum ether = 1/19

Nature: Yellowish solid

MP: 173–175 °C

^{1}H NMR (400 MHz, $CDCl_3$): δ (ppm) 7.52 (dd, J = 8.0 Hz, 0.8 Hz, 1H), 7.37 (dd, J = 7.6 Hz, 0.8 Hz, 1H), 7.33 (s, 1H), 7.31-7.27 (m, 2H), 7.25-7.23 (m, 1H), 7.04 (d, J = 6.8 Hz, 2H), 6.96 (t, J = 7.8 Hz, 1H), 5.79 (s, 2H), 2.35 (s, 3H).

^{13}C{^{1}H} NMR (400 MHz, $CDCl_3$): δ (ppm) 168.4, 138.8, 129.9, 129.6, 128.8, 128.2, 127.6, 126.4, 123.7, 120.8, 120.3, 117.2, 104.2, 51.3, 20.1.

IR (ATR) υ (cm^{-1}): 1737, 1248, 1162, 678, 555.

HRMS (ESI) *m/z* calcd for $[M+H]^+$ $C_{17}H_{15}BrNO_2^+$ 344.0281, found 344.0219.

18. 1-benzyl-7-nitro-1*H*-indol-3-yl acetate (2q)

Reaction condition: The reaction was carried out with 0.050 g (0.2 mM) of **1q** and 0.077 g **DAIB**, under the irradiation of 8W blue LED for 12 h.

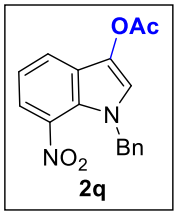

2q

Yield: 51%, 32 mg

R_f: 0.2; EtOAc/Petroleum ether = 1/9

Nature: Yellowish solid

MP: 165–168 °C

^{1}H NMR (400 MHz, $CDCl_3$): δ (ppm) 7.85 (dd, J = 7.6 Hz, 0.8 Hz, 1H), 7.75 (dd, J = 7.6 Hz, 0.4 Hz, 1H), 7.57 (s, 1H), 7.25-7.20 (m, 3H), 7.14 (t, J = 7.8 Hz, 1H), 6.95-6.92 (m, 2H), 5.42 (s, 2H), 2.39 (s, 3H).

^{13}C{^{1}H} NMR (400 MHz, $CDCl_3$): δ (ppm) 168.1, 137.1, 136.7, 130.3, 128.9, 128.0, 127.0, 126.0, 123.9, 123.6, 122.3, 121.0, 118.9, 53.7, 21.0.

IR (ATR) υ (cm^{-1}): 1716, 1478, 1286, 1109, 548.

HRMS (ESI) *m/z* calcd for $[M+H]^+$ $C_{17}H_{15}N_2O_4^+$ 311.1026, found 311.1049.

19. 1-benzyl-7-(benzyloxy)-1*H*-indol-3-yl acetate (2r)

Reaction condition: The reaction was carried out with 0.063 g (0.2 mM) of **1r** and 0.077 g **DAIB**, under the irradiation of 8W blue LED for 12 h.

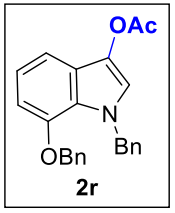

2r

Yield: 58%, 43 mg

R_f: 0.5; EtOAc/Petroleum ether = 1/19

Nature: Greenish solid

MP: 184–186 °C

^{1}H NMR (400 MHz, $CDCl_3$): δ (ppm) 7.36-7.34 (m, 3H), 7.31 (d, J = 4.0 Hz, 1H), 7.28-7.26 (m, 5H), 7.22 (d, J = 8.0 Hz, 1H), 7.05 (t, J = 8.0 Hz, 1H), 7.00-6.98 (m, 2H), 6.73 (d, J = 7.6 Hz, 1H), 5.60 (s, 2H), 5.12 (s, 2H), 2.39 (s, 3H).

^{13}C{^{1}H} NMR (400 MHz, $CDCl_3$): δ (ppm) 168.6, 146.8, 139.5, 136.8, 129.9, 128.62, 128.60, 128.1, 127.8, 127.2, 126.5, 123.4, 122.9, 120.2, 118.6, 110.6, 104.5, 70.5, 52.7, 21.1.

IR (ATR) υ (cm^{-1}): 2818, 1762, 1485, 1275, 1107, 749, 655, 549.

HRMS (ESI) *m/z* calcd for $[M+H]^+$ $C_{24}H_{22}NO_3^+$ 372.1594, found 372.1624.

---

20. ethyl 3-acetoxy-1-benzyl-1H-indole-2-carboxylate (2s)

Reaction condition: The reaction was carried out with 0.056 g (0.2 mM) of **1s** and 0.077 g **DAIB**, under the irradiation of 8W blue LED for 12 h.

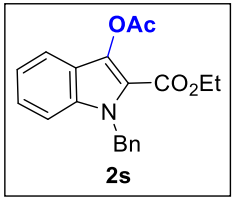

2s

Yield: 56%, 37 mg

R_f: 0.4; EtOAc/Petroleum ether = 1/9

Nature: White solid

MP: 110–112 °C

^{1}H NMR (400 MHz, $CDCl_3$): δ (ppm) 7.57 (d, J = 8.0 Hz, 1H), 7.33 (d, J = 5.2 Hz, 2H), 7.25 (d, J = 7.6 Hz, 2H), 7.21 (d, J = 6.8 Hz, 1H), 7.19-7.15 (m, 1H), 7.05 (d, J = 7.2 Hz, 2H), 5.80 (s, 2H), 4.30 (q, J = 7.2 Hz, 2H), 2.42 (s, 3H), 1.32 (t, J = 7.2 Hz, 3H).

$^{13}C\{^{1}H\}$ NMR (400 MHz, $CDCl_3$): δ(ppm) 169.2, 161.0, 138.2, 136.7, 135.0, 128.7, 127.3, 126.4, 126.3, 121.2, 120.0, 119.3, 117.6, 111.0, 60.8, 48.2, 20.9, 14.3.

IR (ATR) υ (cm^{-1}): 1769,1695, 1618, 364, 1193, 1124, 740, 696, 666.

HRMS (ESI) *m/z* calcd for $[M+ Na]^+$ $C_{20}H_{19}NNaO_4^+$ 360.1206, found 360.1201.

---

31. 1-benzyl-1*H*-indol-3-yl propionate (3a)

Reaction condition: The reaction was carried out with 0.041 g (0.2 mM) of **1a** and 0.084 g **DEIB**, under the irradiation of 8W blue LED for 12 h.

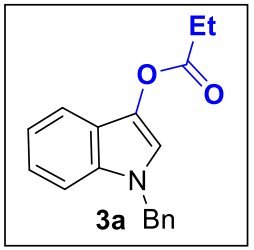

Yield: 43%, 24 mg

R_f: 0.5; EtOAc/Petroleum ether = 1/49

Nature: Yellowish liquid

^{1}H NMR (400 MHz, $CDCl_3$): δ(ppm) 7.45 (dd, J_1 = 8.0 Hz, J_2 = 0.8 Hz, 1H), 7.37 (s, 1H), 7.31-7.27 (m, 4H), 7.23-7.19 (m, 1H), 7.14 (dd, J_1 = 7.6 Hz, J_2 = 0.8 Hz, 3H), 5.28 (s, 2H), 2.67 (q, J = 7.6 Hz, 2H), 1.32 (t, J = 7.6 Hz, 2H).

$^{13}C\{^{1}H\}$ NMR (400 MHz, $CDCl_3$): δ(ppm) 172.2, 137.4, 133.5, 129.9, 128.9, 127., 127.0, 122.7, 120.6, 119.6, 17.8, 117.4, 109.8, 50.2, 27.8, 9.4.

IR (ATR) υ (cm^{-1}): 1749, 1614, 1453, 1345, 1334, 1174, 1076, 895, 702.

HRMS (ESI) *m/z* calcd for $[M+ H]^+$ $C_{18}H_{18}NO_2^+$ 280.1332, found 280.1328..

---

21. 1-benzylindoline-2,3-dione (4a)[2]

Reaction condition: The reaction was carried out with 0.041 g (0.2 mM) of **1a** and 0.322 g **DAIB**,

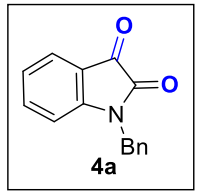

under the irradiation of 8W blue LED for 12 h.

Yield: 92%, 44 mg

R_f: 0.3; EtOAc/Petroleum ether = 1/9

Nature: Yellow solid

MP: 208–210 °C

^{1}H NMR (400 MHz, $CDCl_3$): δ (ppm) 7.60 (d, J = 7.2 Hz, 1H), 7.50-7.46 (m, 1H), 7.34-7.31 (m, 5H), 7.08 (t, J = 7.6 Hz, 1H), 6.78 (d, J = 8.0 Hz, 1H), 4.93 (s, 2H).

^{13}C{^{1}H} NMR (400 MHz, $CDCl_3$): δ (ppm) 183.4, 158.4, 150.8, 138.4, 134.6, 129.1, 128.3, 127.5, 125.5, 124.0, 117.7, 111.1, 44.1.

IR (ATR) υ (cm^{-1}): 1739, 1618, 1309, 1181, 778, 695.

22. 1-methylindoline-2,3-dione (4b)[2]

Reaction condition: The reaction was carried out with 0.026 g (0.2 mM) of **1b** and 0.322 g **DAIB**, under the irradiation of 8W blue LED for 12 h.

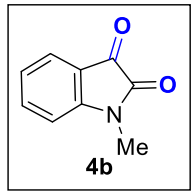

4b

Yield: 89%, 29 mg

R_f: 0.3; EtOAc/Petroleum ether = 1/9

Nature: Radish solid

MP: 184–186 °C

^{1}H NMR (400 MHz, $CDCl_3$): δ (ppm) 7.58 (dt, J = 7.8 Hz, 1.2 Hz, 1H), 7.53 (d, J = 7.2 Hz, 1H), 7.08 (t, J = 7.6 Hz, 1H), 6.78 (d, J = 7.6 Hz, 1H), 3.21 (s, 3H).

^{13}C{^{1}H} NMR (400 MHz, $CDCl_3$): δ (ppm) 183.4, 158.2, 151.5, 138.5, 125.2, 123.6, 117.4, 110.1, 26.2.

IR (ATR) υ (cm^{-1}): 1731, 1628, 1458, 1325, 1091, 1073, 891, 659, 515.

23. 1-allylindoline-2,3-dione (4c)[2]

Reaction condition: The reaction was carried out with 0.023 g (0.2 mM) of **1c** and 0.322 g **DAIB**, under the irradiation of 8W blue LED for 12 h.

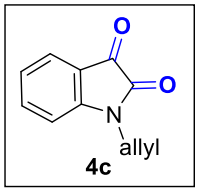

4c

Yield: 83%, 24 mg

R_f: 0.3; EtOAc/Petroleum ether = 1/9

Nature: Orange solid

MP: 172–174 °C

^{1}H NMR (400 MHz, $CDCl_3$): δ (ppm) 7.56-7.52 (m, 2H), 7.11-7.06 (m, 1H), 6.87 (d, J = 7.6 Hz, 1H), 5.86-5.76 (m, 1H), 5.31-5.24 (m, 2H), 4.34 (t, J = 1.6 Hz, 1H), 4.32 (t, J = 1.6 Hz, 1H).

^{13}C{^{1}H} NMR (400 MHz, $CDCl_3$): δ (ppm) 183.3, 157.9, 150.8, 138.5, 130.3, 125.3, 123.8, 118.6, 117.5, 111.0, 42.5.

IR (ATR) υ (cm^{-1}): 1769, 1603, 1181, 1092, 629, 532.

24. 1-benzyl-2,3-dioxoindoline-4-carbonitrile (4d)

Reaction condition: The reaction was carried out with 0.046 g (0.2 mM) of **1h** and 0.322 g **DAIB**, under the irradiation of 8W blue LED for 12 h.

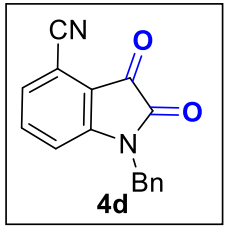

4d

Yield: 71%, 37 mg

R_f: 0.4; EtOAc/Petroleum ether = 3/17

Nature: Yellow solid

MP: 203–205 °C

^{1}H NMR (400 MHz, $CDCl_3$): δ (ppm) 7.60 (t, J = 8.0 Hz, 1H), 7.39-7.30 (m, 6H), 7.04 (d, J = 8.0 Hz, 1H), 4.97 (s, 2H).

^{13}C{^{1}H} NMR (400 MHz, $CDCl_3$): δ (ppm) 179.8, 156.9, 151.4, 138.3, 133.7, 129.4, 128.7, 127.8, 127.5, 117.4, 115.2, 114.5, 108.7, 44.5.

IR (ATR) υ (cm^{-1}): 2248, 1741, 1682, 1168, 635, 529.

HRMS (ESI) *m/z* calcd for $[M+H]^+$ $C_{16}H_{11}N_2O_2^+$ 263.0821, found 263.0849.

---

25. 1-benzyl-5-methoxyindoline-2,3-dione (4e)[3]

Reaction condition: The reaction was carried out with 0.047 g (0.2 mM) of **1i** and 0.322 g **DAIB**, under the irradiation of 8W blue LED for 12 h.

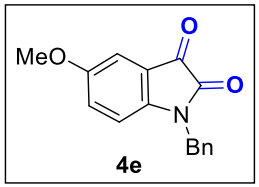

4e

Yield: 81%, 43 mg

R_f: 0.4; EtOAc/Petroleum ether = 1/9

Nature: Orange solid

MP: 190–192 °C

^{1}H NMR (400 MHz, $CDCl_3$): δ (ppm) 7.36-7.30 (m, 6H), 6.84 (d, J = 8.8 Hz, 1H), 6.65 (d, J = 8.8 Hz, 1H), 4.92 (s, 2H), 3.84 (s, 3H).

^{13}C{^{1}H} NMR (400 MHz, $CDCl_3$): δ (ppm) 182.3, 157.4, 155.7, 145.8, 134.3, 129.1, 128.2, 127.4, 120.5, 118.0, 110.9, 86.9, 57.3, 43.3.

IR (ATR) υ (cm^{-1}): 1748, 1729, 1678, 1305, 1021, 822, 659.

---

26. 1-benzyl-5-bromoindoline-2,3-dione (4f)[3]

Reaction condition: The reaction was carried out with 0.057 g (0.2 mM) of **1k** and 0.322 g **DAIB**, under the irradiation of 8W blue LED for 12 h.

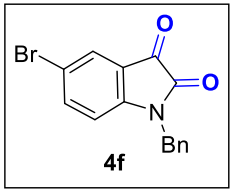

4f

Yield: 72%, 45 mg

R_f: 0.4; EtOAc/Petroleum ether = 1/9

Nature: Pale-yellow solid

MP: 210–212 °C

^{1}H NMR (400 MHz, $CDCl_3$): δ (ppm) 7.46 (d, J = 8.0 Hz, 1H), 7.3-7.31 (m, 5H), 7.25 (d, J = 7.2 Hz, 1H), 6.49 (s, 1H), 4.91 (s, 2H).

^{13}C{^{1}H} NMR (400 MHz, $CDCl_3$): δ (ppm) 182.1, 158.2, 151.6, 134.1, 133.7, 128.3, 1285, 127.5, 127.3, 126.5, 116.5, 114.6, 44.3.

IR (ATR) υ (cm^{-1}): 1749, 1706, 1251, 748, 579.

---

27. 1-benzyl-5-nitroindoline-2,3-dione (4g)

Reaction condition: The reaction was carried out with 0.050 g (0.2 mM) of **1j** and 0.322 g **DAIB**, under the irradiation of 8W blue LED for 12 h.

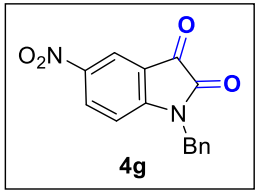

4g

Yield: 75%, 42 mg

R_f: 0.3; EtOAc/Petroleum ether = 3/17

Nature: Orange solid

MP: 195–198 °C

^{1}H NMR (400 MHz, $CDCl_3$): δ (ppm) 8.44 (d, J = 2.0 Hz, 1H), 8.40 (dd, J = 8.8 Hz, 2.4 Hz, 1H), 7.38-7.31 (m, 5H), 6.95 (d, J = 8.4 Hz, 1H), 5.01 (s, 2H).

^{13}C{^{1}H} NMR (400 MHz, $CDCl_3$): δ (ppm) 181.3, 158.0, 154.8, 144.3, 13.6, 133.5, 129.4, 128.8, 127.5, 121.0, 117.4, 111.4, 44.7.

IR (ATR) υ (cm^{-1}): 1762, 1572, 1635, 1248, 1181, 706, 561

HRMS (ESI) *m/z* calcd for $[M+H]^+$ $C_{15}H_{11}N_2O_2^+$ 283.0719, found 283.0744.

---

28. 1-benzyl-6-fluoroindoline-2,3-dione (4h)

Reaction condition: The reaction was carried out with 0.045 g (0.2 mM) of **1n** and 0.322 g **DAIB**, under the irradiation of 8W blue LED for 12 h.

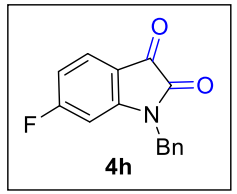

4h

Yield: 62%, 32 mg

R_f: 0.5; EtOAc/Petroleum ether = 1/9

Nature: Yellow solid

MP: 205–207 °C

^{1}H NMR (400 MHz, $CDCl_3$): δ (ppm) 7.63 (dd, J_1 = 8.4 Hz, J_2 = 5.6 Hz, 1H), 7.38-7.31 (m, 5H), 6.77-6.72 (m, 1H), 6.49 (dd, J = 8.8 Hz, 1.6 Hz, 1H), 4.91 (s, 2H).

^{13}C{^{1}H} NMR (400 MHz, $CDCl_3$): δ (ppm) 181.1, 158.6, 134.1, 129.3, 128.5, 128.3, 128.2, 127.5, 111.1, 110.8, 100.2, 99.9, 44.4.

^{19}F NMR (373 MHz, $CDCl_3$): δ (ppm) -92.8.

IR (ATR) υ (cm^{-1}): 1768, 1692, 708, 648, 547.

HRMS (ESI) *m/z* calcd for $[M+H]^+$ $C_{15}H_{11}FNO_2^+$ 256.0777, found 256.0802.

29. methyl 1-benzyl-2,3-dioxoindoline-6-carboxylate (4i)

Reaction condition: The reaction was carried out with 0.045 g (0.2 mM) of **1o** and 0.322 g **DAIB**, under the irradiation of 8W blue LED for 12 h.

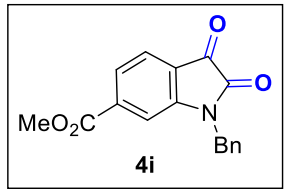

4i

Yield: 65%, 38 mg

R_f: 0.5; EtOAc/Petroleum ether = 1/9

Nature: Yellow solid

MP: 212–215 °C

^{1}H NMR (400 MHz, $CDCl_3$): δ (ppm) 7.77 (d, J = 7.6 Hz, 1H), 7.67 (d, J = 7.6 Hz, 1H), 7.45 (s, 1H), 7.36 (d, J = 4.4 Hz, 4H), 7.32 (t, J = 4.2 Hz, 1H), 4.97 (s, 2H), 3.92 (s, 3H).

^{13}C{^{1}H} NMR (400 MHz, $CDCl_3$): δ (ppm) 183.2, 165.3, 157.8, 150.6, 138.6, 134.2, 129.3, 128.5, 127.7, 125.41, 125.36, 120.4, 111.6, 53.0, 44.3.

IR (ATR) υ (cm^{-1}): 1759, 1708, 1642, 655, 513.

HRMS (ESI) *m/z* calcd for $[M+H]^+$ $C_{17}H_{14}NO_4^+$ 296.0923, found 296.0950.

---

30. 1-benzyl-7-methylindoline-2,3-dione (4j)

Reaction condition: The reaction was carried out with 0.044 g (0.2 mM) of **1s** and 0.322 g **DAIB**, under the irradiation of 8W blue LED for 12 h.

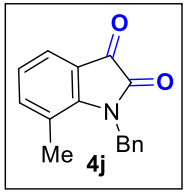

Yield: 79%, 40 mg

R_f: 0.5; EtOAc/Petroleum ether = 1/9

Nature: Yellow solid

MP: 140–142 °C

^{1}H NMR (400 MHz, $CDCl_3$): δ (ppm) 7.51 (d, J = 7.2 Hz, 1H), 7.33 (t, J = 7.0 Hz, 2H), 7.27 (t, J = 8.0 Hz, 2H), 7.20 (d, J = 7.2 Hz, 2H), 7.01 (t, J = 7.6 Hz, 1H), 5.19 (s, 2H), 2.25 (s, 3H).

^{13}C{^{1}H} NMR (400 MHz, $CDCl_3$): δ (ppm) 183.8, 159.7, 148.7, 142.7, 136.3, 129.2, 127.8, 125.7, 124.2, 123.7, 122.2, 118.9, 45.4, 18.7.

IR (ATR) υ (cm^{-1}): 1754,1738, 1445, 1395, 1108, 914, 754, 569.

HRMS (ESI) *m/z* calcd for $[M+H]^+$ $C_{16}H_{14}NO_2^+$ 252.1025, found 252.1052.

---

32. Synthesis of 1-benzyl-5-(4-cyanophenyl)-1*H*-indol-3-yl acetate (5): An oven dried round bottom flask was equipped with a rubber septum and magnetic stir bar and charged with **2l** (0.020 g, 0.05 mmol), 4-cyanobenzeneboronic acid (0.015 g, 2.0 equiv.), triphenylphosphine (0.001 g, 6.0 mol%), potassium carbonate (0.042 g, 0.30 mmol, 6.0 equiv.) and palladium acetate (0.001 g, 3.0 mol%). The reaction vessel was evacuated and backfilled with argon. 2.0 mL 1,4-dioxane was added to the reaction mixture under argon atmosphere and stirred for 8 hours at 110°C. After completion, the reaction mixture was diluted with ethyl acetate (10 mL) and washed with water for three times (3×10 mL). The organic layer was separated and collected over Na_2SO_4 and evaporated under reduced pressure. The crude product was purified *via* silica gel and the pure product **4** was obtained as white solid.

1-benzyl-5-(4-cyanophenyl)-1*H*-indol-3-yl acetate (5)

Yield: 79%, 15 mg

R_f: 0.5; EtOAc/Petroleum ether = 1/9

Nature: White solid

MP: 205–207 °C

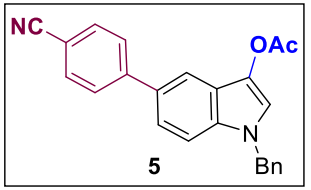

^{1}H NMR (400 MHz, $CDCl_3$): δ (ppm) 7.79 (s, 1H), 7.71 (dd, *J* = 13.2 Hz, 8.4 Hz, 4H), 7.42 (d, *J* = 10.0 Hz, 2H), 7.35-7.28 (m, 4H), 7.15 (d, *J* = 6.8 Hz, 2H), 5.30 (s, 2H), 2.38 (s, 3H).

^{13}C{^{1}H} NMR (400 MHz, $CDCl_3$): δ (ppm) 168.6, 146.8, 137.0, 133.5, 132.6, 131.1, 130.3, 129.0, 128.0, 127.9, 126.9, 122.2, 121.2, 119.4, 118.6, 116.8, 110.6, 110.0, 50.5, 21.1.

IR (ATR) υ (cm^{-1}): 2242, 1757, 1367, 1122, 817, 609, 575.

HRMS (ESI) *m/z* calcd for $[M+H]^+$ $C_{24}H_{19}N_2O_2^+$ 367.1441, found 367.1718.

33. Synthesis of 1-benzyl-6-phenyl-1*H*-indol-3-yl acetate (6): An oven dried round bottom flask was equipped with a rubber septum and magnetic stir bar and charged with **2m** (0.020 g, 0.06 mmol), benzeneboronic acid (0.014 g, 2.0 equiv.), triphenylphosphine (0.001 g, 6.0 mol%),

potassium carbonate (0.048 g, 0.35 mmol, 6.0 equiv.) and palladium acetate (0.001 g, 3.0 mol%). The reaction vessel was evacuated and backfilled with argon. 2.0 mL 1,4-dioxane was added to the reaction mixture under argon atmosphere and stirred for 8 hours at 110°C. After completion, the reaction mixture was diluted with ethyl acetate (10 mL) and washed with water for three times (3×10 mL). The organic layer was separated and collected over Na_2SO_4 and evaporated under reduced pressure. The crude product was purified *via* silica gel and the pure product **5** was obtained as white solid.

1-benzyl-6-phenyl-1*H*-indol-3-yl acetate (6)

Yield: 81%, 16 mg

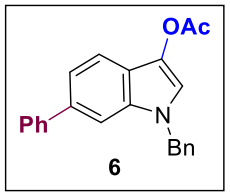

6

R_f: 0.6; EtOAc/Petroleum ether = 1/9

Nature: Grey solid

MP: 212–213 °C

^{1}H NMR (400 MHz, $CDCl_3$): δ (ppm) 7.63 (q, J = 8.0 Hz, 3H), 7.47-7.40 (m, 4H), 7.37 (s, 1H), 7.33-7.28 (m, 4H), 7.17 (d, J = 6.8 Hz, 2H), 5.33 (s, 2H), 2.38 (s, 3H).

^{13}C{^{1}H} NMR (400 MHz, $CDCl_3$): δ (ppm) 168.7, 137.2, 136.3, 134.1, 129.0, 128.8, 127.9, 127.6, 127.0, 119.84, 119.78, 118.1, 118.0, 108.3, 50.2, 21.1.

IR (ATR) υ (cm^{-1}): 1751, 1421, 1306, 1125, 775, 666.

HRMS (ESI) *m/z* calcd for $[M+ H]^+$ $C_{23}H_{20}NO_2^+$ 342.1494, found 342.1519.

34. methyl (*E*)-3-(3-acetoxy-1-benzyl-1*H*-indol-5-yl)acrylate (7). An oven dried round-bottom flak was equipped with a rubber septum and magnetic bar and charged with **2l** (0.023 g, 0.06 mmol), potassium carbonate (0.044 g, 0.35 mmol, 5.0 equiv.) and palladium acetate (0.001 g, 5.0 mol%). The reaction vessel was evacuated and backfilled with argon. Finally, methyl acrylate (0.011 g, 2.0 equiv.) and 2.0 mL dioxane were added to the reaction mixture and stirred for 10 h at 110 °C. After completion, the reaction mixture was diluted with 10 mL ethyl acetate and

washed with water (3×10 mL) for three times. The organic layer was separated and collected over Na_2SO_4 and evaporated under reduced pressure. The crude product was purified *via* silica gel and the pure product **5** was obtained as white solid.

methyl (*E*)-3-(3-acetoxy-1-benzyl-1*H*-indol-5-yl)acrylate (7)

Yield: 51%, 11 mg

R_f: 0.6; EtOAc/Petroleum ether = 1/9

Nature: Off-white solid

MP: 189–191 °C

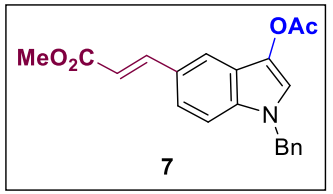

7

^{1}H NMR (400 MHz, $CDCl_3$): δ (ppm) 7.82 (d, *J* = 16.0 Hz, 1H), 7.74 (d, *J* = 1.2 Hz, 1H), 7.40 (dd, *J* = 8.8 Hz, 1.6 Hz, 1H), 7.37 (s, 1H), 7.32-7.28 (m, 3H), 7.22 (d, *J* = 10.8 Hz, 1H), 7.12 (d, *J* = 6.8 Hz, 2H), 6.41 (d, *J* = 16.0 Hz, 1H), 5.27 (s, 2H), 3.80 (s, 3H), 2.37 (s, 3H).

^{13}C{^{1}H} NMR (400 MHz, $CDCl_3$): δ (ppm) 168.5, 168.0, 146.3, 136.8, 134.4, 130.5, 129.0, 128.1, 127.0, 126.5, 122.3, 120.9, 119.4, 118.5, 115.2, 110.4, 51.7, 50.5, 21.1.

IR (ATR) υ (cm^{-1}): 1762, 1737, 1652, 1208, 1175, 951, 779, 615, 507.

HRMS (ESI) *m/z* calcd for $[M+H]^+$ $C_{21}H_{20}NO_4^+$ 350.1387, found 350.1383.

11.2 NMR spectra (^{1}H and ^{13}C spectra)

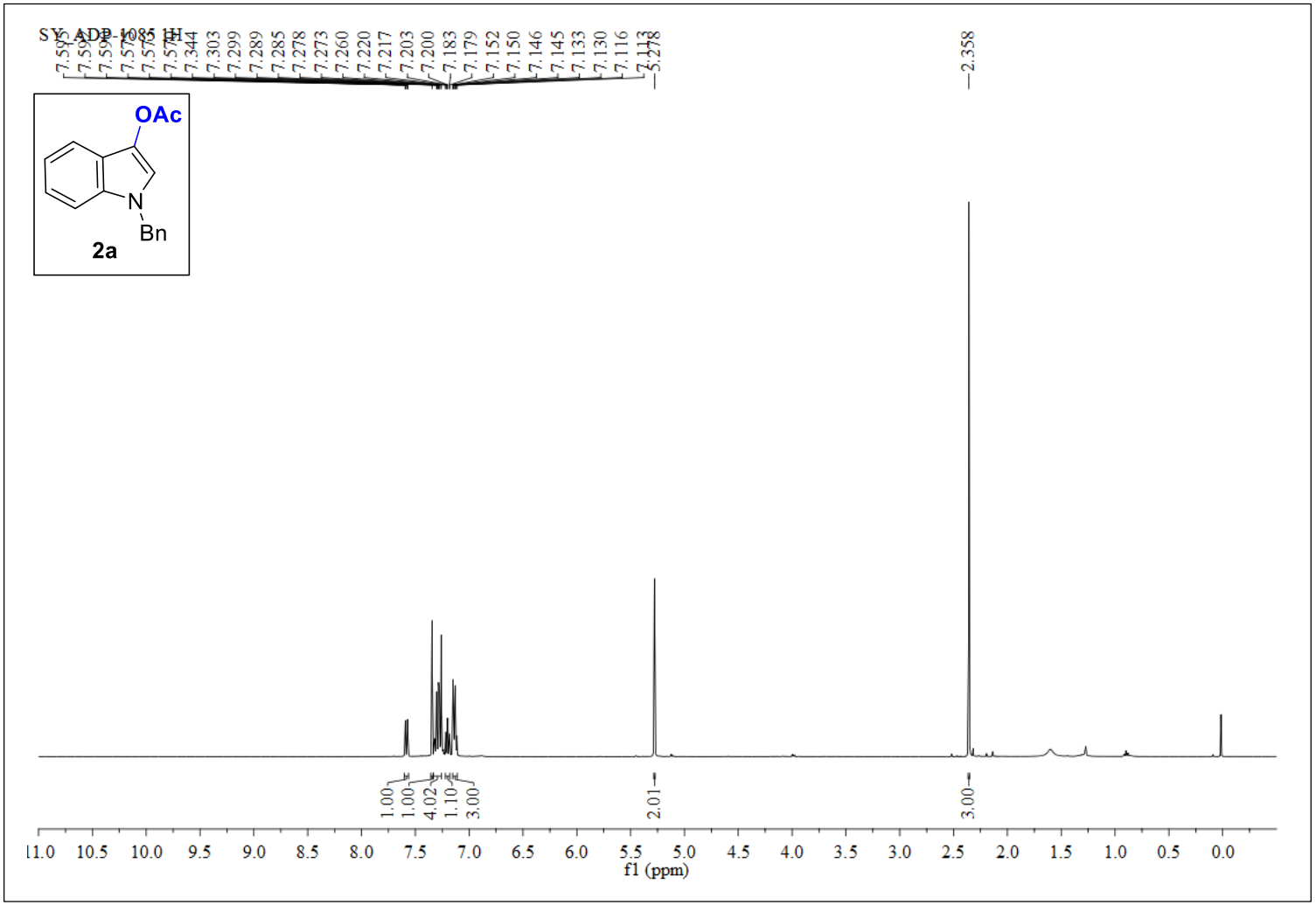

Figure S22. ^{1}H NMR (400 MHz, $CDCl_3$) of **2a**.

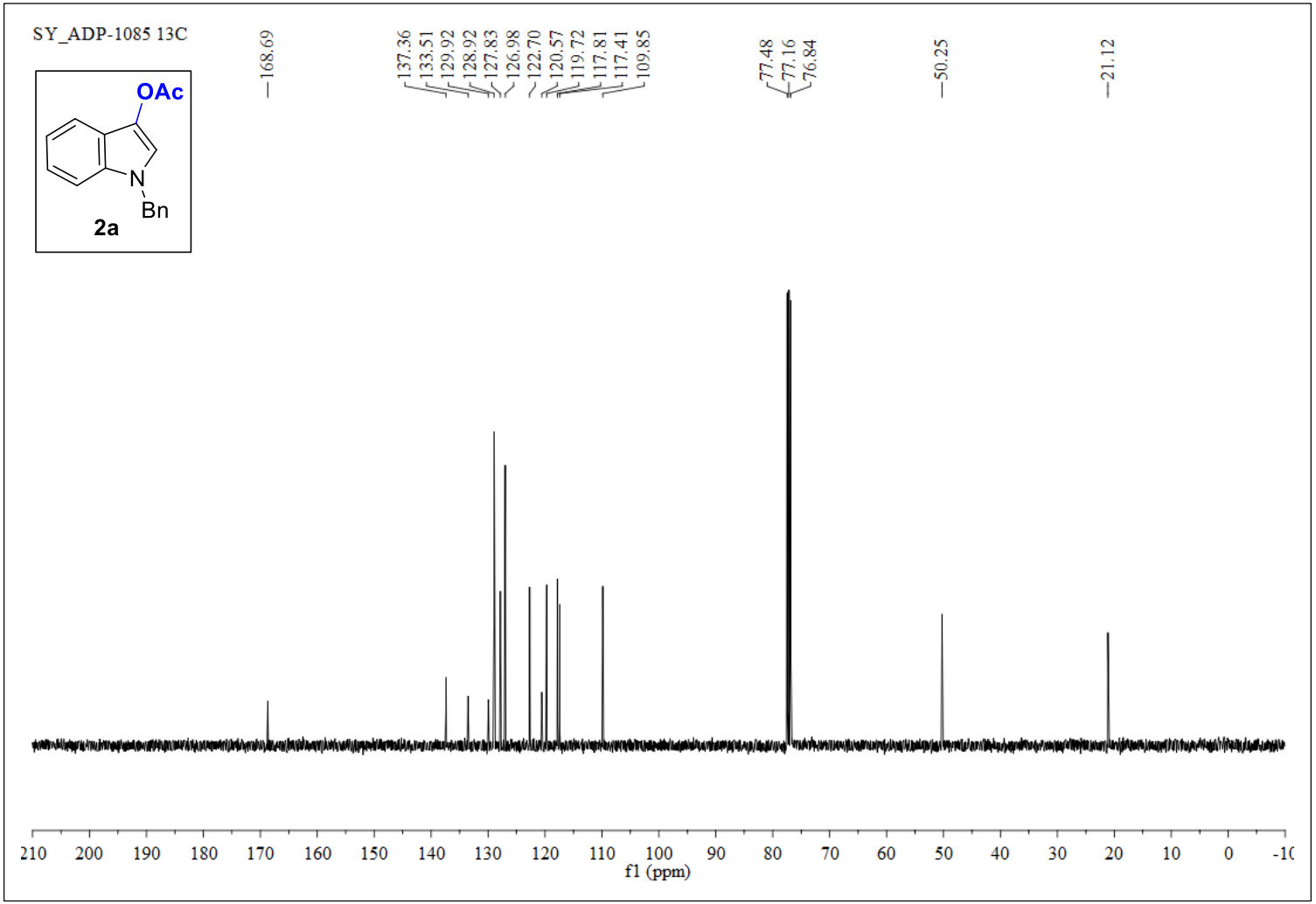

Figure S23. $^{13}C\{^{1}H\}$ NMR (100 MHz, $CDCl_3$) of **2a**.

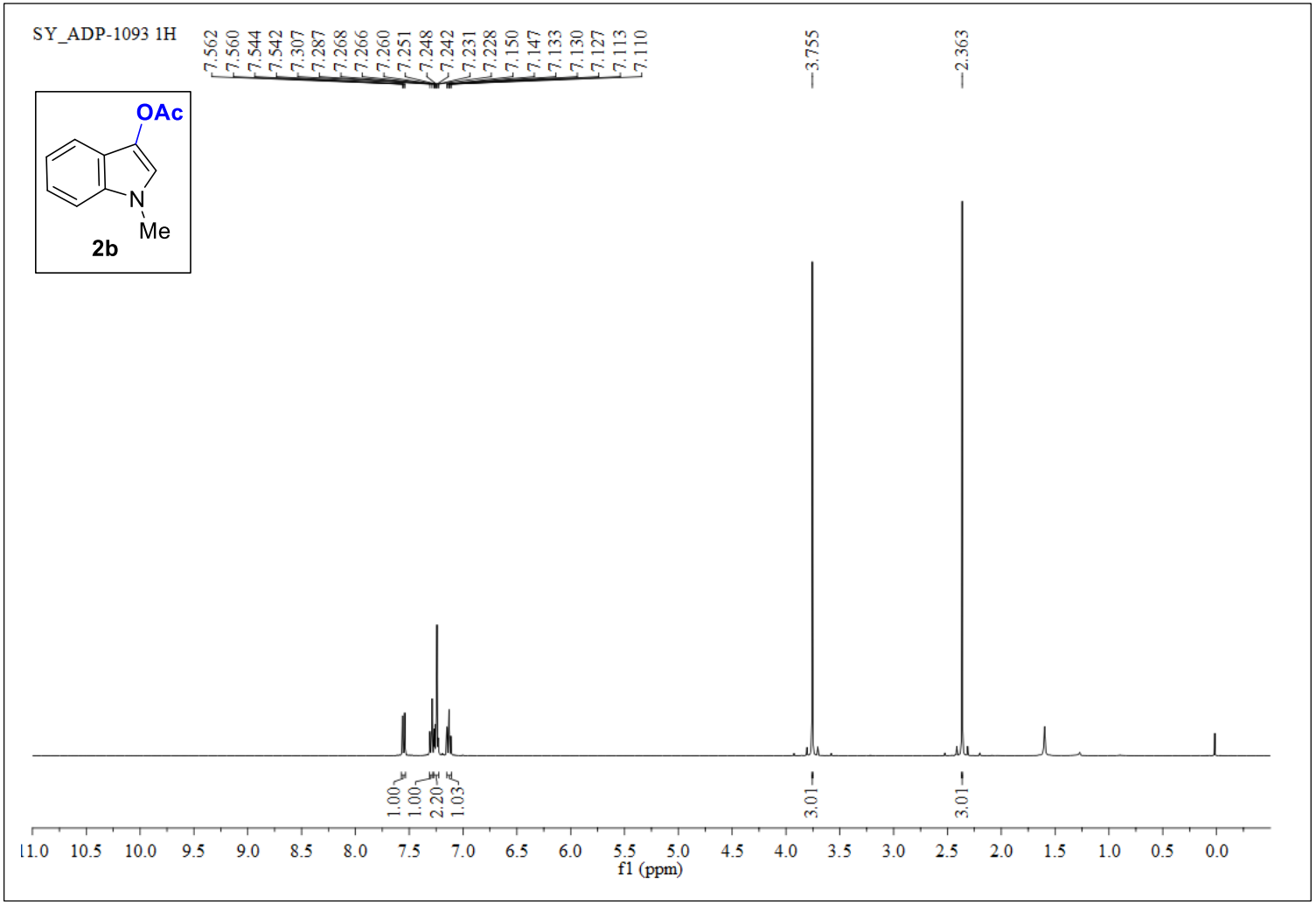

Figure S24. ^{1}H NMR (400 MHz, $CDCl_3$) of **2b**.

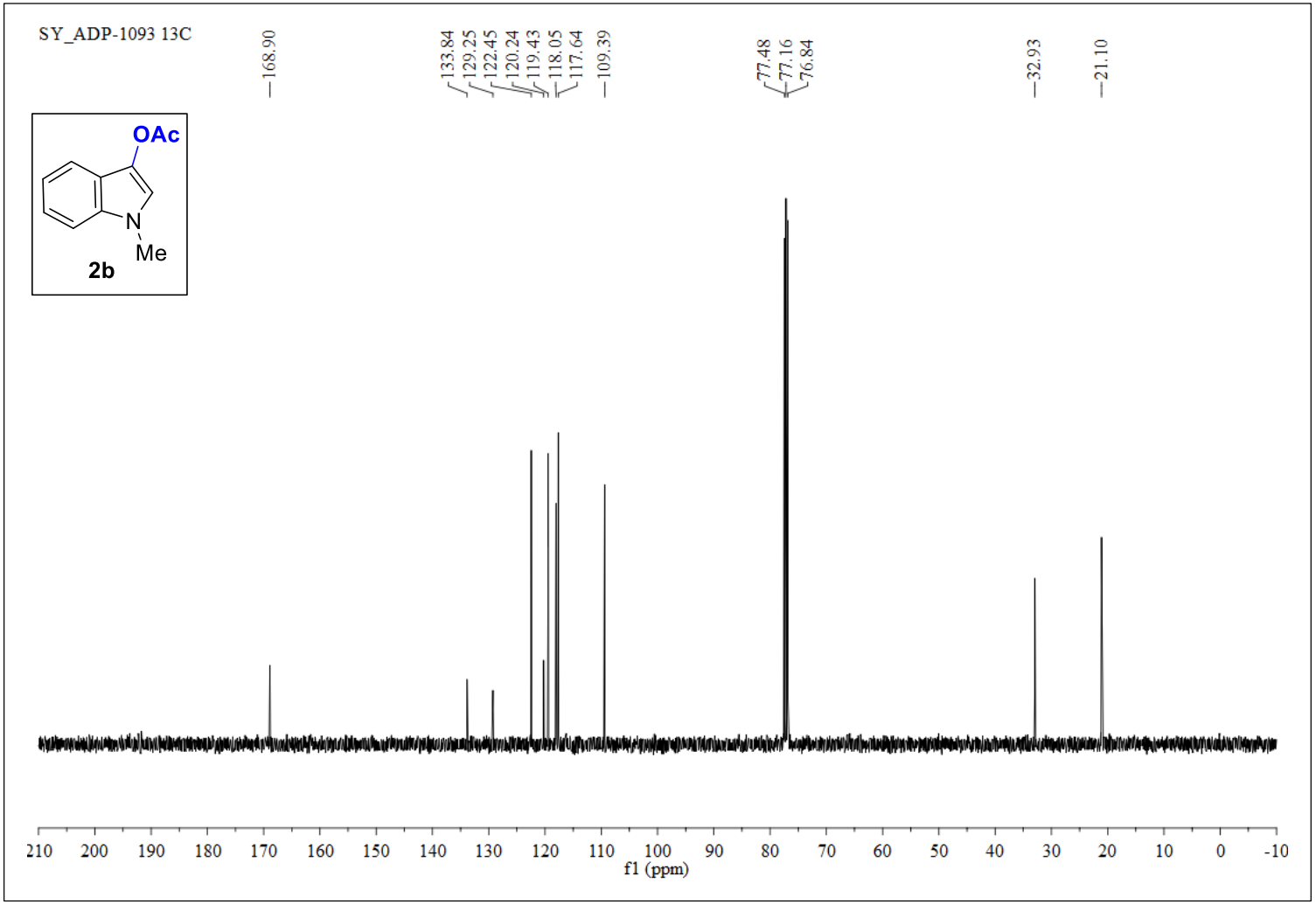

Figure S25. $^{13}C\{^{1}H\}$ NMR (100 MHz, $CDCl_3$) of **2b**.

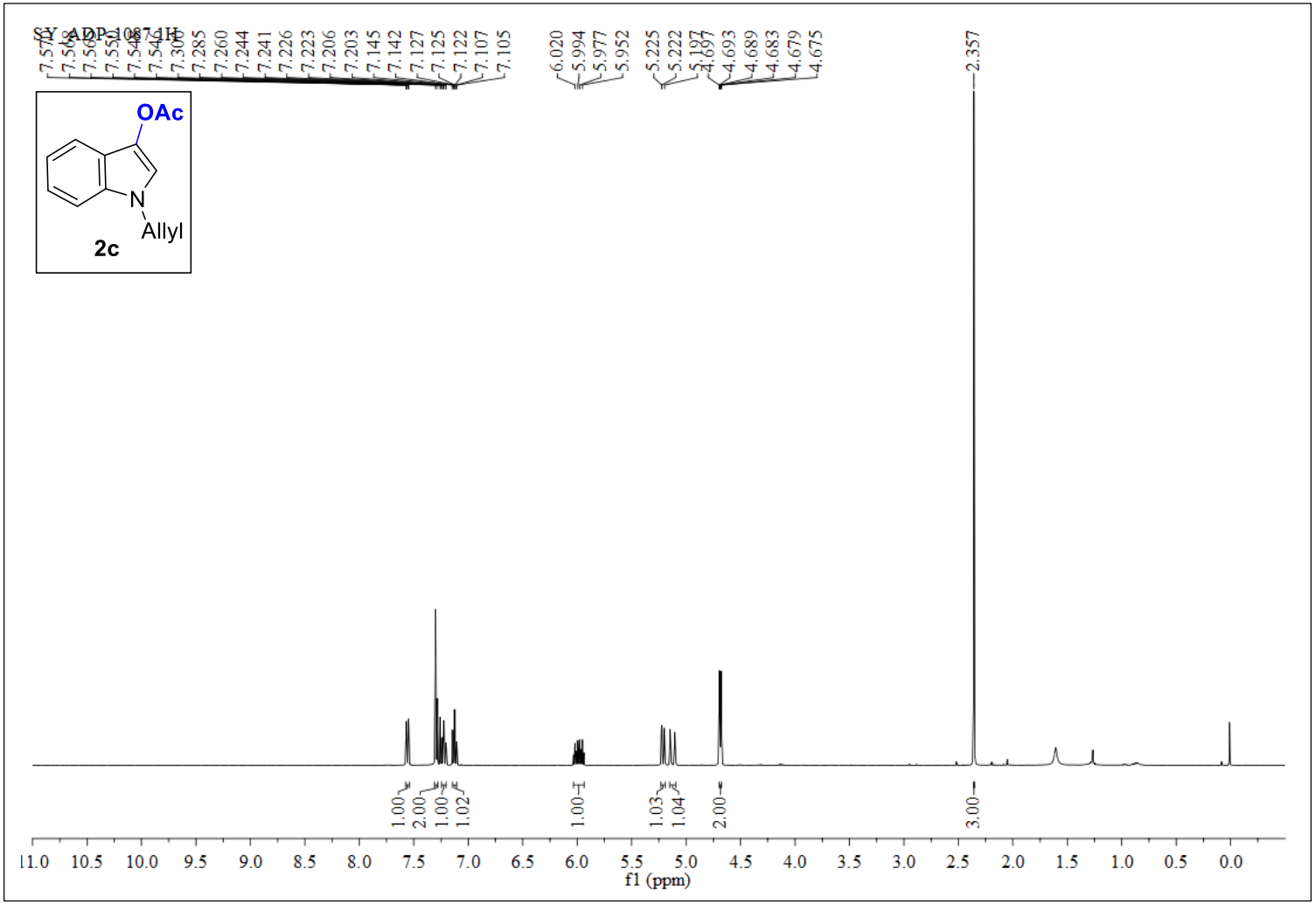

Figure S26. ^{1}H NMR (400 MHz, $CDCl_3$) of **2c**.

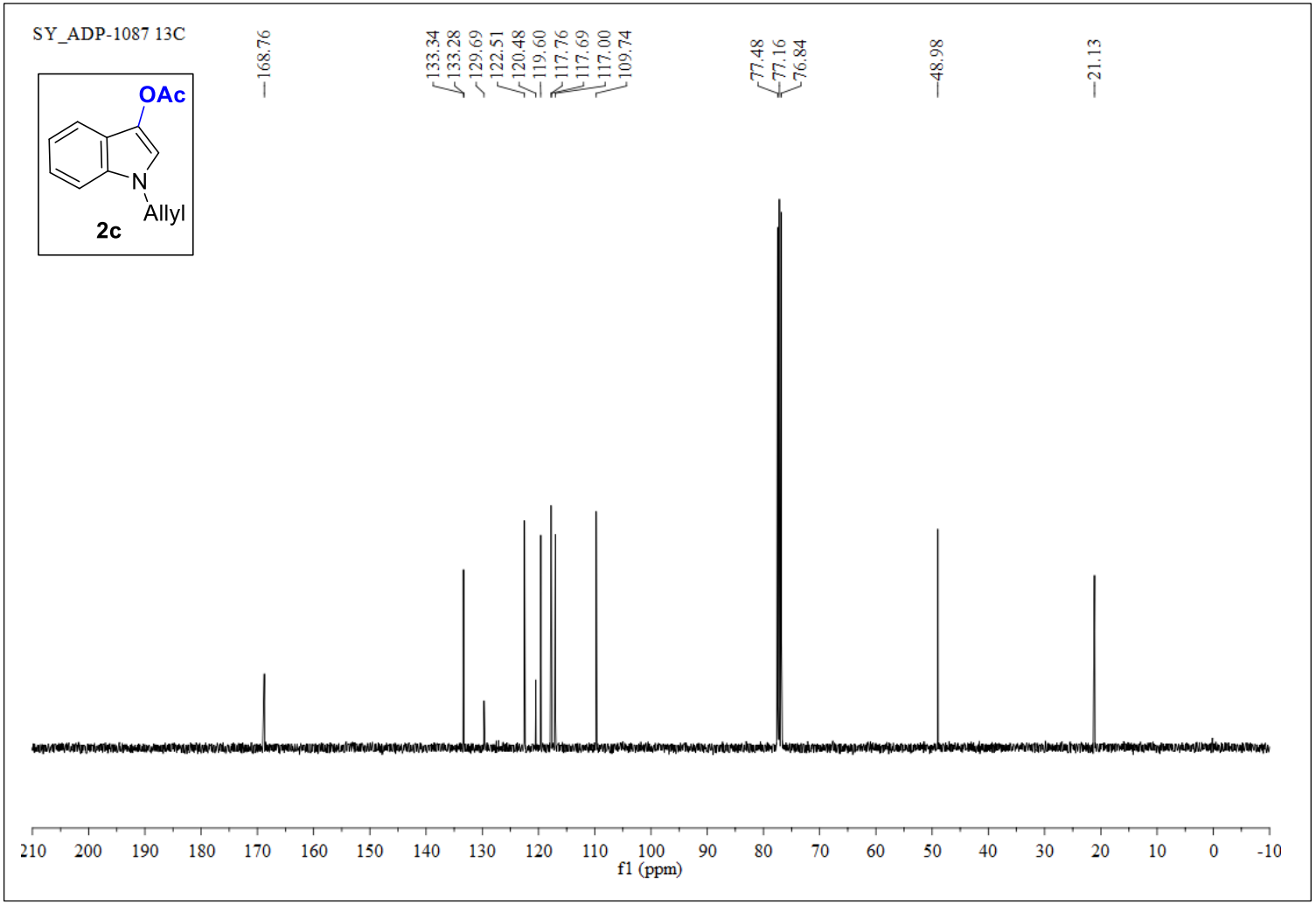

Figure S27. $^{13}C\{^{1}H\}$ NMR (100 MHz, $CDCl_3$) of **2c**.

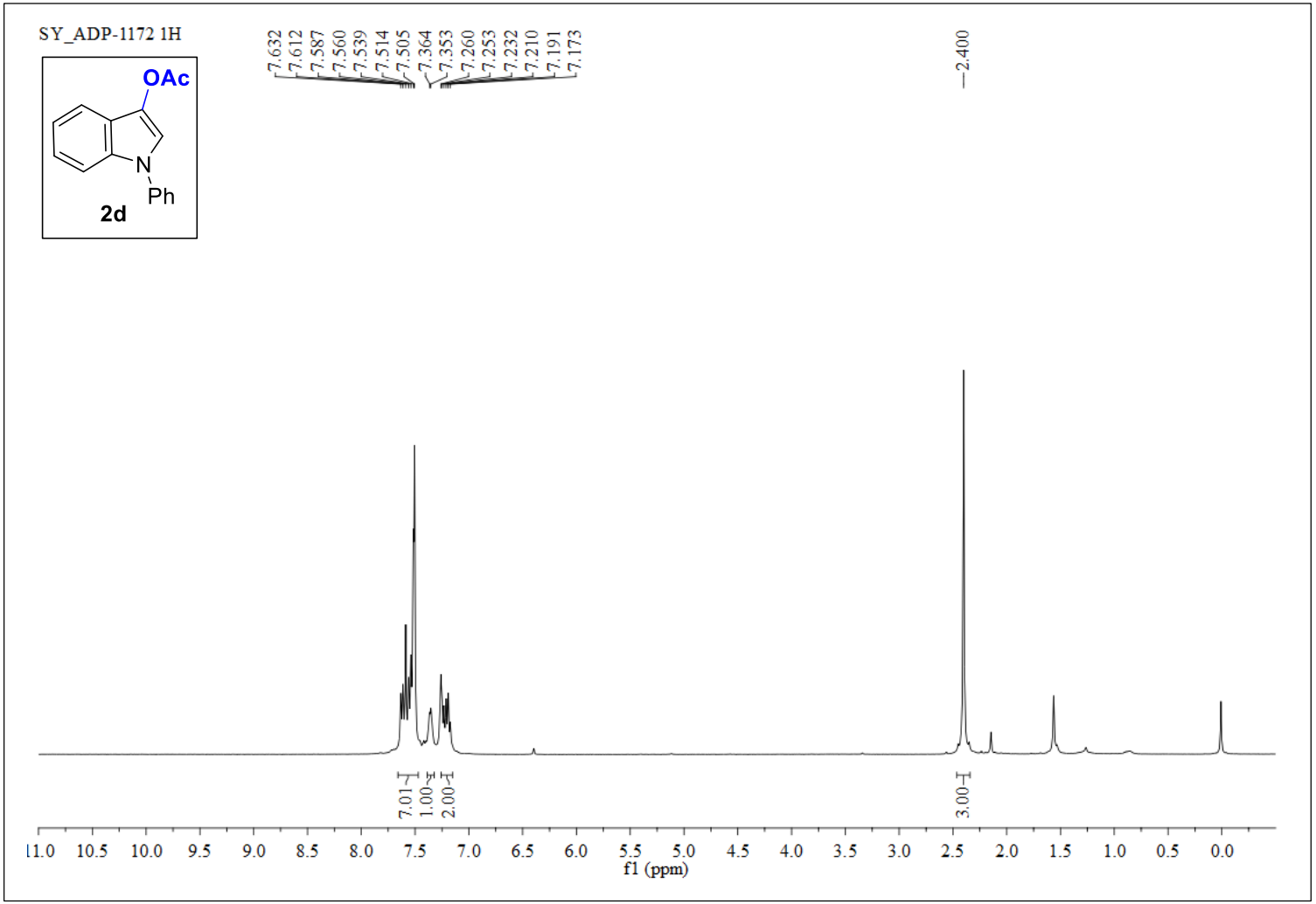

Figure S28. ^{1}H NMR (400 MHz, $CDCl_3$) of **2d**.

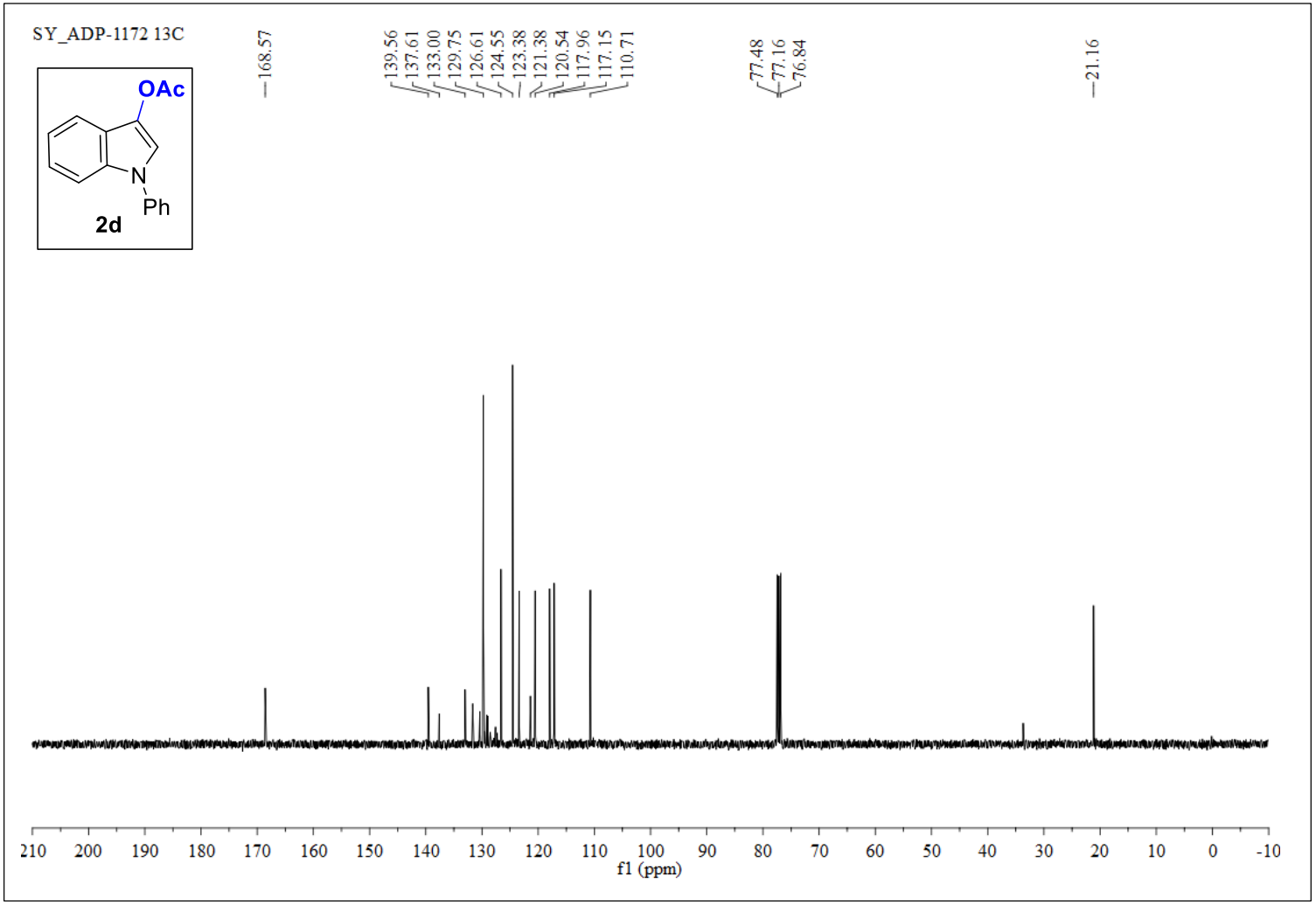

Figure S29. $^{13}C\{^{1}H\}$ NMR (100 MHz, $CDCl_3$) of **2d**.

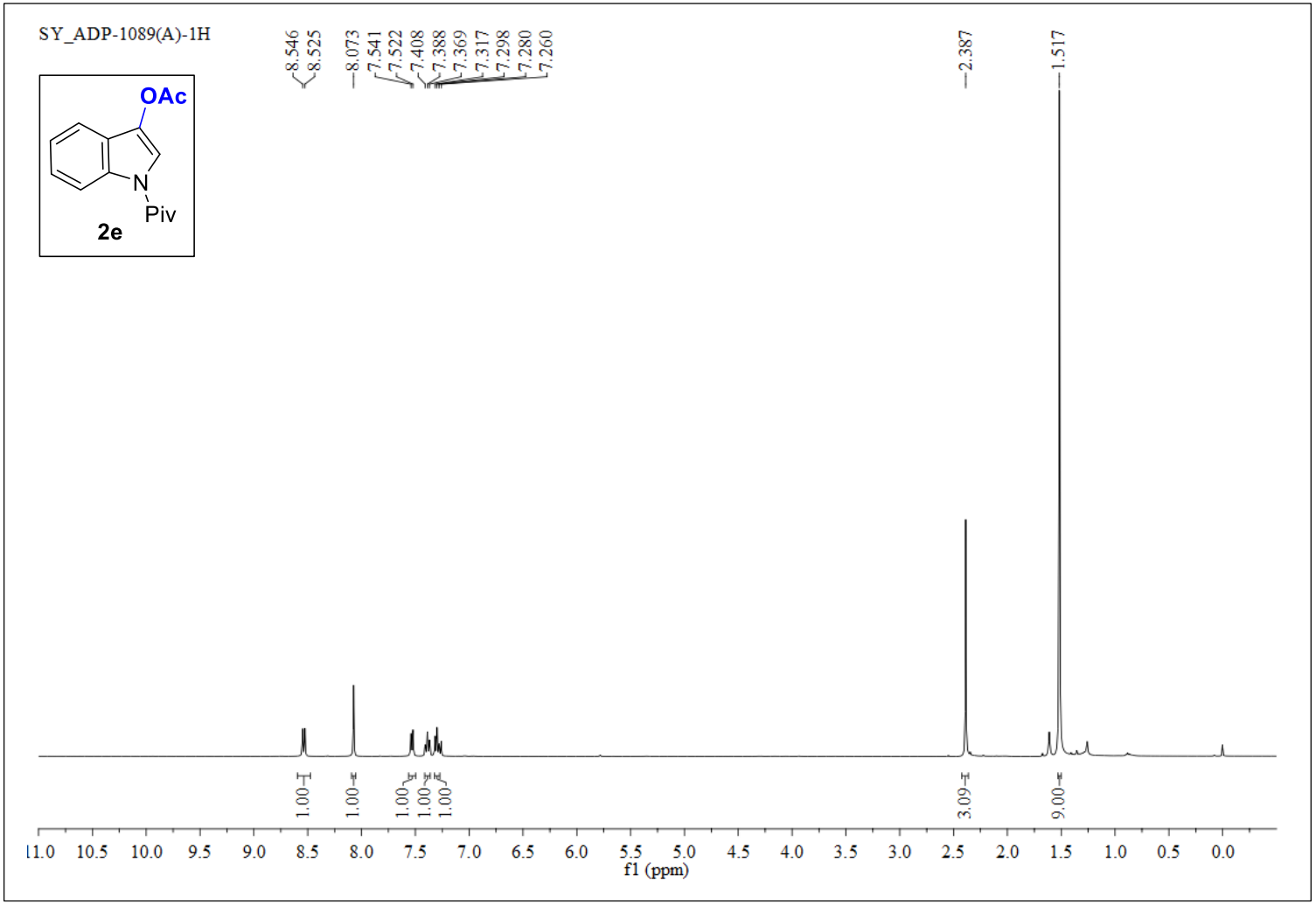

Figure S30. ^{1}H NMR (400 MHz, $CDCl_3$) of **2e**.

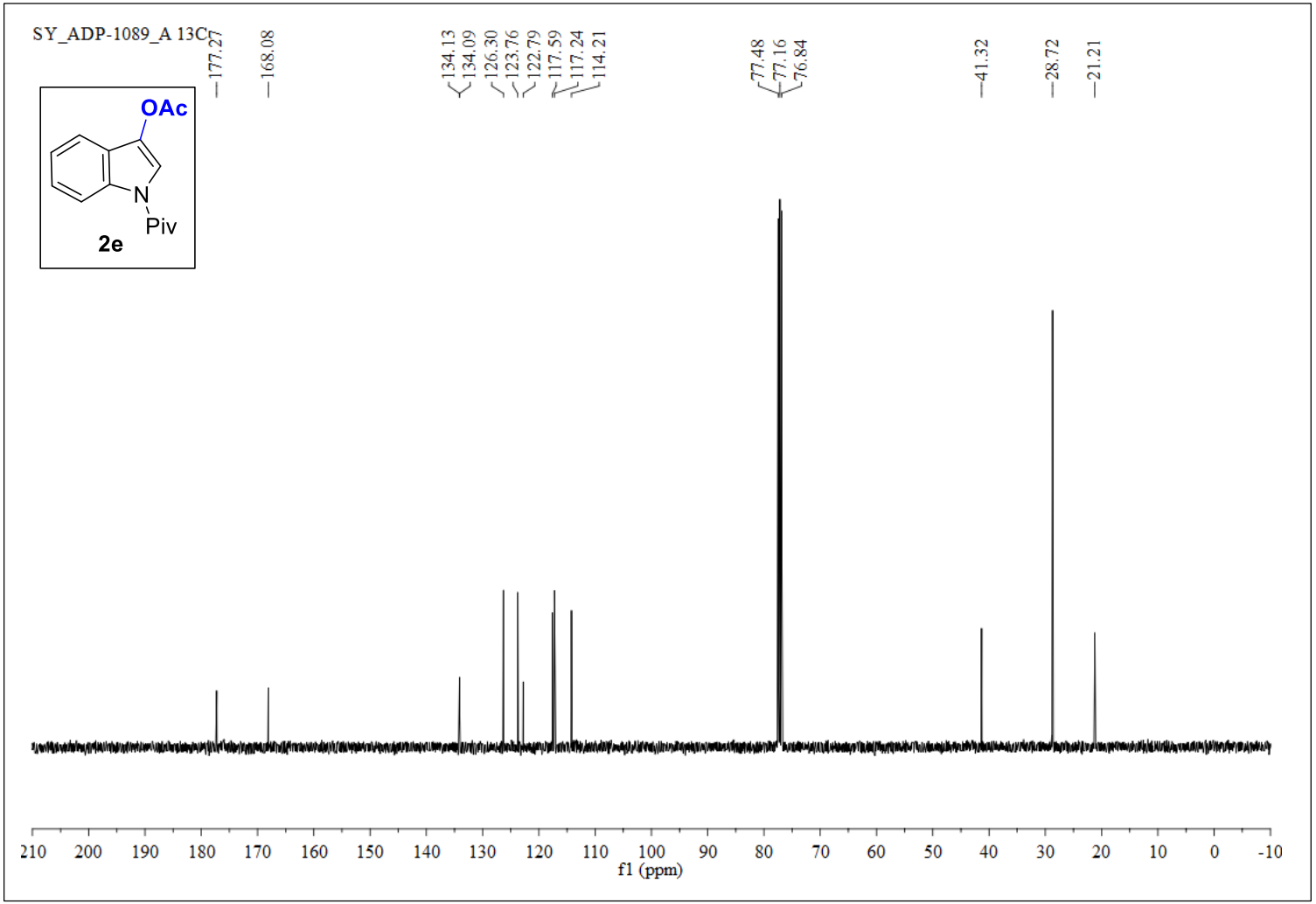

Figure S31. $^{13}C\{^{1}H\}$ NMR (100 MHz, $CDCl_3$) of **2e**.

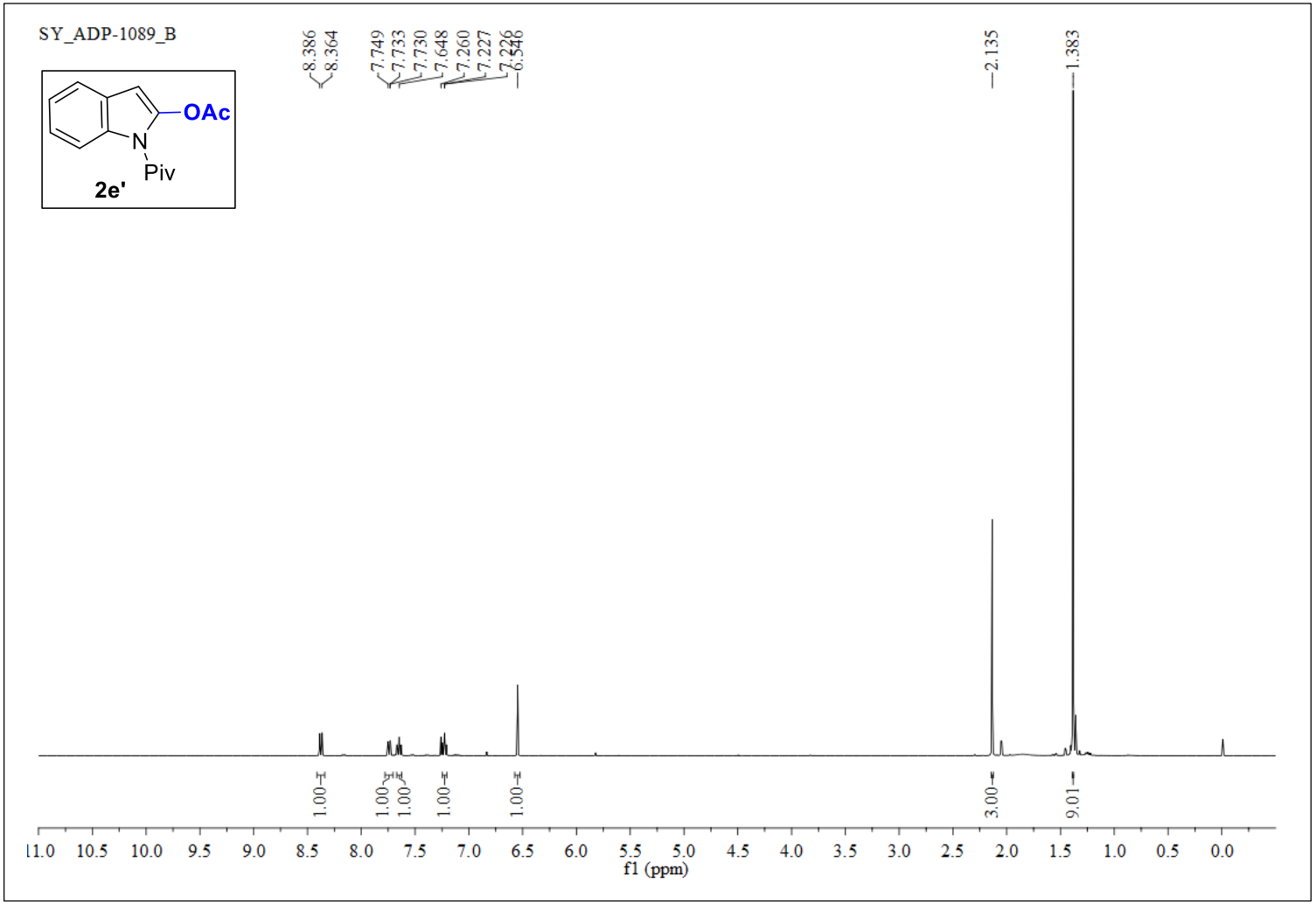

Figure S32. ^{1}H NMR (400 MHz, $CDCl_3$) of **2e′**.

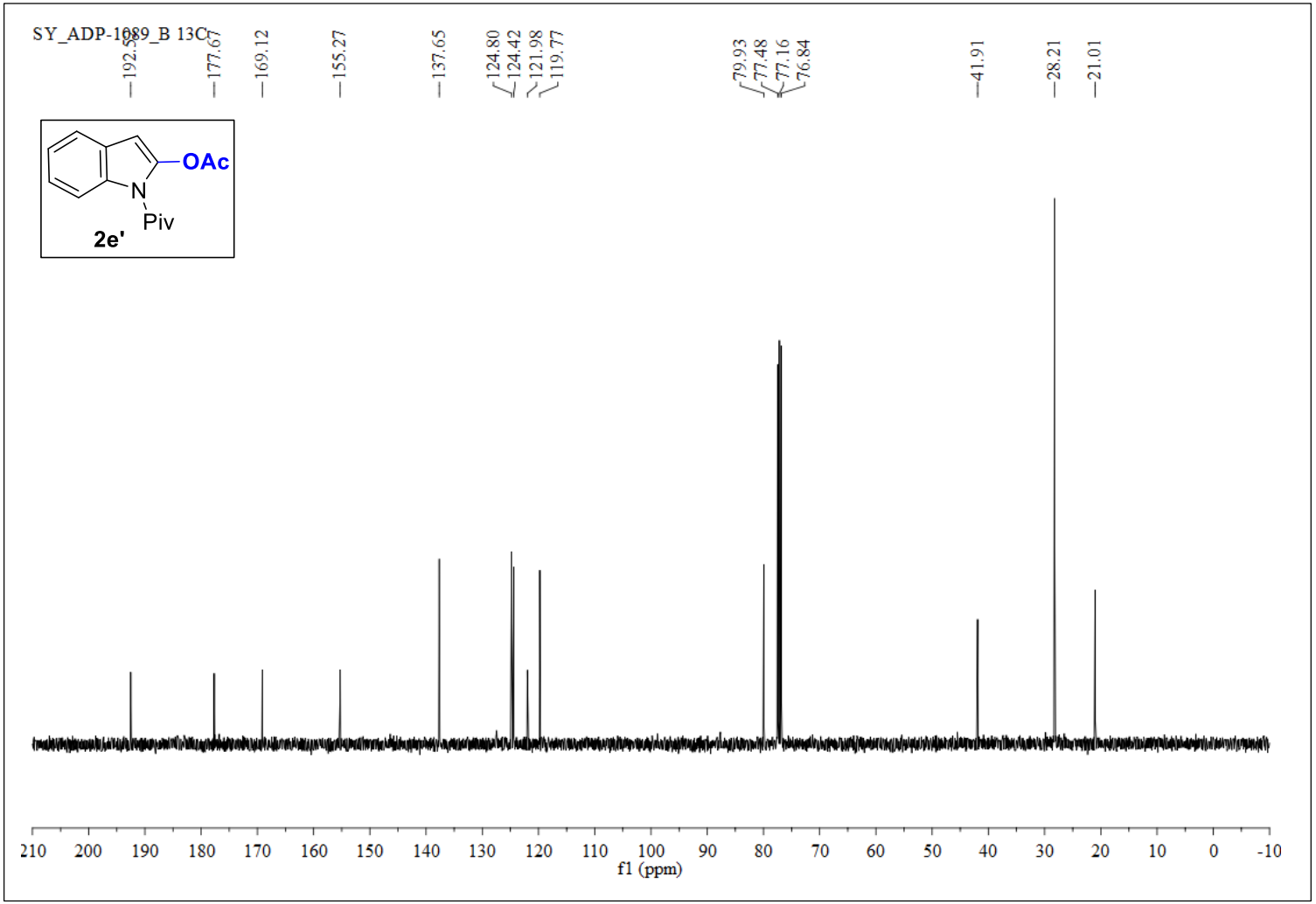

Figure S33. $^{13}C\{^{1}H\}$ NMR (100 MHz, $CDCl_3$) of **2e′**.

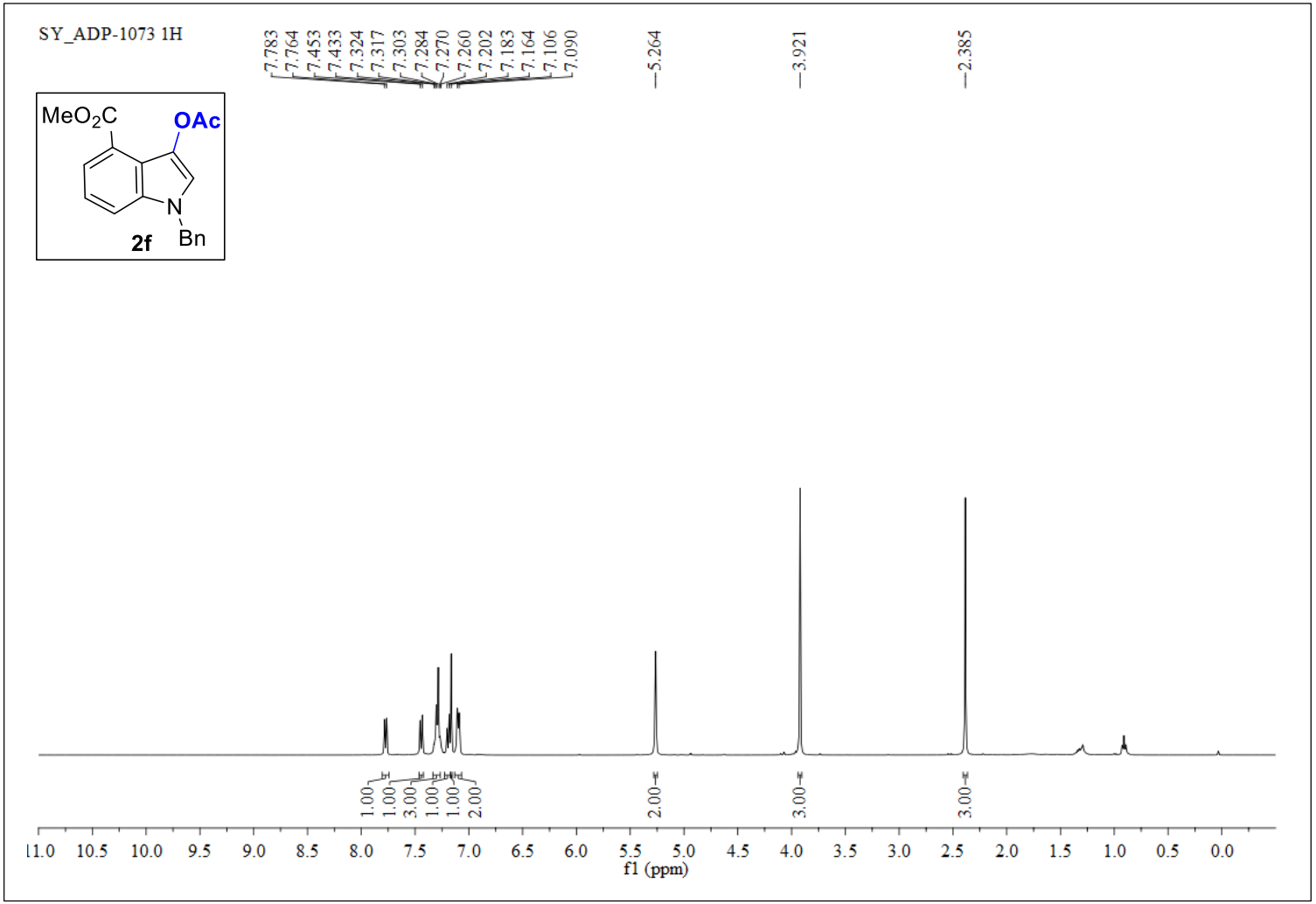

Figure S34. ^{1}H NMR (400 MHz, $CDCl_3$) of **2f**.

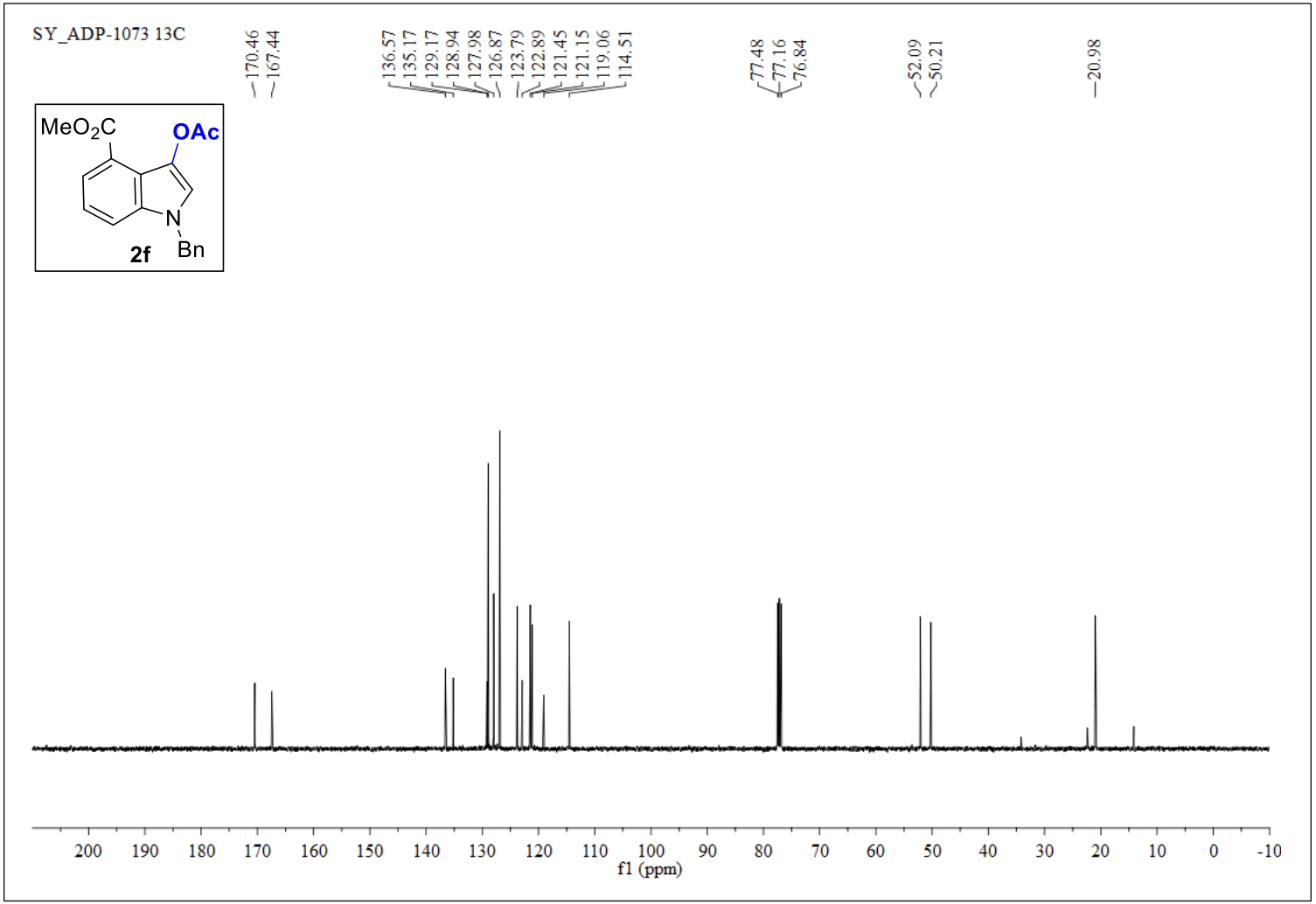

Figure S35. $^{13}C\{^{1}H\}$ NMR (100 MHz, $CDCl_3$) of **2f**.

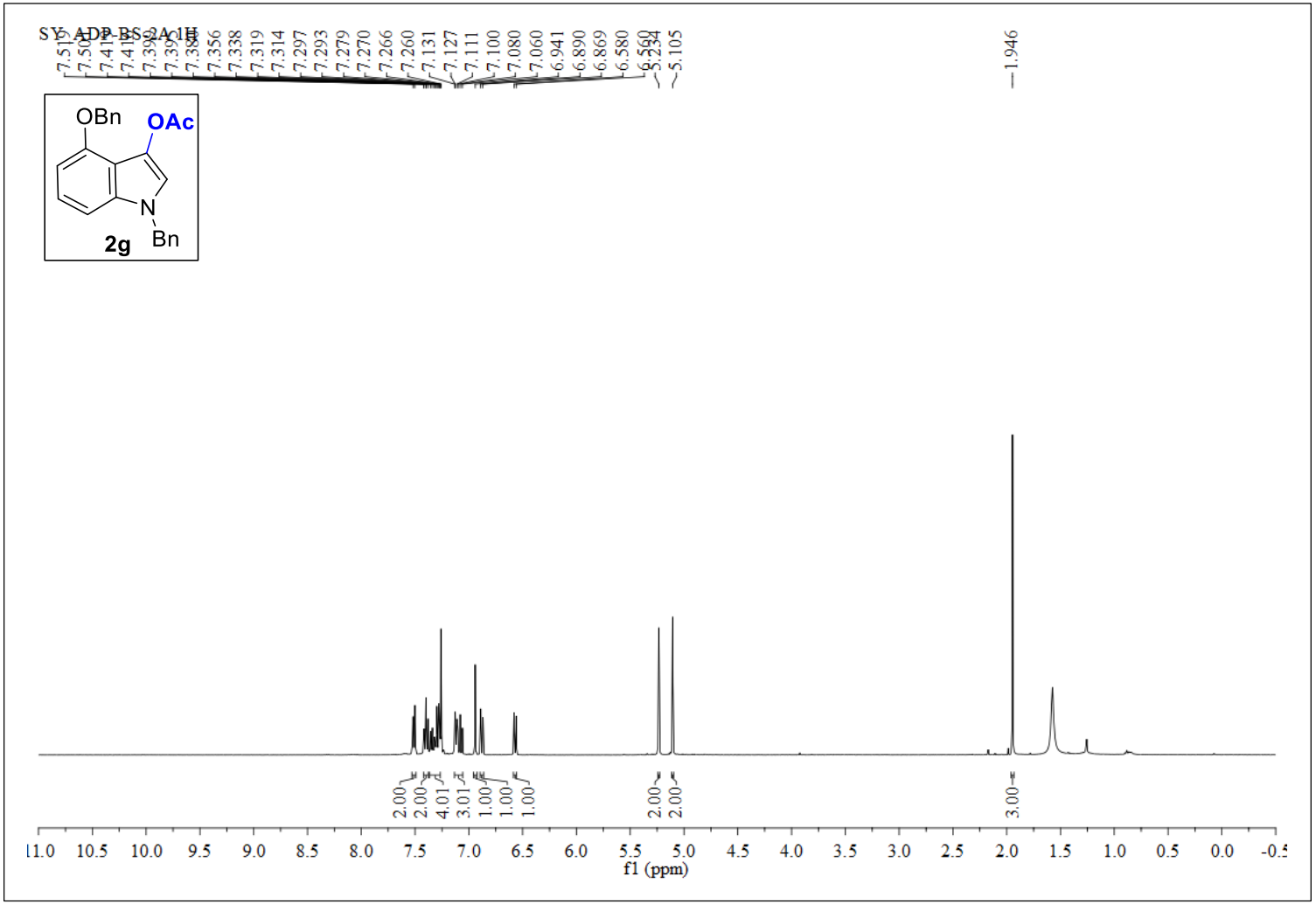

Figure S36. ^{1}H NMR (400 MHz, $CDCl_3$) of **2g**.

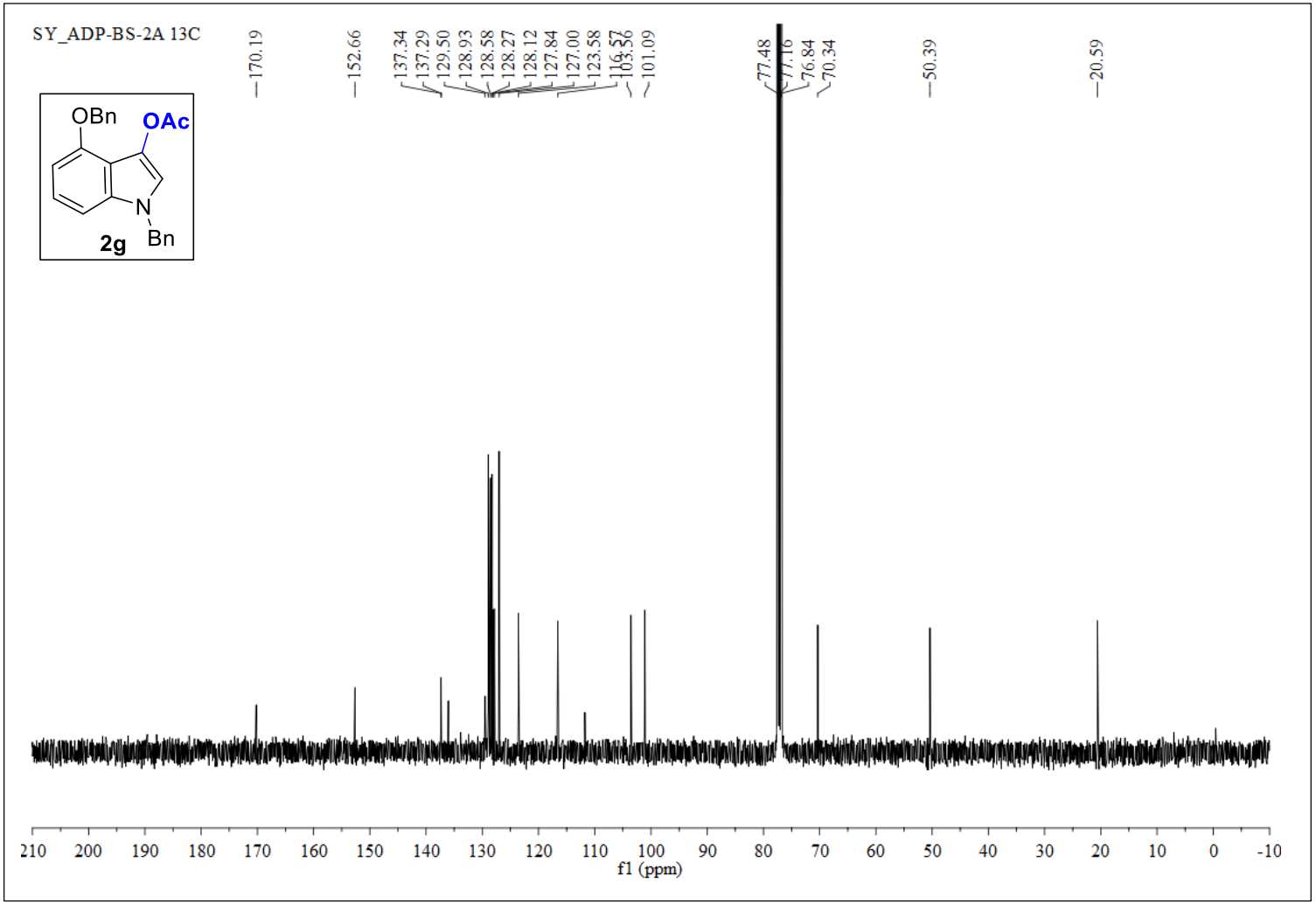

Figure S37. $^{13}C\{^{1}H\}$ NMR (100 MHz, $CDCl_3$) of **2g**.

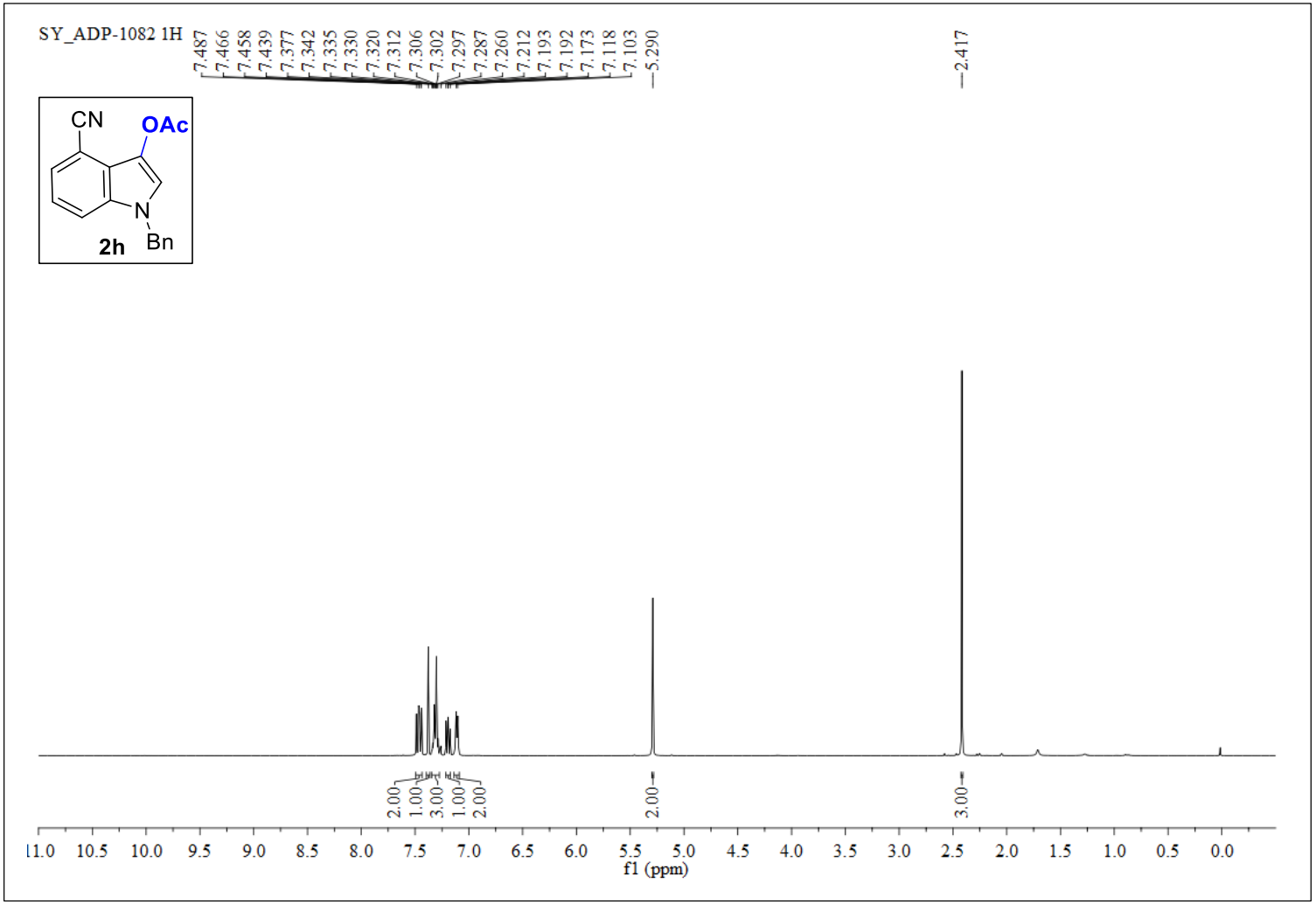

Figure S38. ^{1}H NMR (400 MHz, $CDCl_3$) of **2h**.

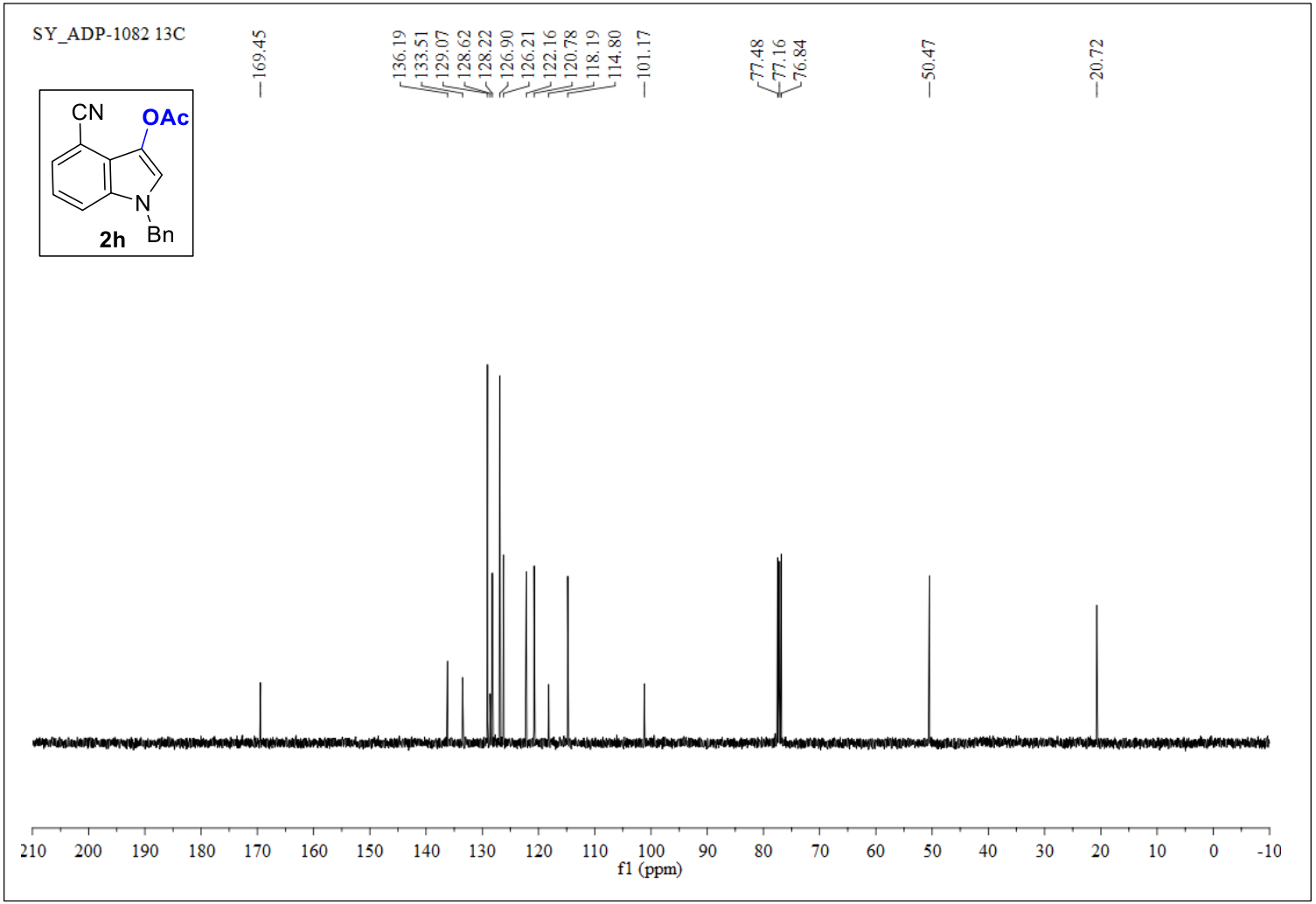

Figure S39. $^{13}C\{^{1}H\}$ NMR (100 MHz, $CDCl_3$) of **2h**.

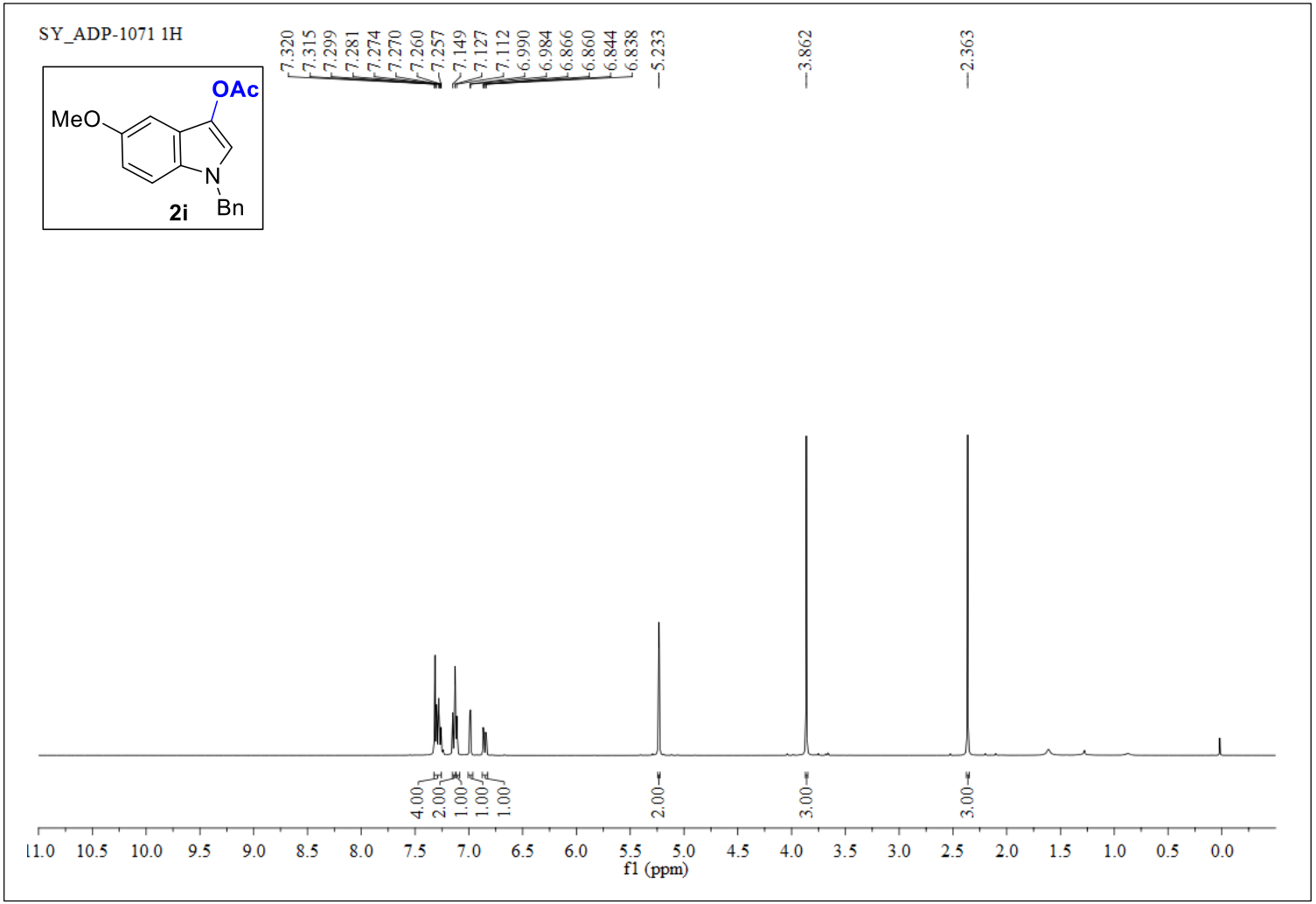

Figure S40. ^{1}H NMR (400 MHz, $CDCl_3$) of **2i**.

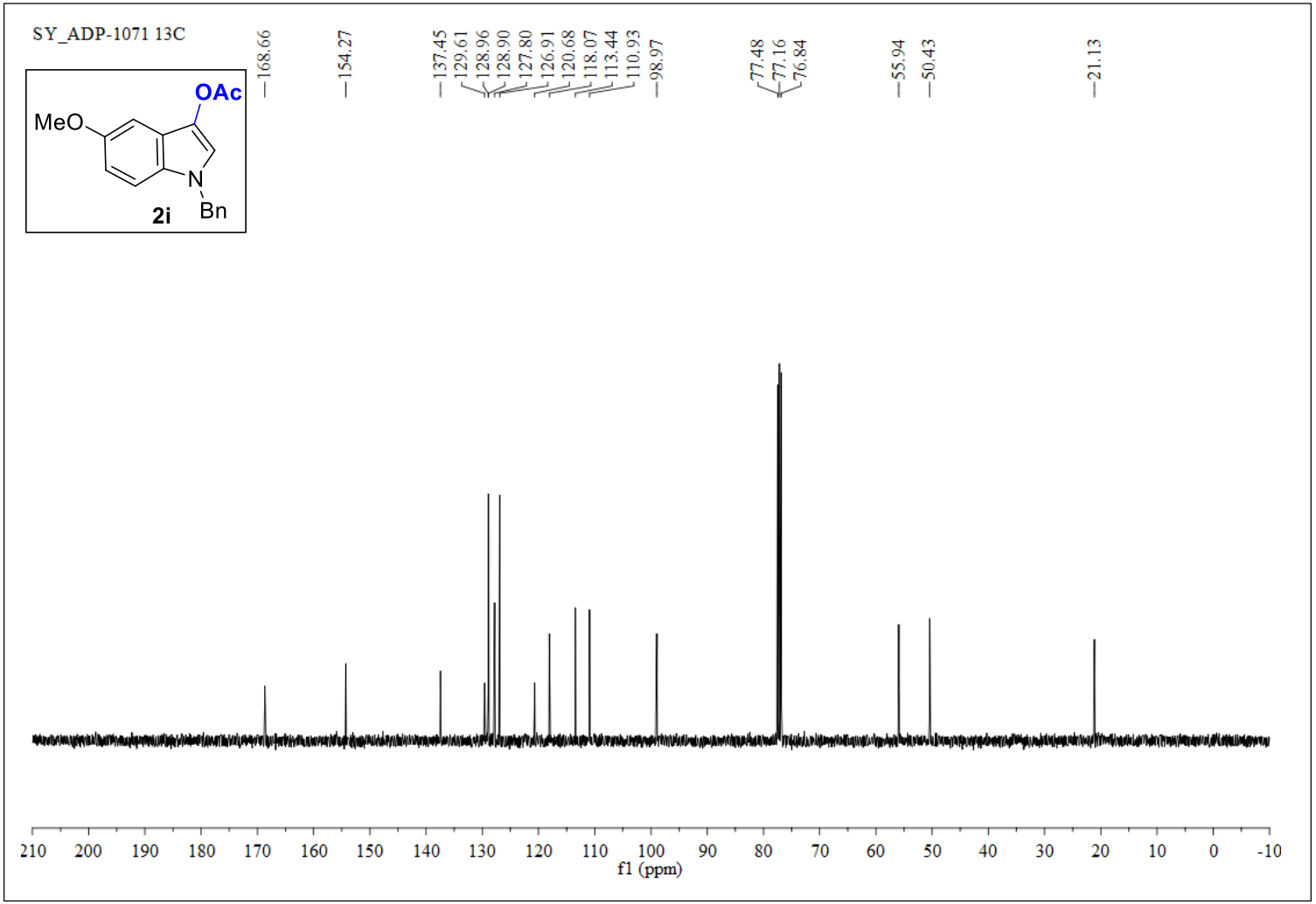

Figure S41. $^{13}C\{^{1}H\}$ NMR (100 MHz, $CDCl_3$) of **2i**.

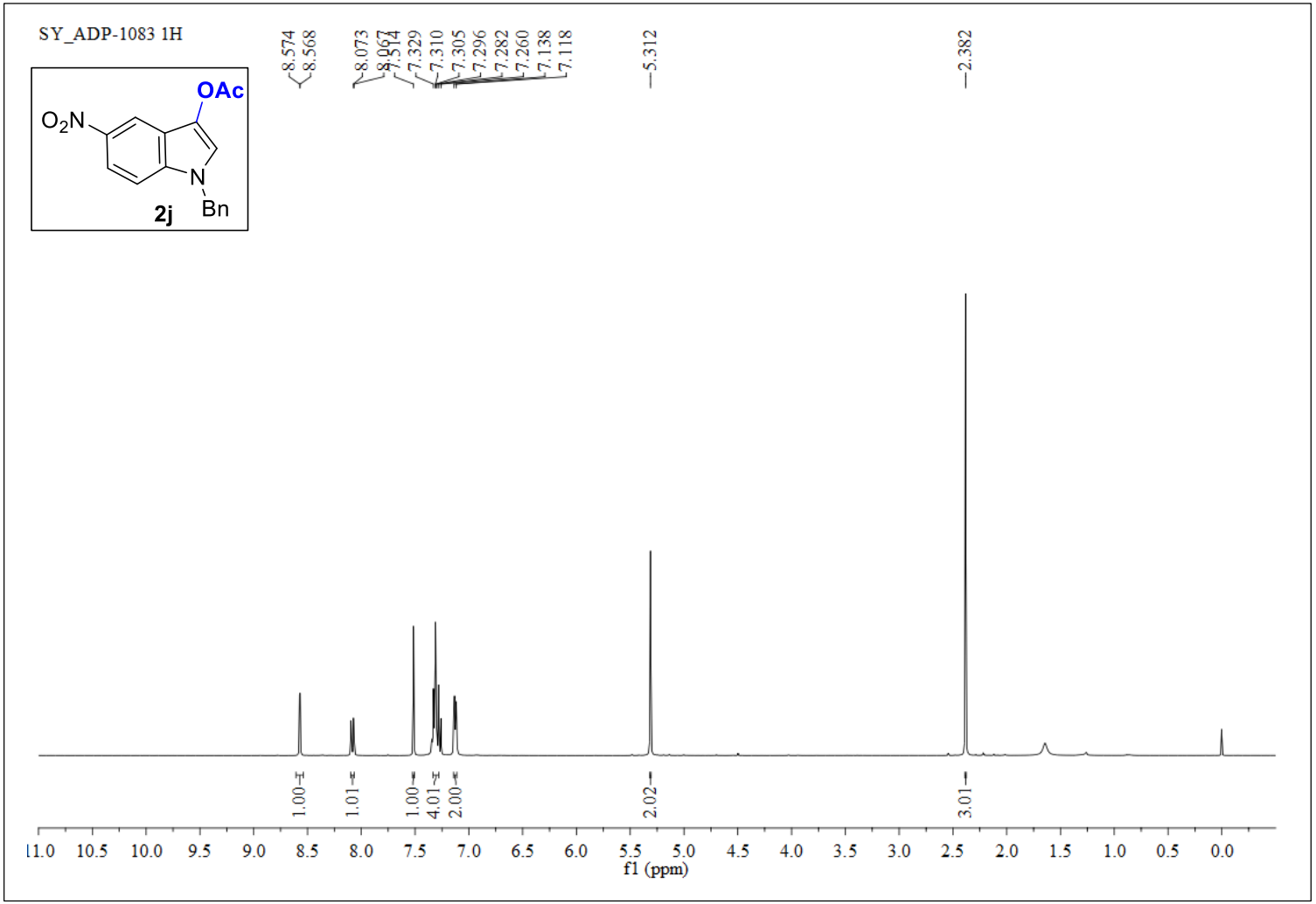

Figure S42. ^{1}H NMR (400 MHz, $CDCl_3$) of **2j**.

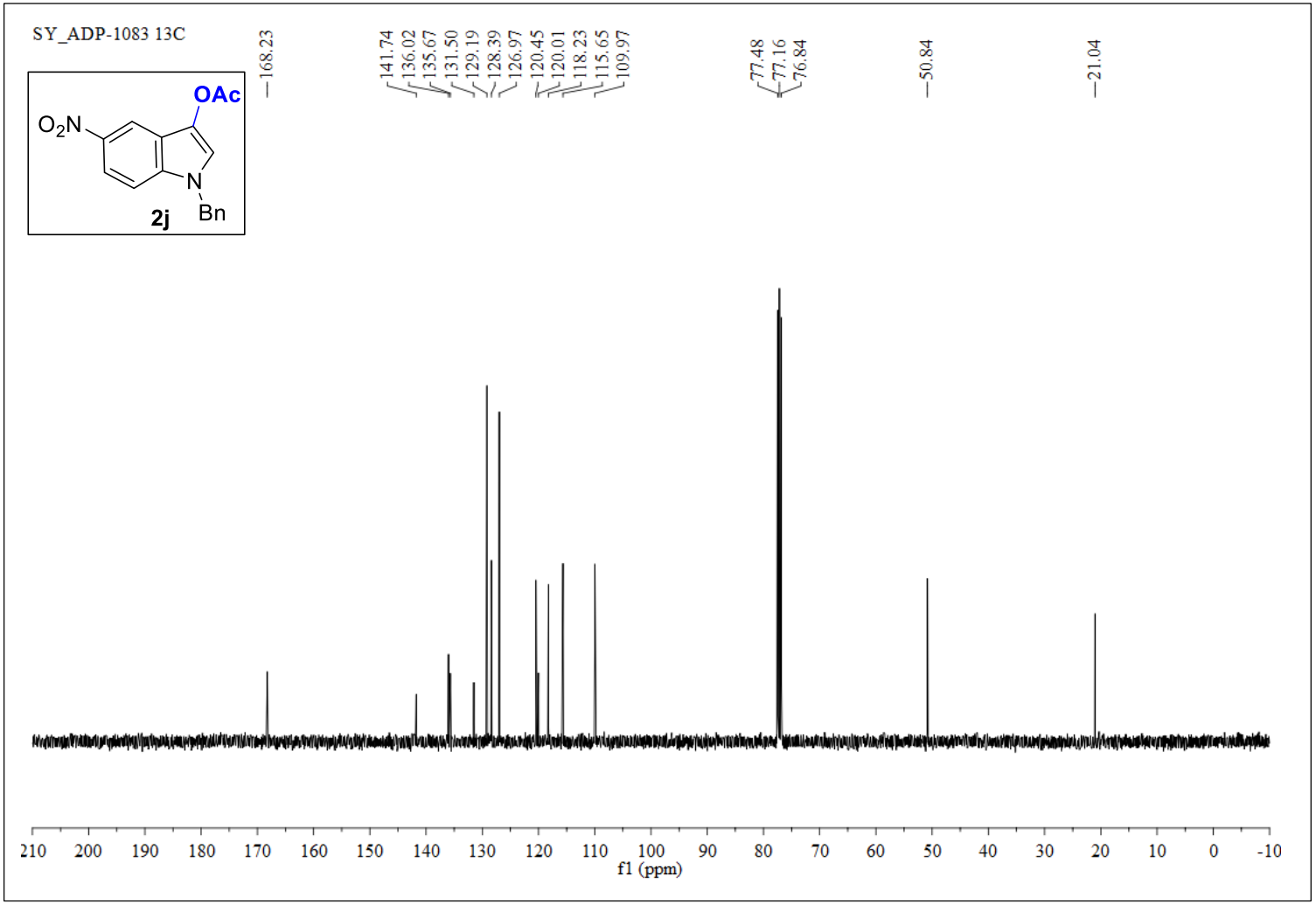

Figure S43. $^{13}C\{^{1}H\}$ NMR (100 MHz, $CDCl_3$) of **2j**.

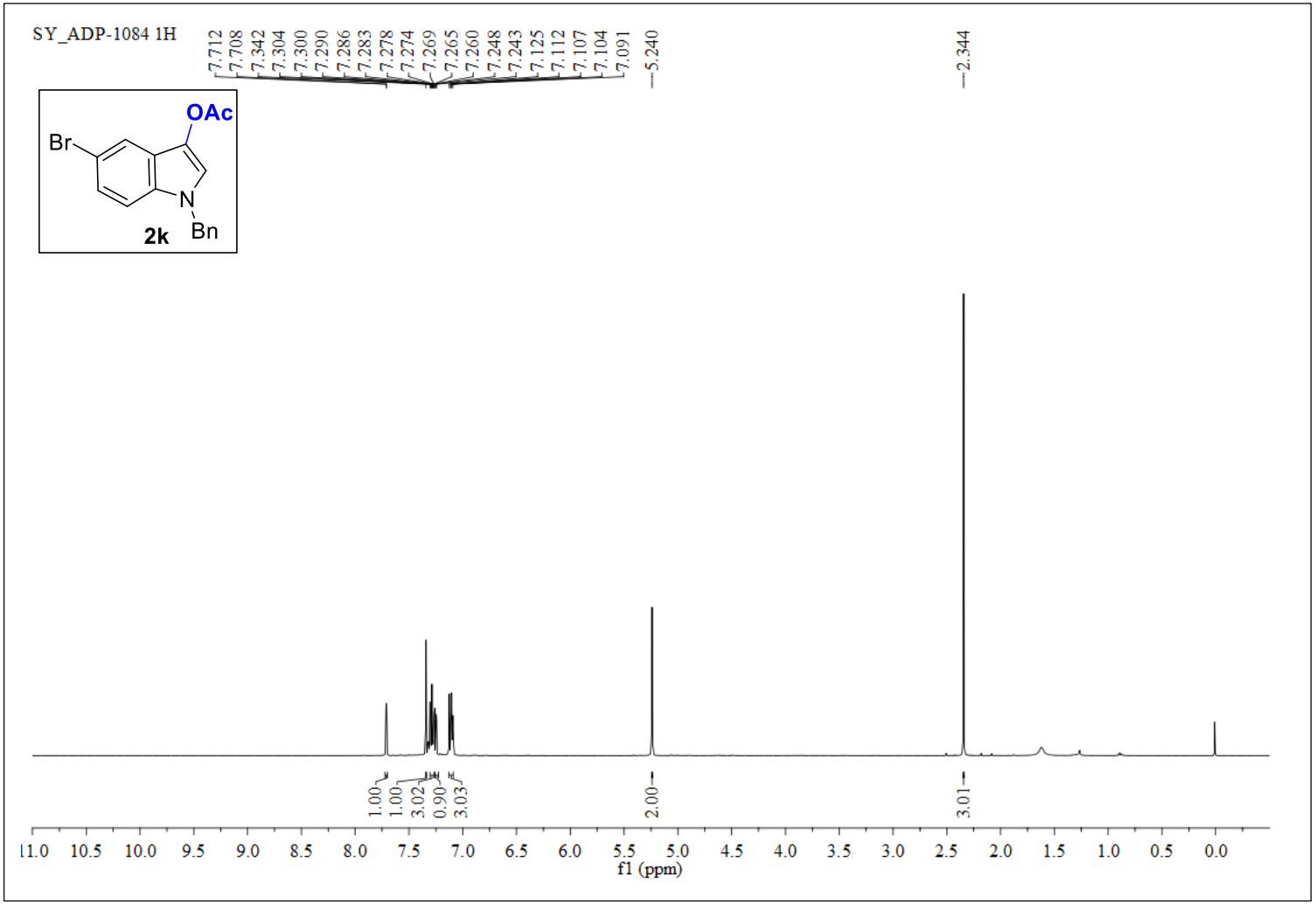

Figure S44. ^{1}H NMR (400 MHz, $CDCl_3$) of **2k**.

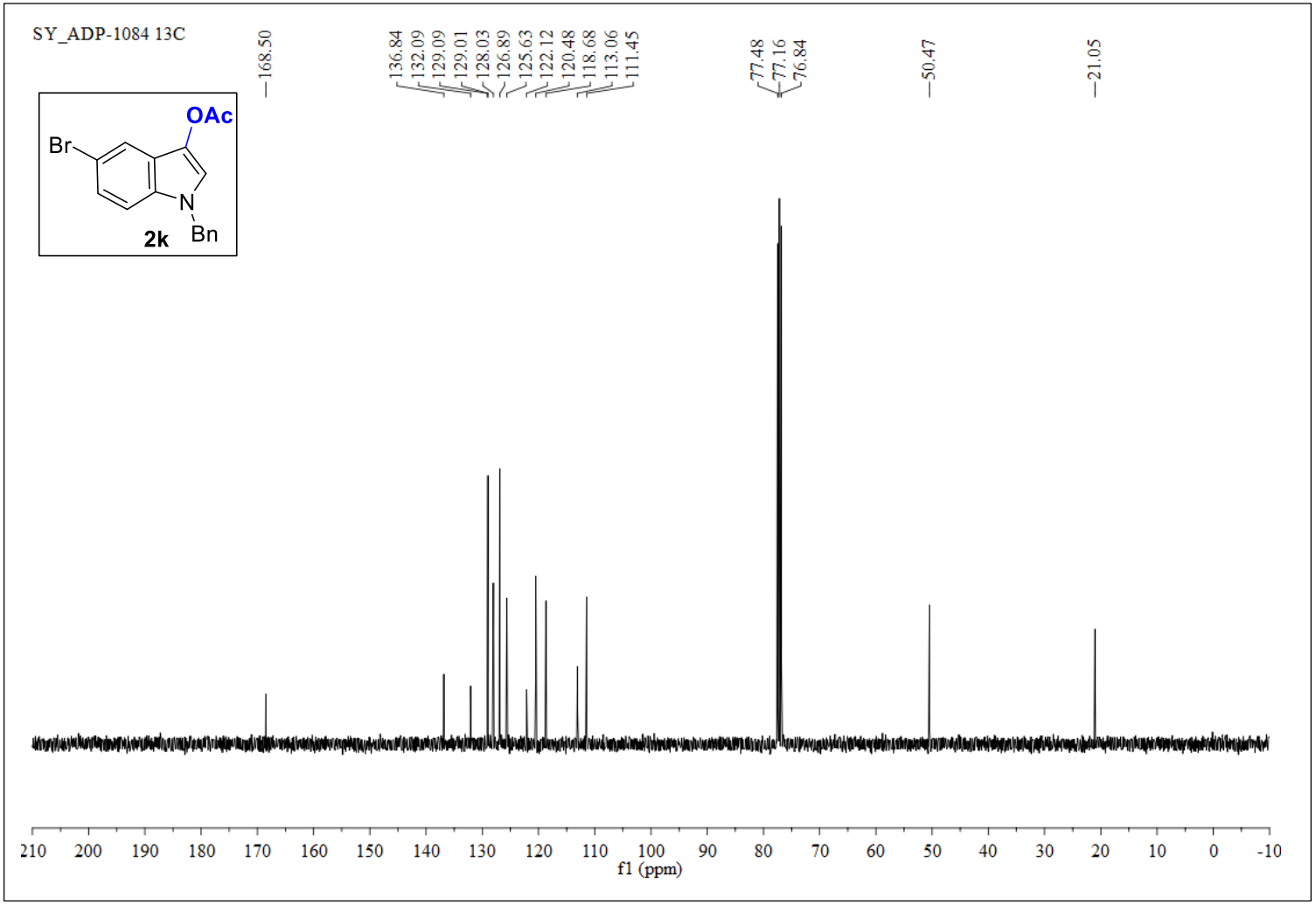

Figure S45. $^{13}C\{^{1}H\}$ NMR (100 MHz, $CDCl_3$) of **2k**.

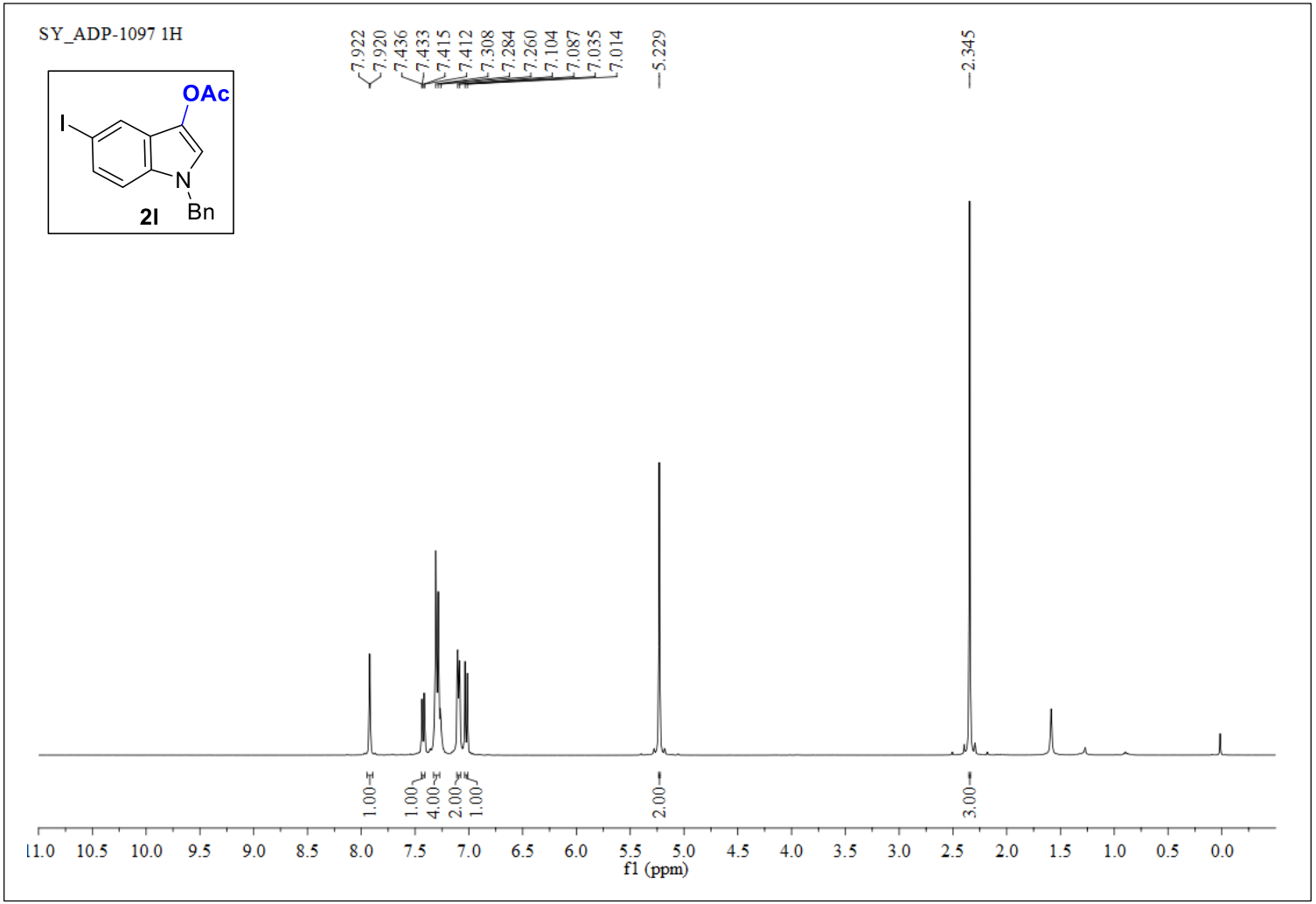

Figure S46. ^{1}H NMR (400 MHz, $CDCl_3$) of **2l**.

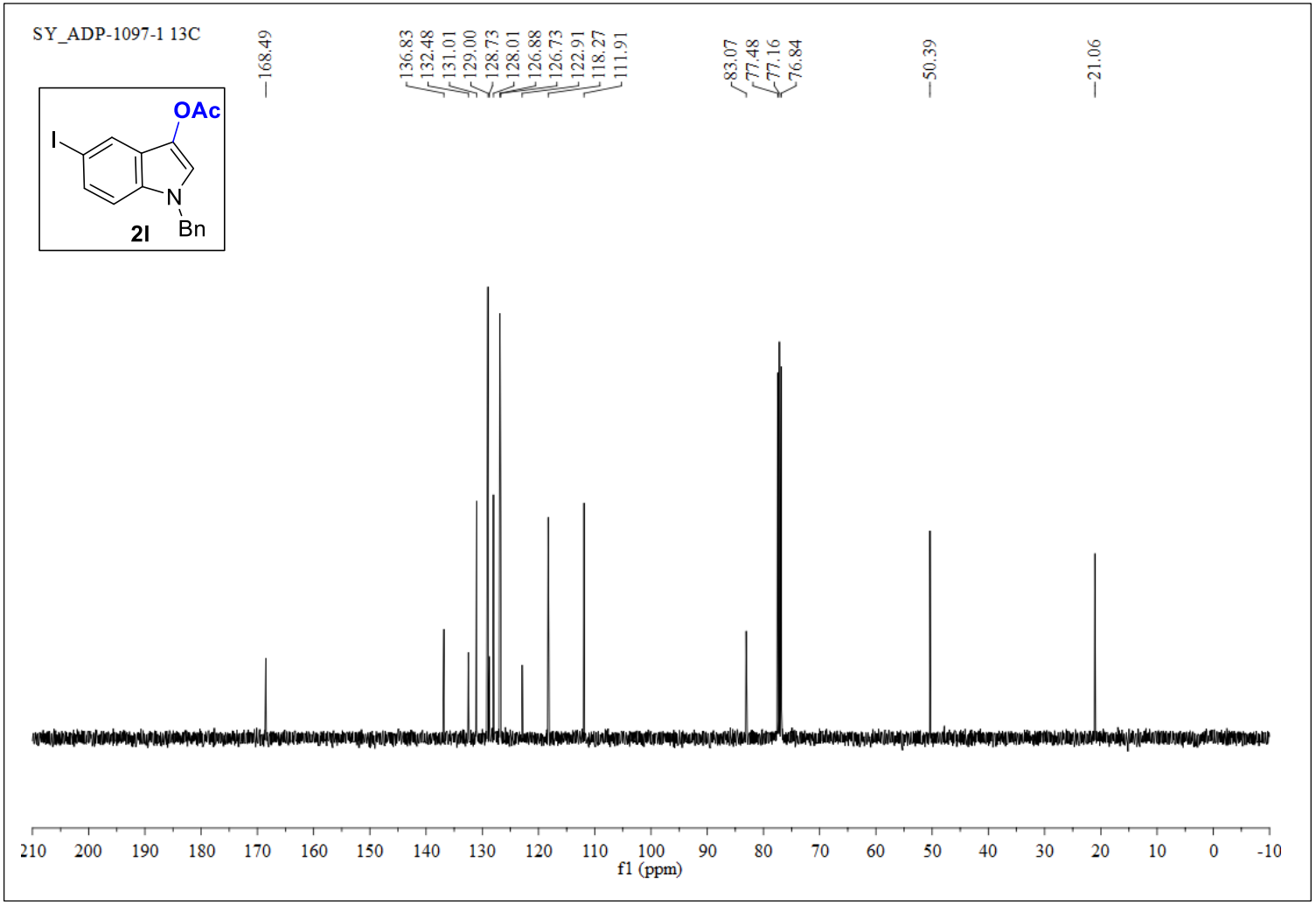

Figure S47. $^{13}C\{^{1}H\}$ NMR (100 MHz, $CDCl_3$) of **2l**.

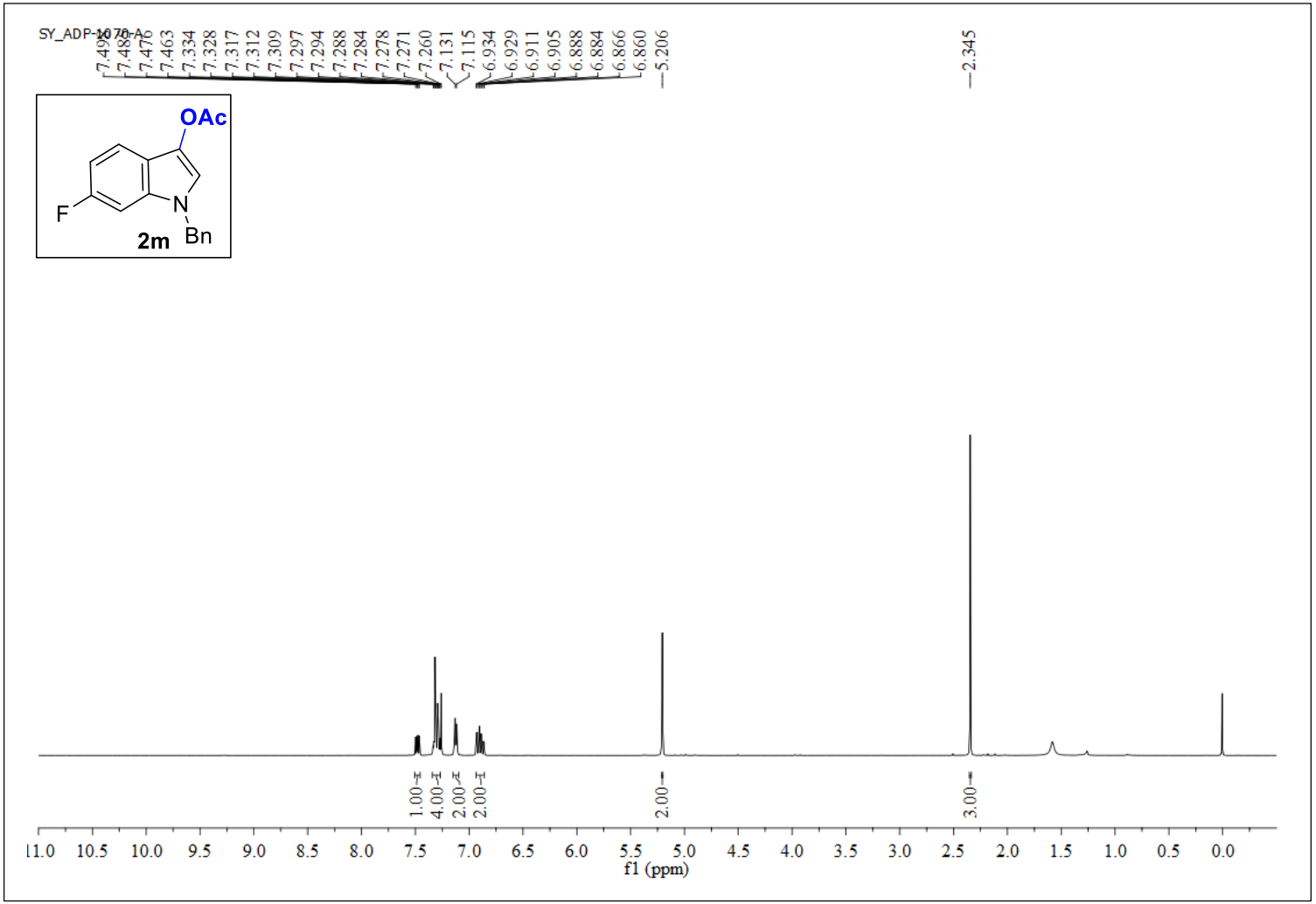

Figure S48. ^{1}H NMR (400 MHz, $CDCl_3$) of **2m**.

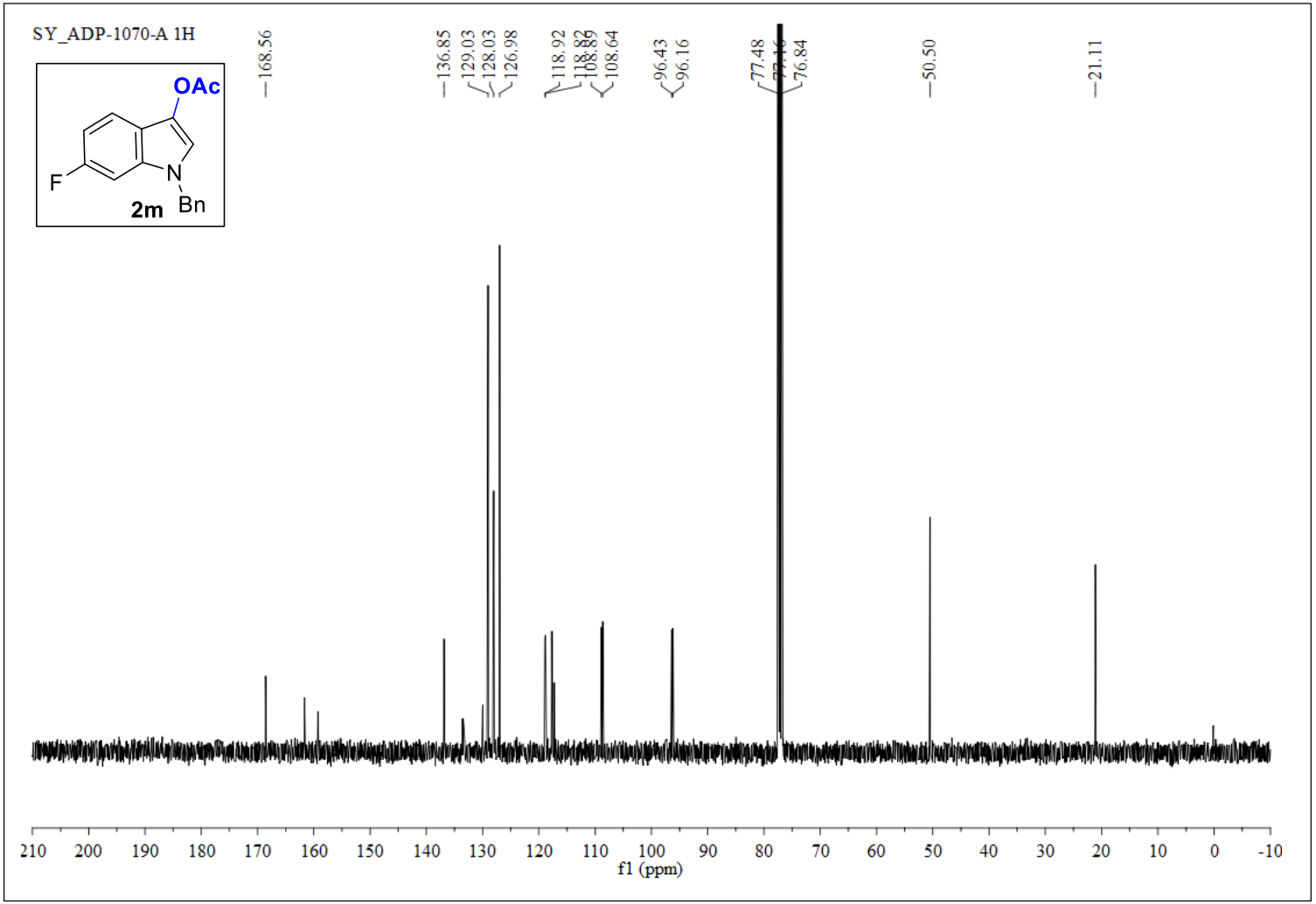

Figure S49. $^{13}C\{^{1}H\}$ NMR (100 MHz, $CDCl_3$) of **2m**.

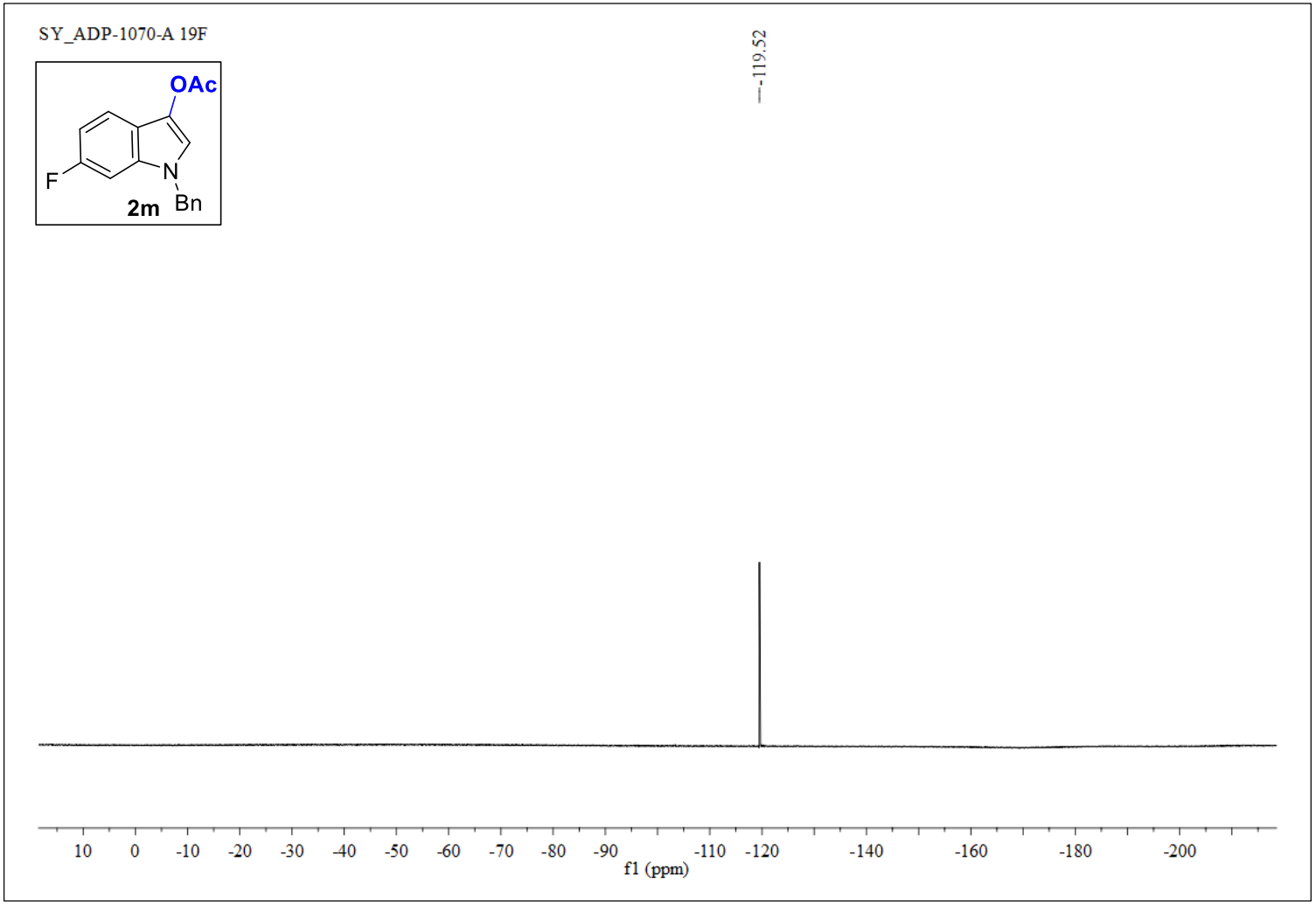

Figure S50. ^{19}F NMR (373 MHz, $CDCl_3$) of **2m**.

.

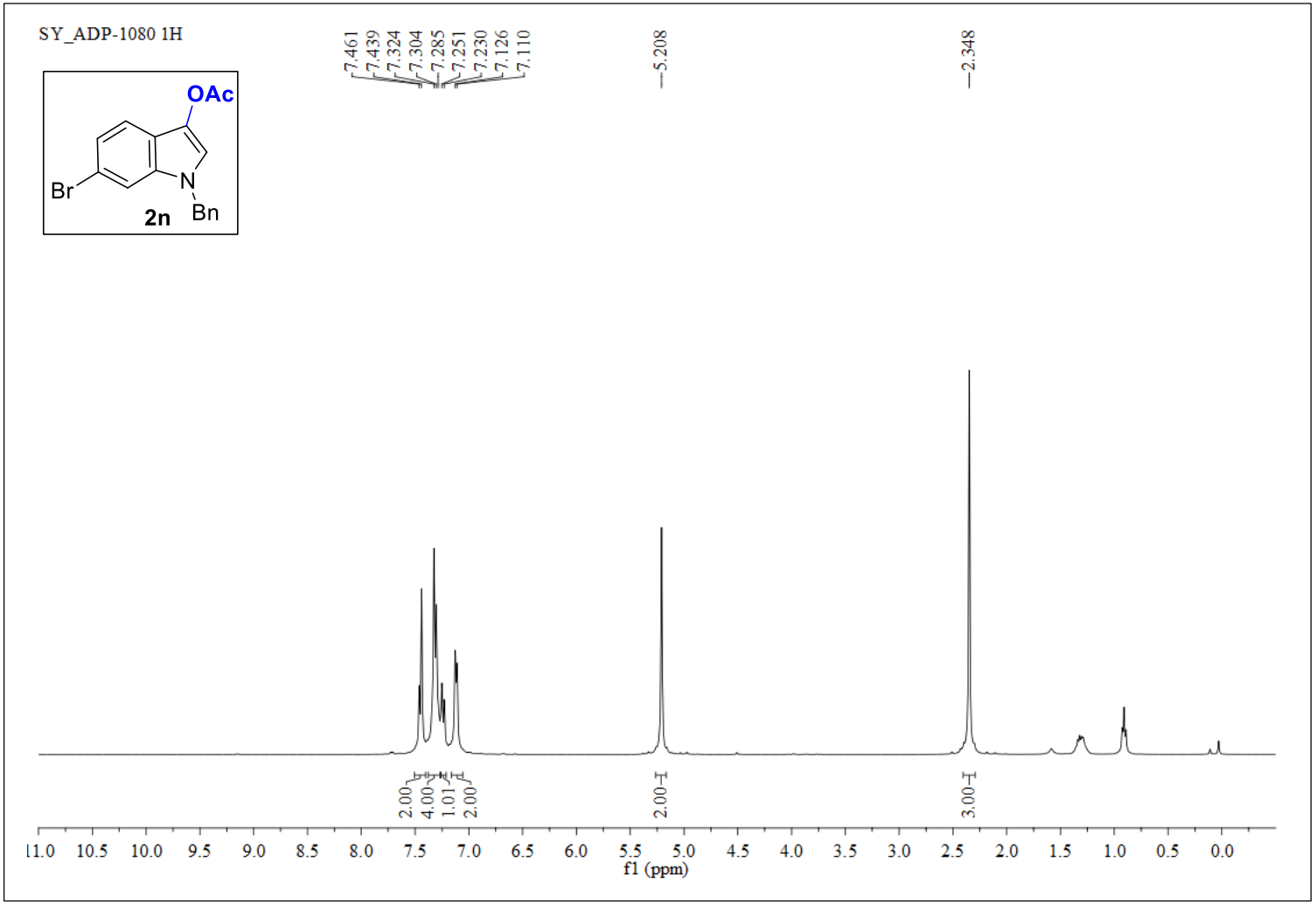

Figure S51. ^{1}H NMR (400 MHz, $CDCl_3$) of **2n**.

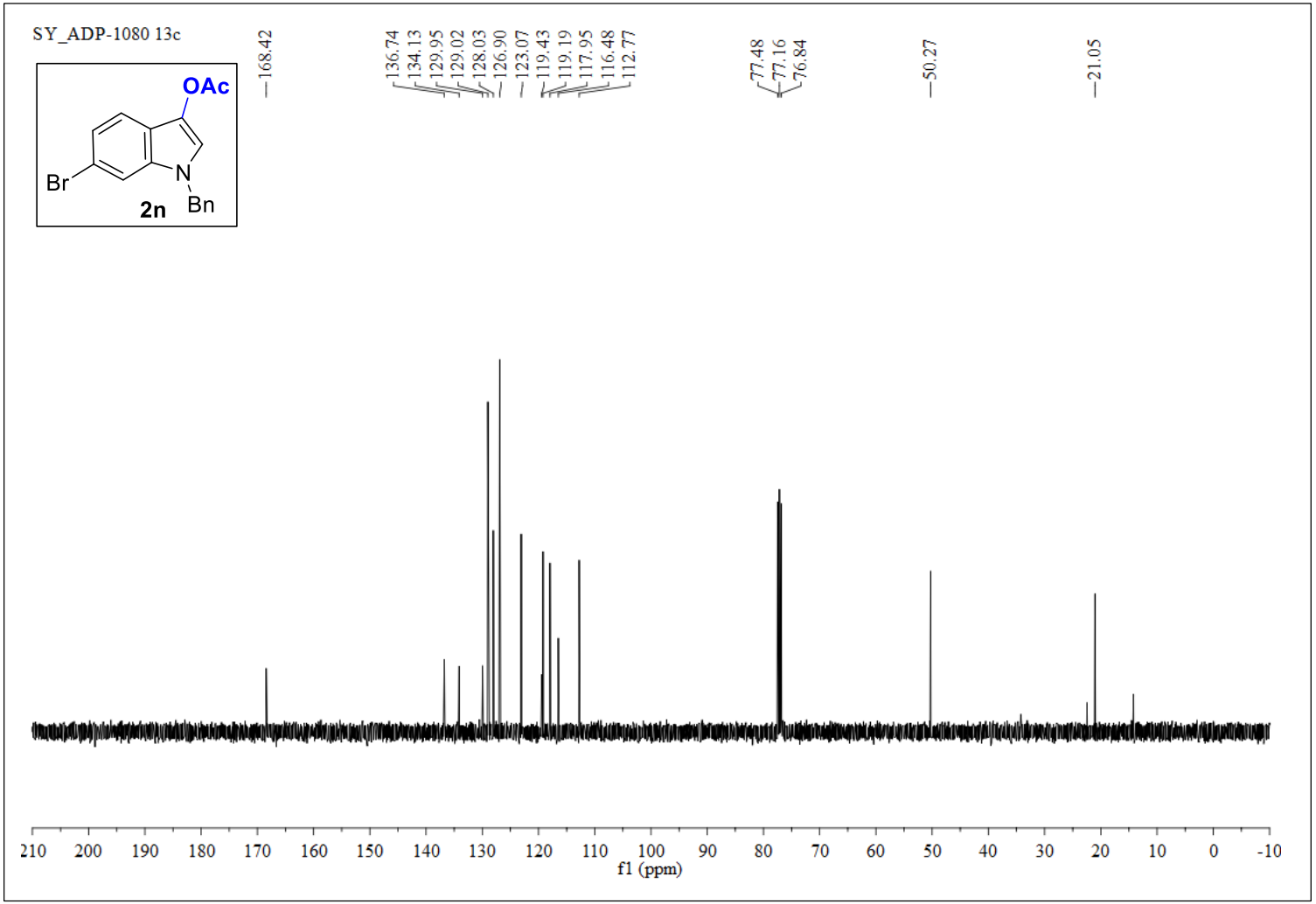

Figure S52. $^{13}C\{^{1}H\}$ NMR (100 MHz, $CDCl_3$) of **2n**.

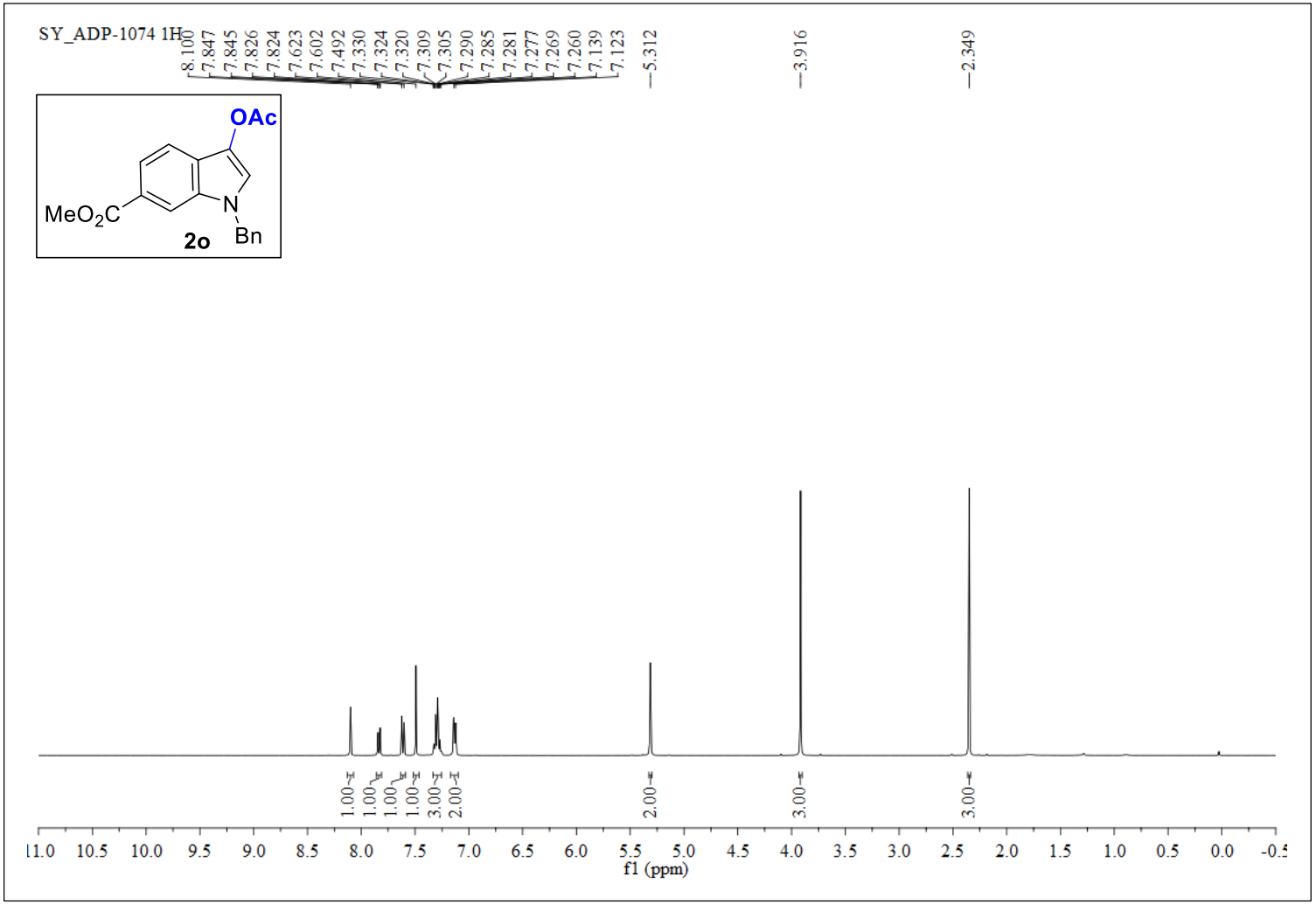

Figure S53. ^{1}H NMR (400 MHz, $CDCl_3$) of **2o**.

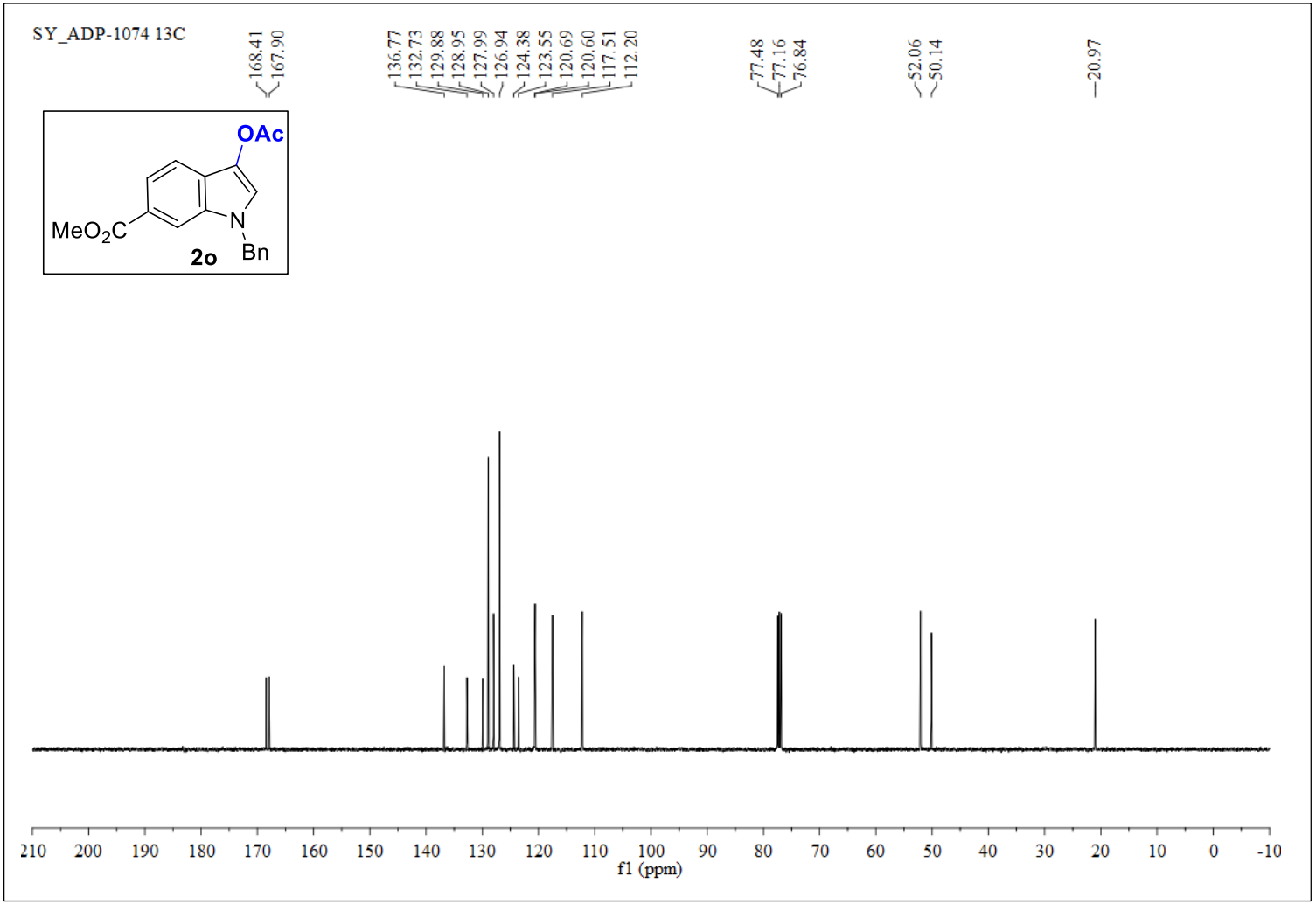

Figure S54. $^{13}C\{^{1}H\}$ NMR (100 MHz, $CDCl_3$) of **2o**.

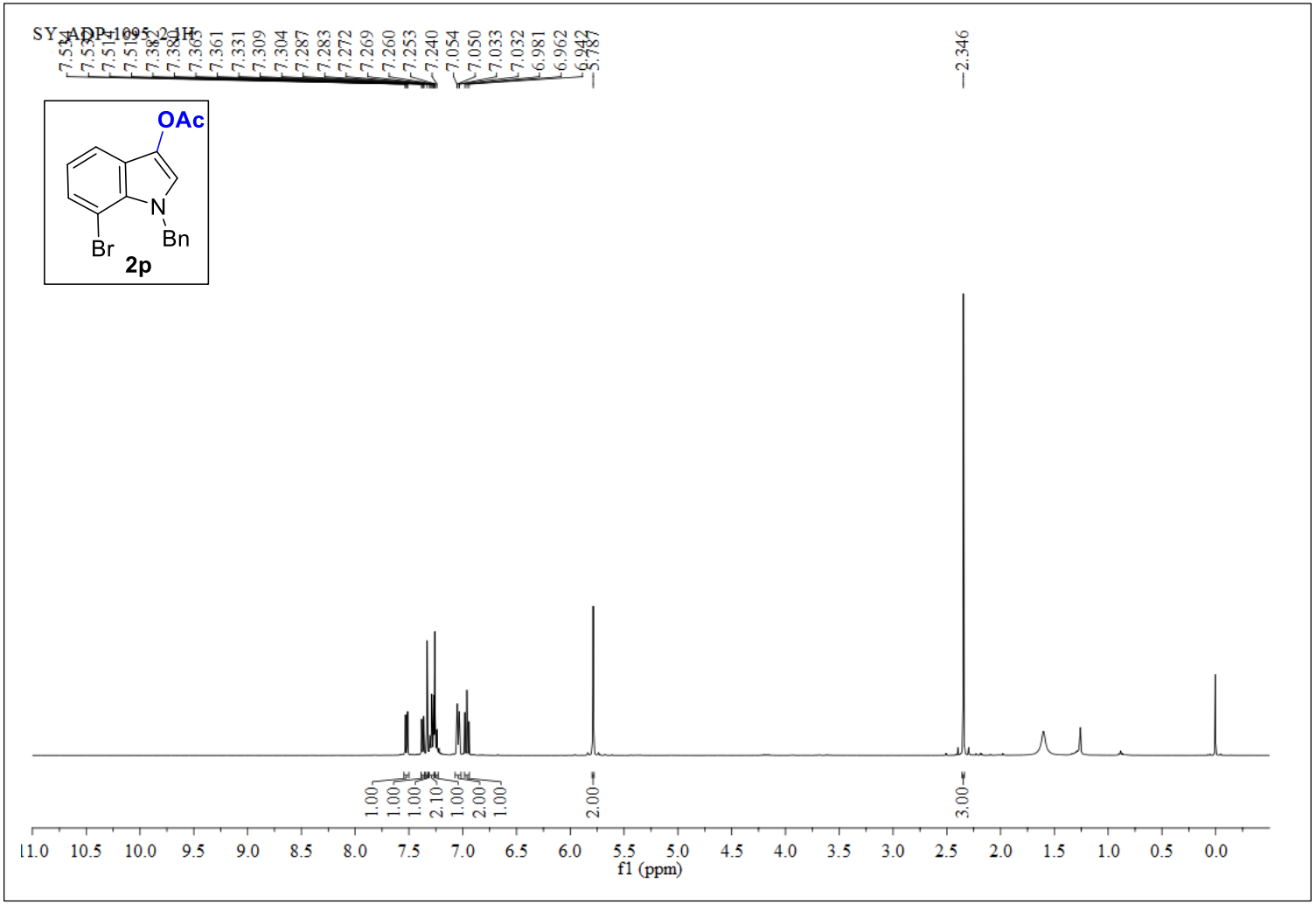

Figure S55. ^{1}H NMR (400 MHz, $CDCl_3$) of **2p**.

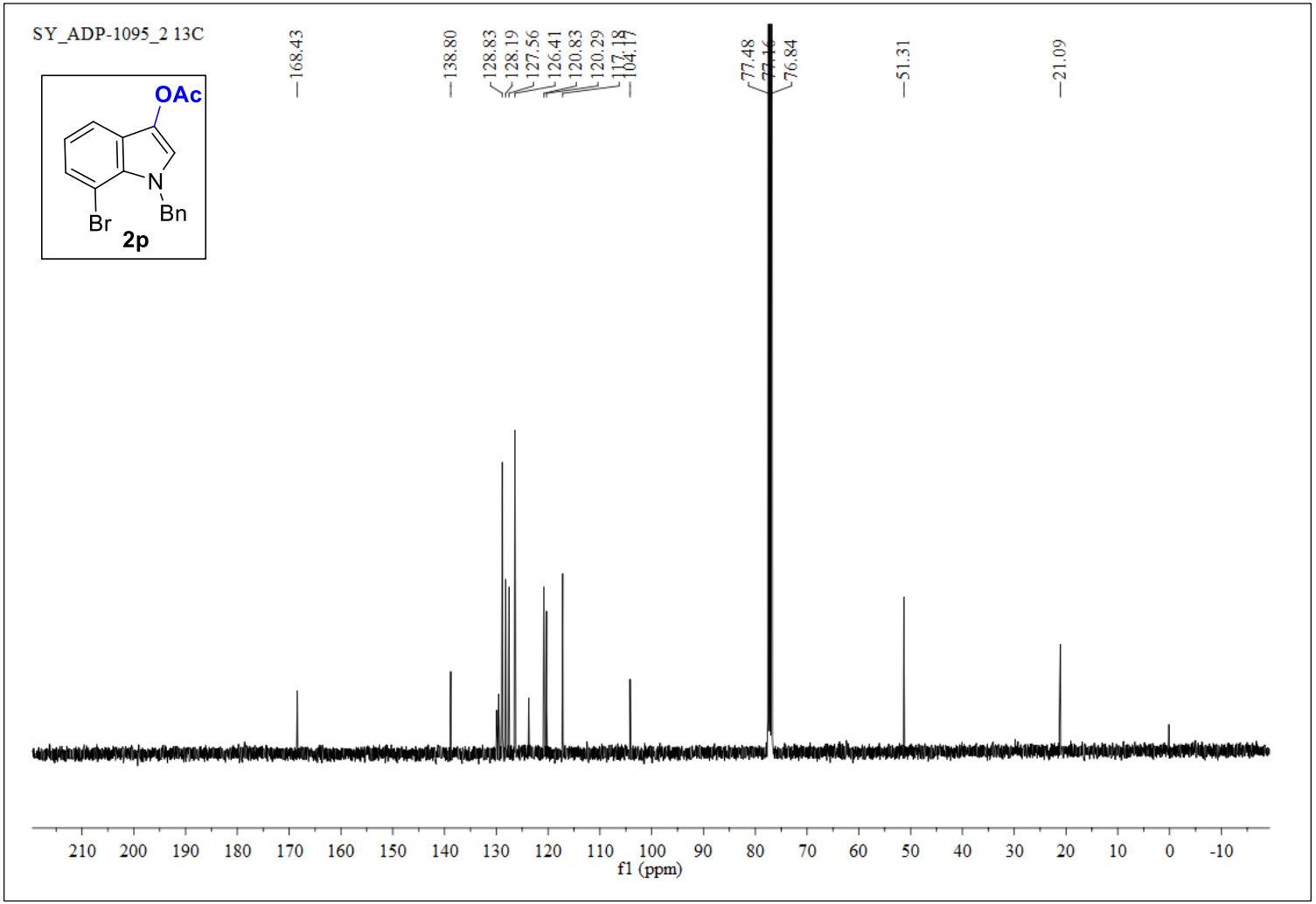

Figure S56. $^{13}C\{^{1}H\}$ NMR (100 MHz, $CDCl_3$) of **2p**.

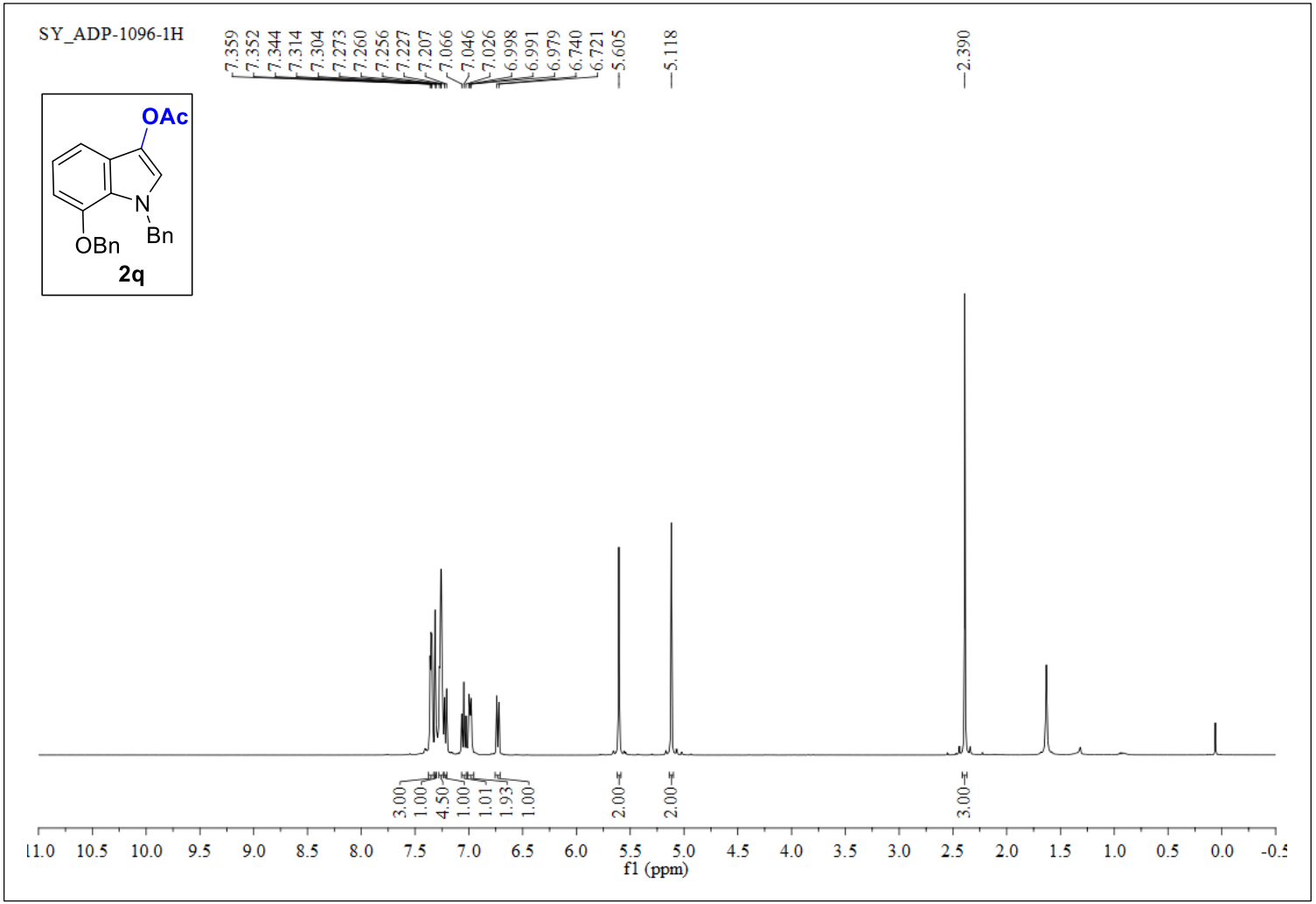

Figure S57. ^{1}H NMR (400 MHz, $CDCl_3$) of **2q**.

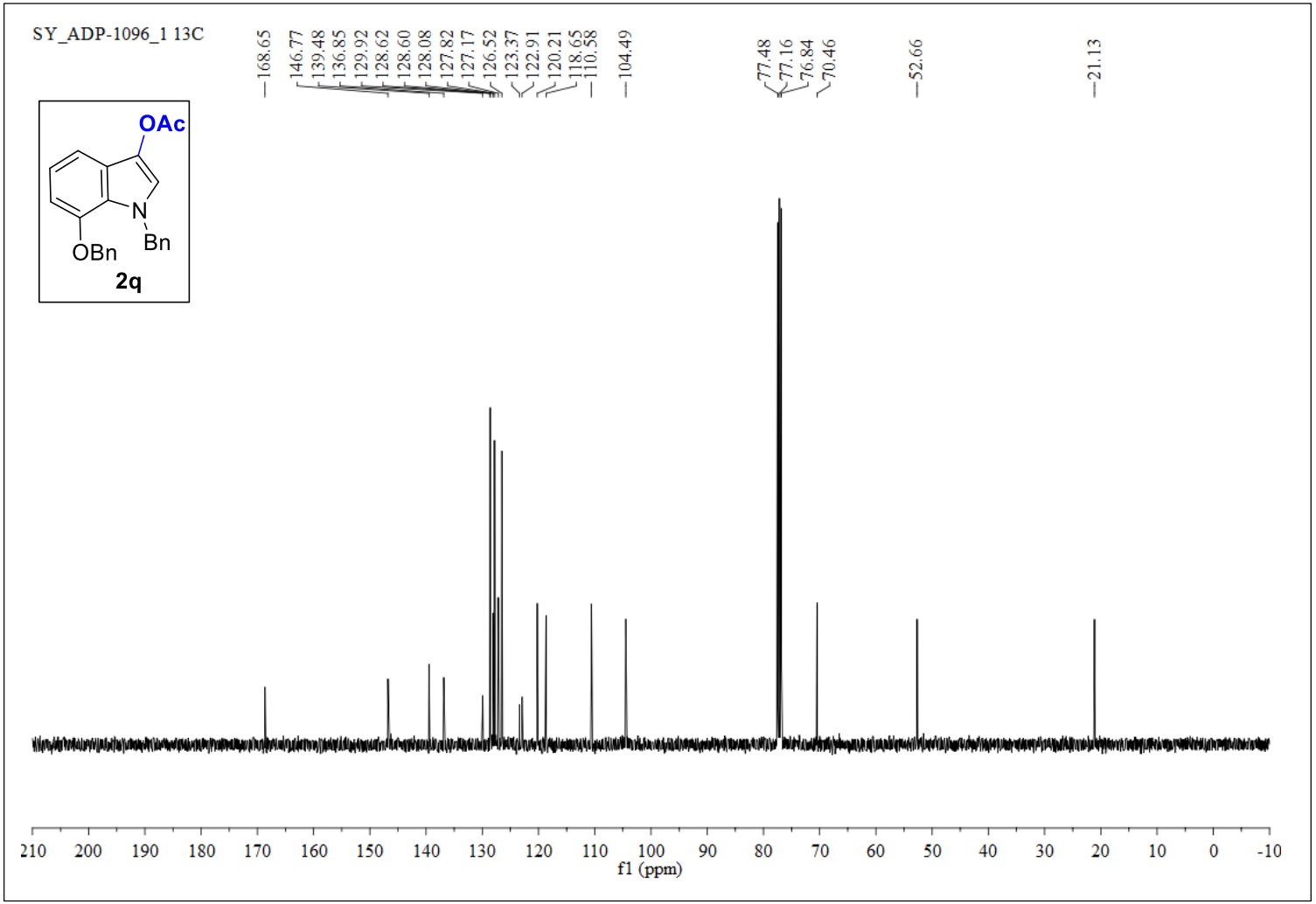

Figure S58. $^{13}C\{^{1}H\}$ NMR (100 MHz, $CDCl_3$) of **2q**.

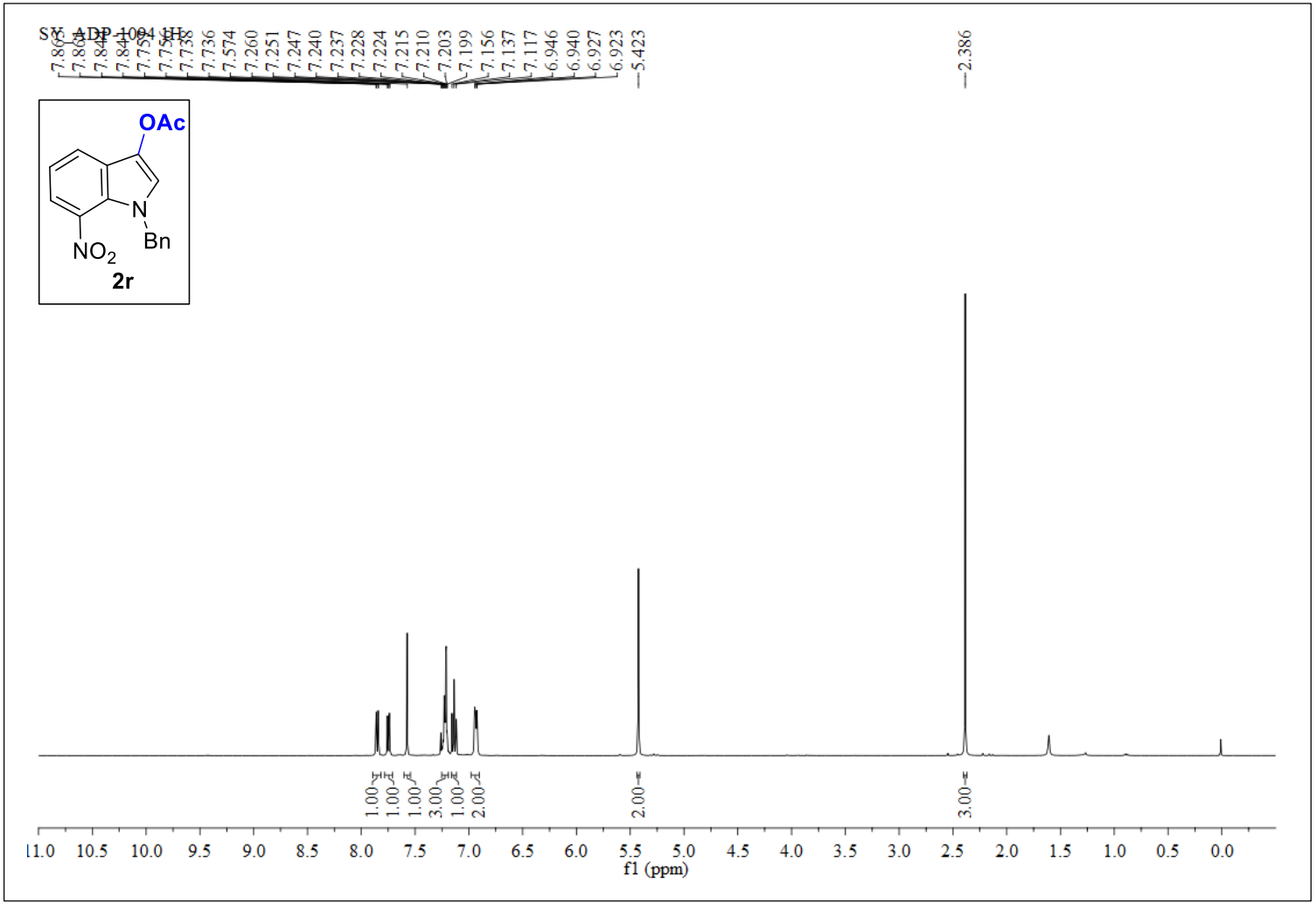

Figure S59. ^{1}H NMR (400 MHz, $CDCl_3$) of **2r**.

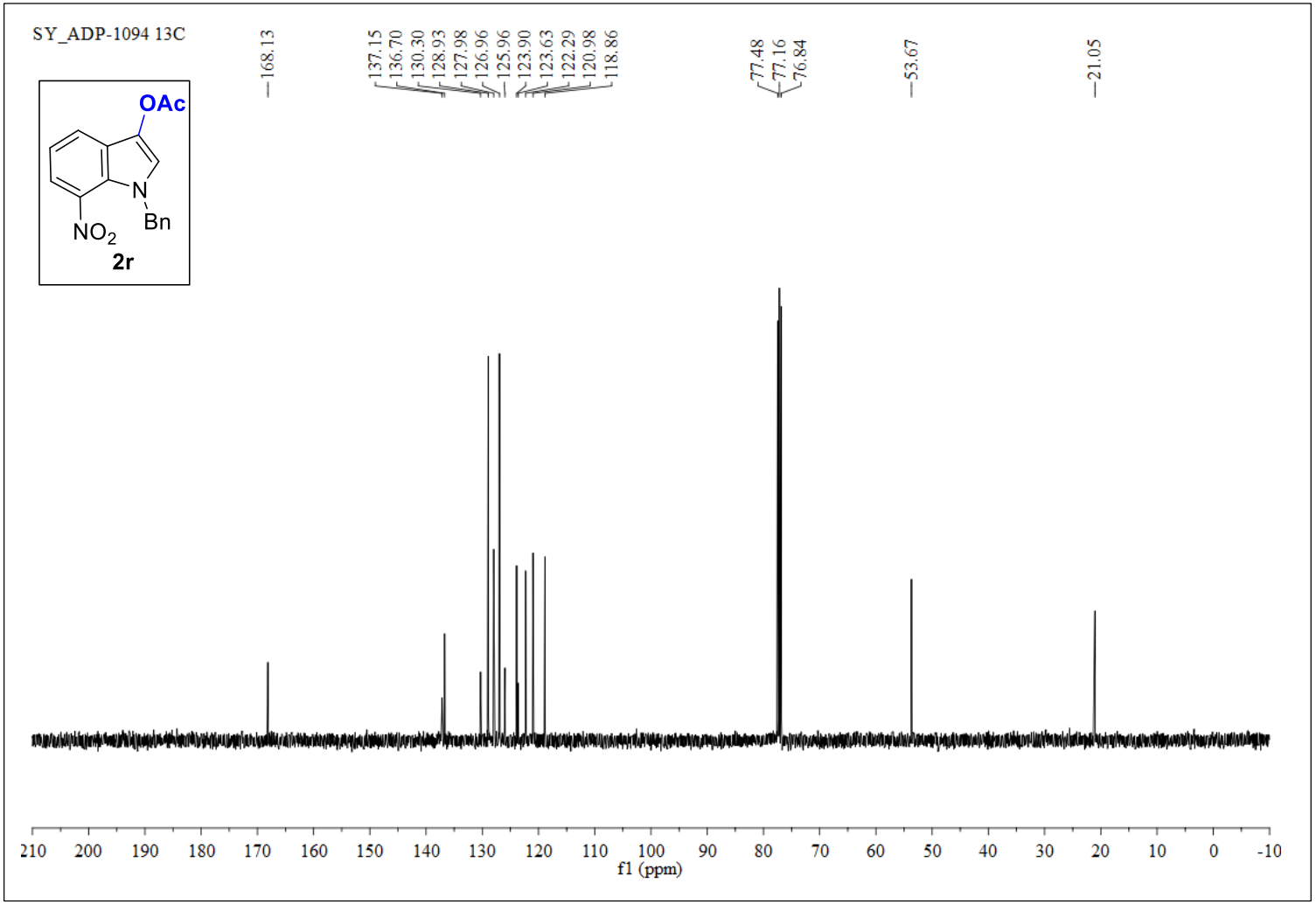

Figure S60. $^{13}C\{^{1}H\}$ NMR (100 MHz, $CDCl_3$) of **2r**.

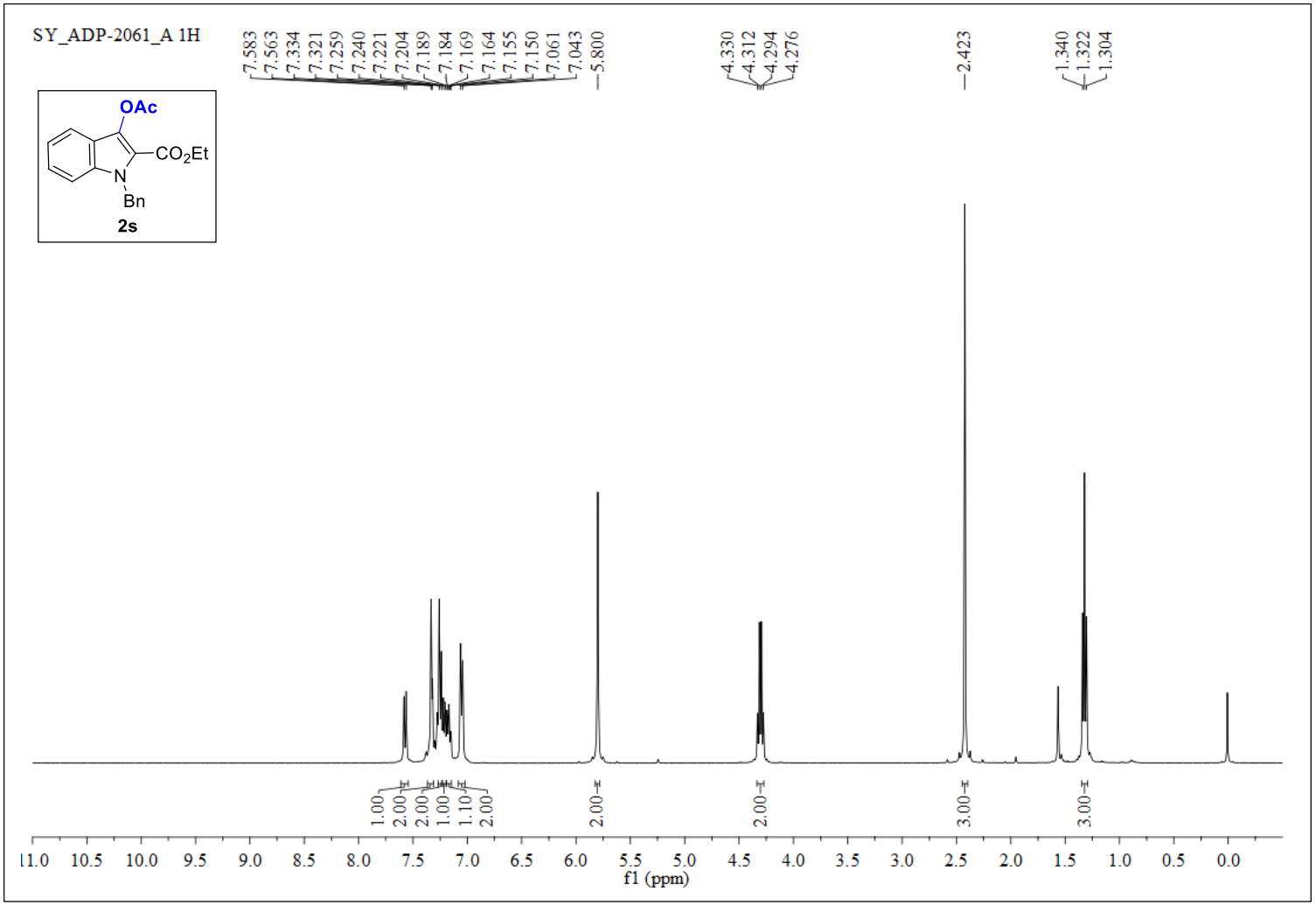

Figure S61. ^{1}H NMR (400 MHz, $CDCl_3$) of **2s**.

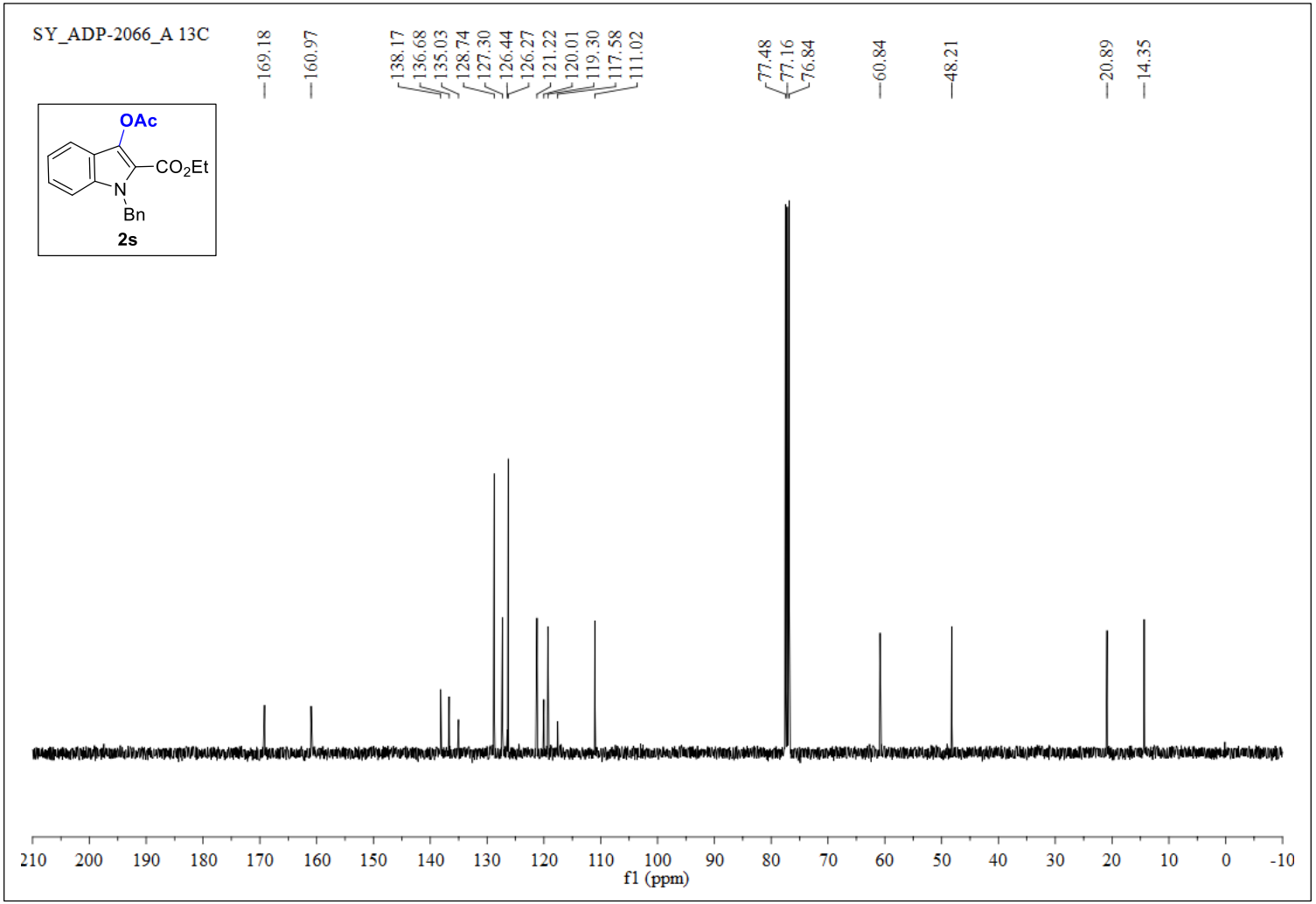

Figure S62. $^{13}C\{^{1}H\}$ NMR (100 MHz, $CDCl_3$) of **2s**.

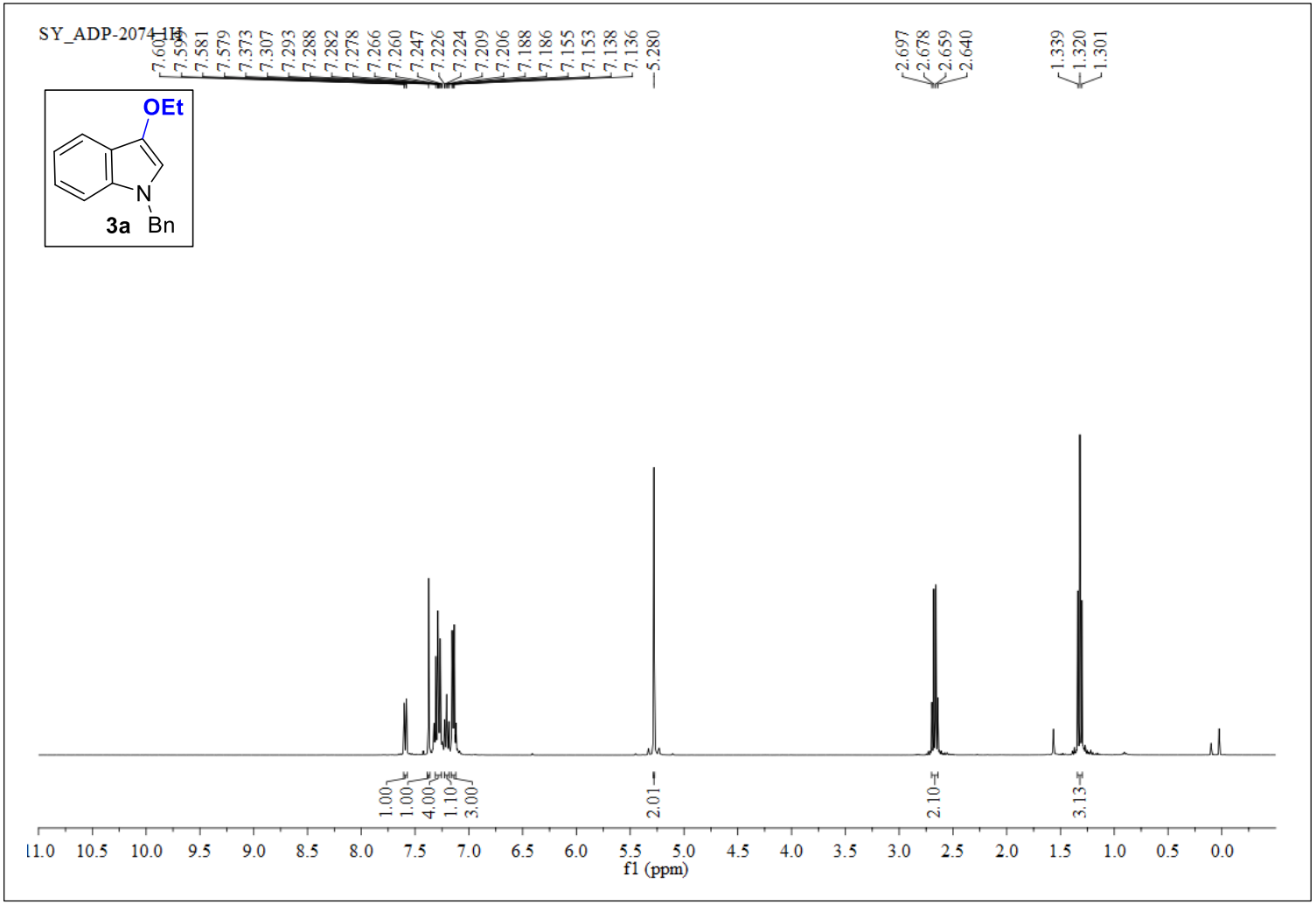

Figure S63. ^{1}H NMR (400 MHz, $CDCl_3$) of **3a**.

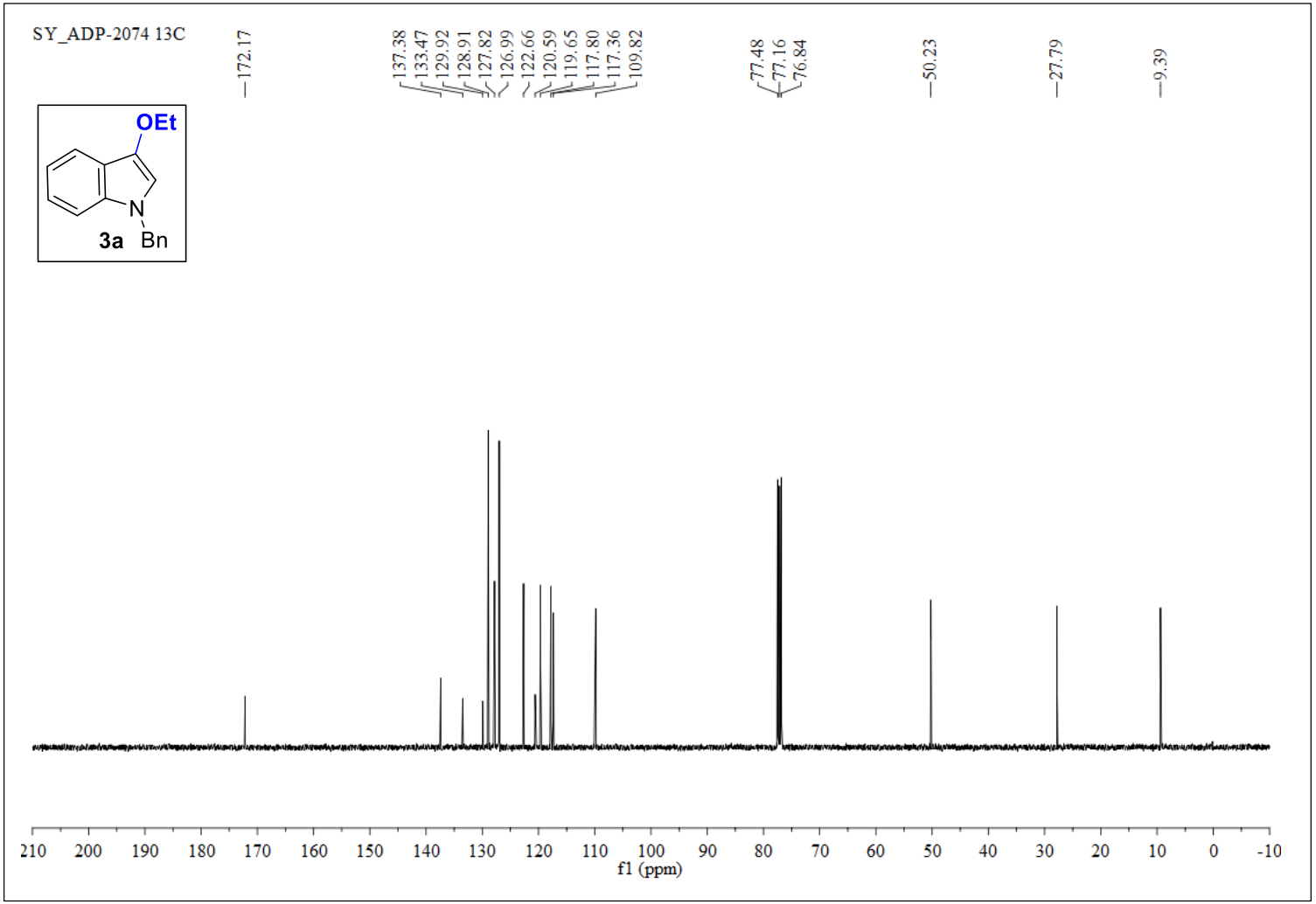

Figure S64. $^{13}C\{^{1}H\}$ NMR (100 MHz, $CDCl_3$) of **3a**.

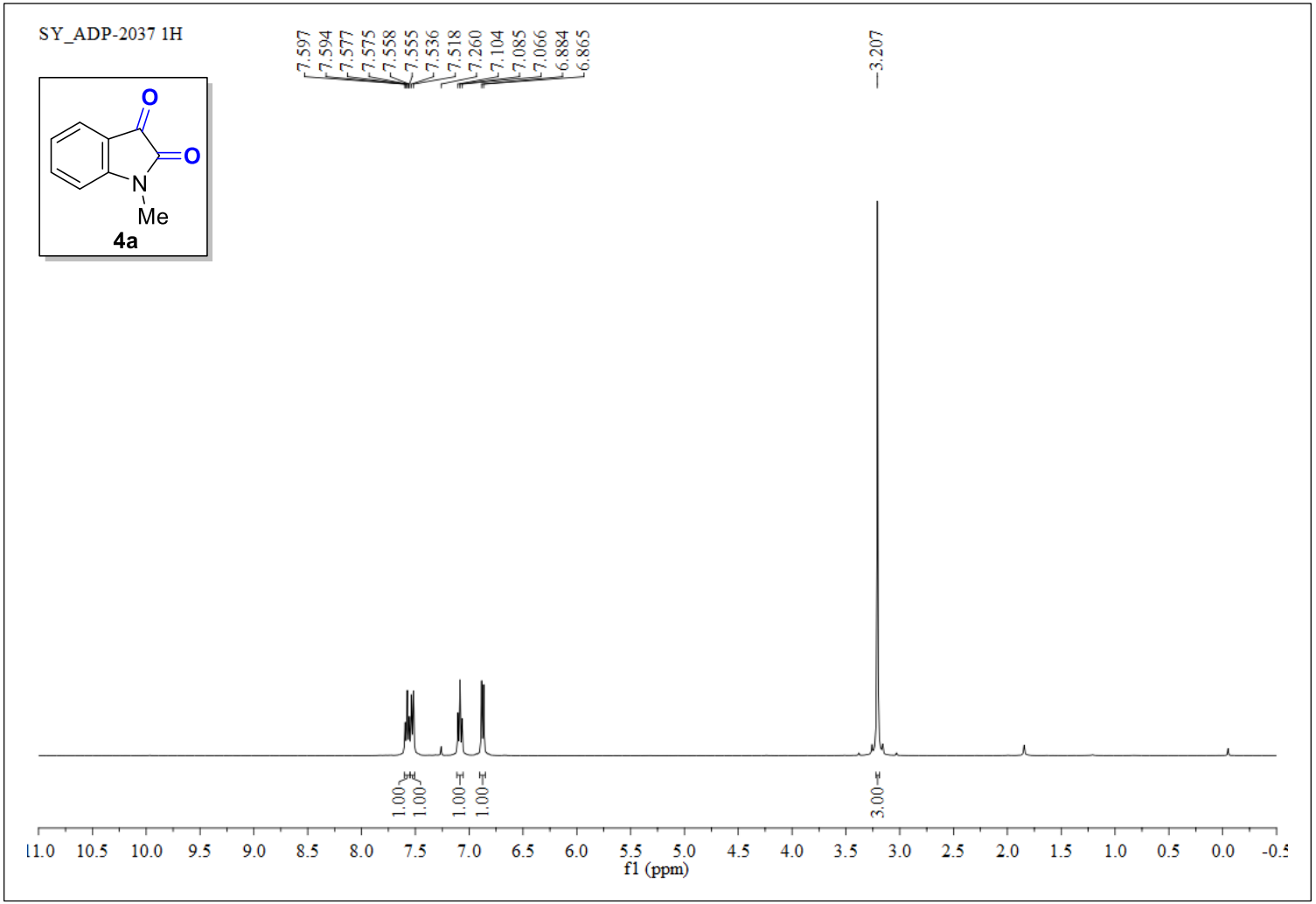

Figure S65. ^{1}H NMR (400 MHz, $CDCl_3$) of **4a**.

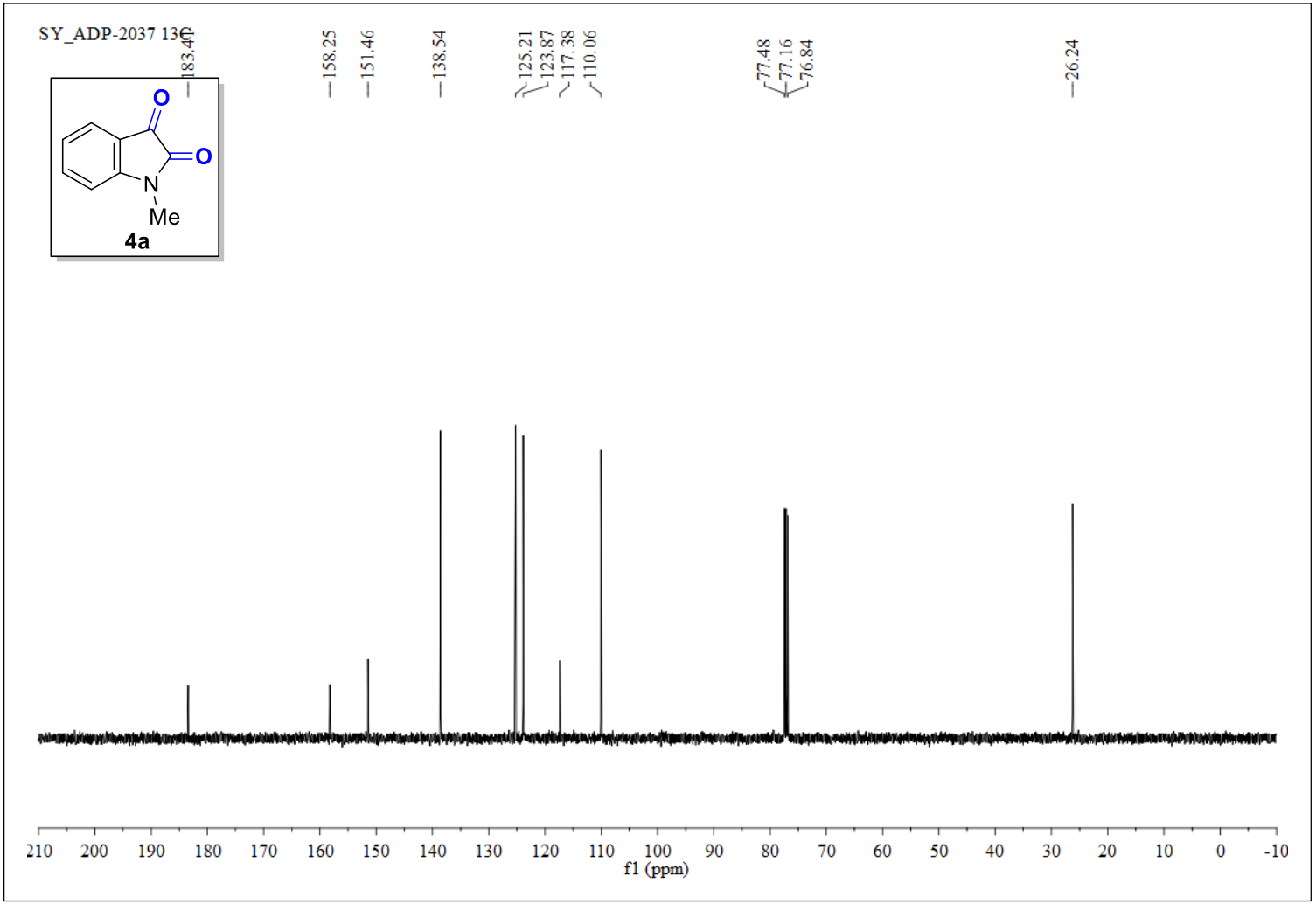

Figure S66. $^{13}C\{^{1}H\}$ NMR (100 MHz, $CDCl_3$) of **4a**.

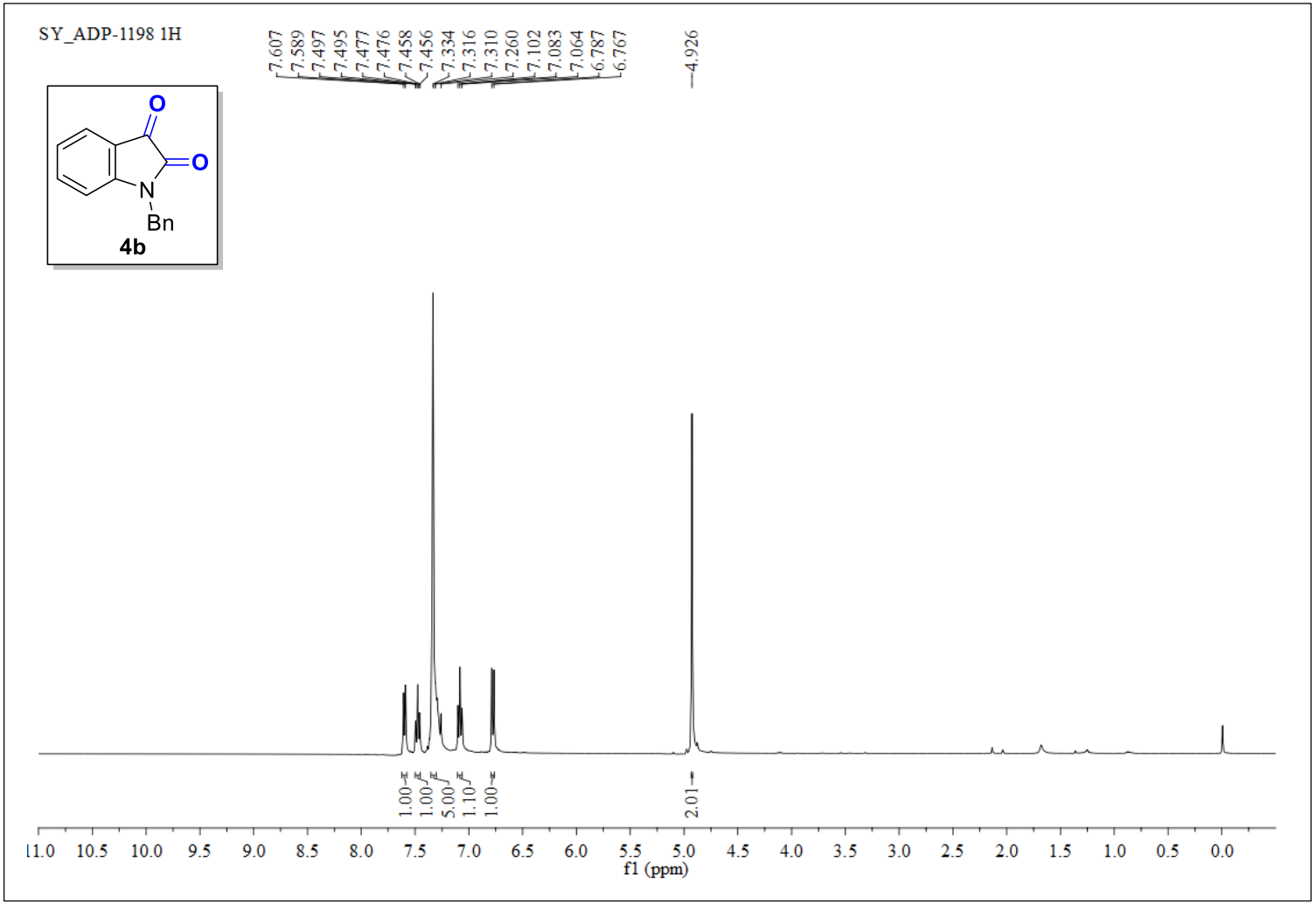

Figure S67. ^{1}H NMR (400 MHz, $CDCl_3$) of **4b**.

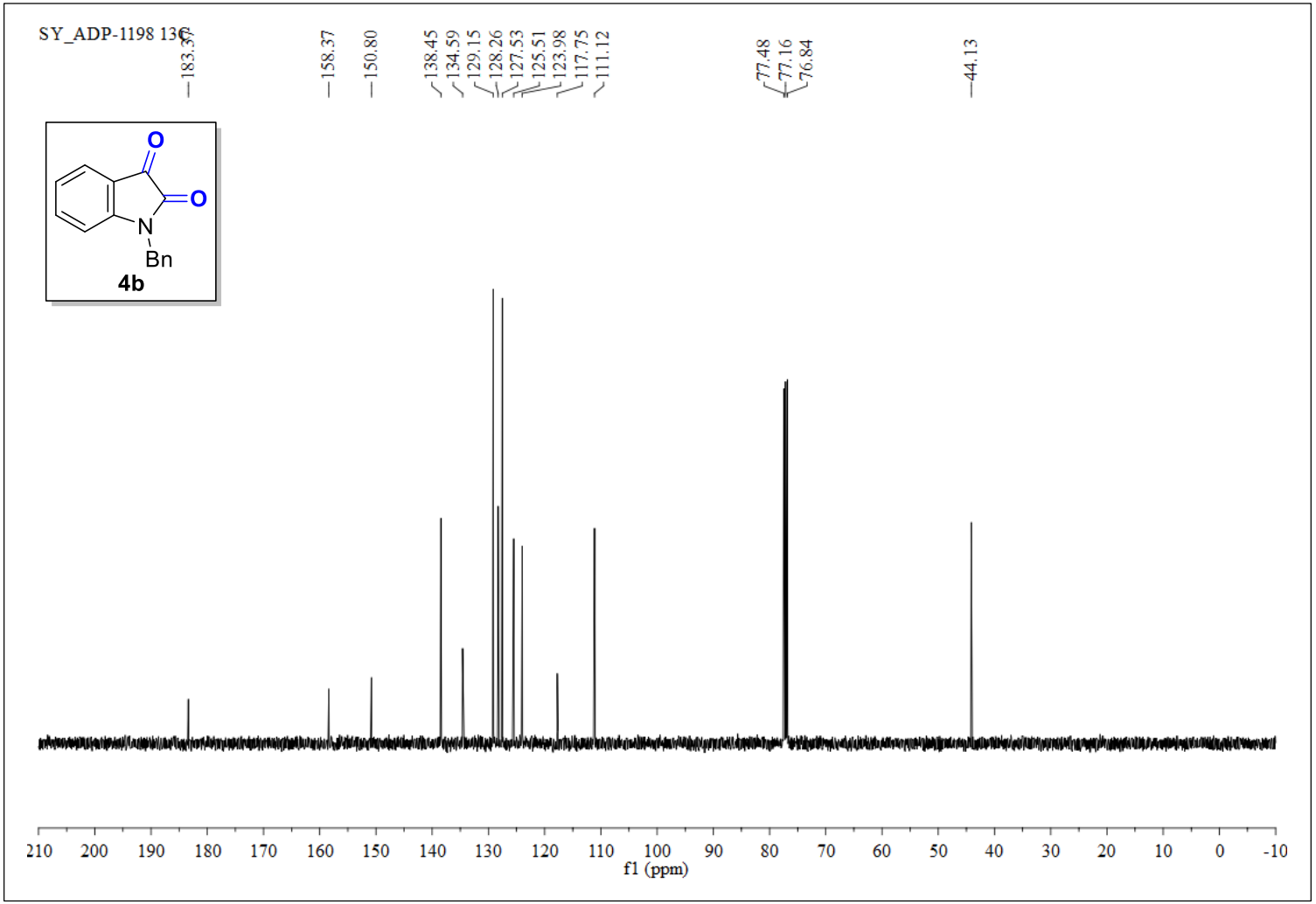

Figure S68. $^{13}C\{^{1}H\}$ NMR (100 MHz, $CDCl_3$) of **4b**.

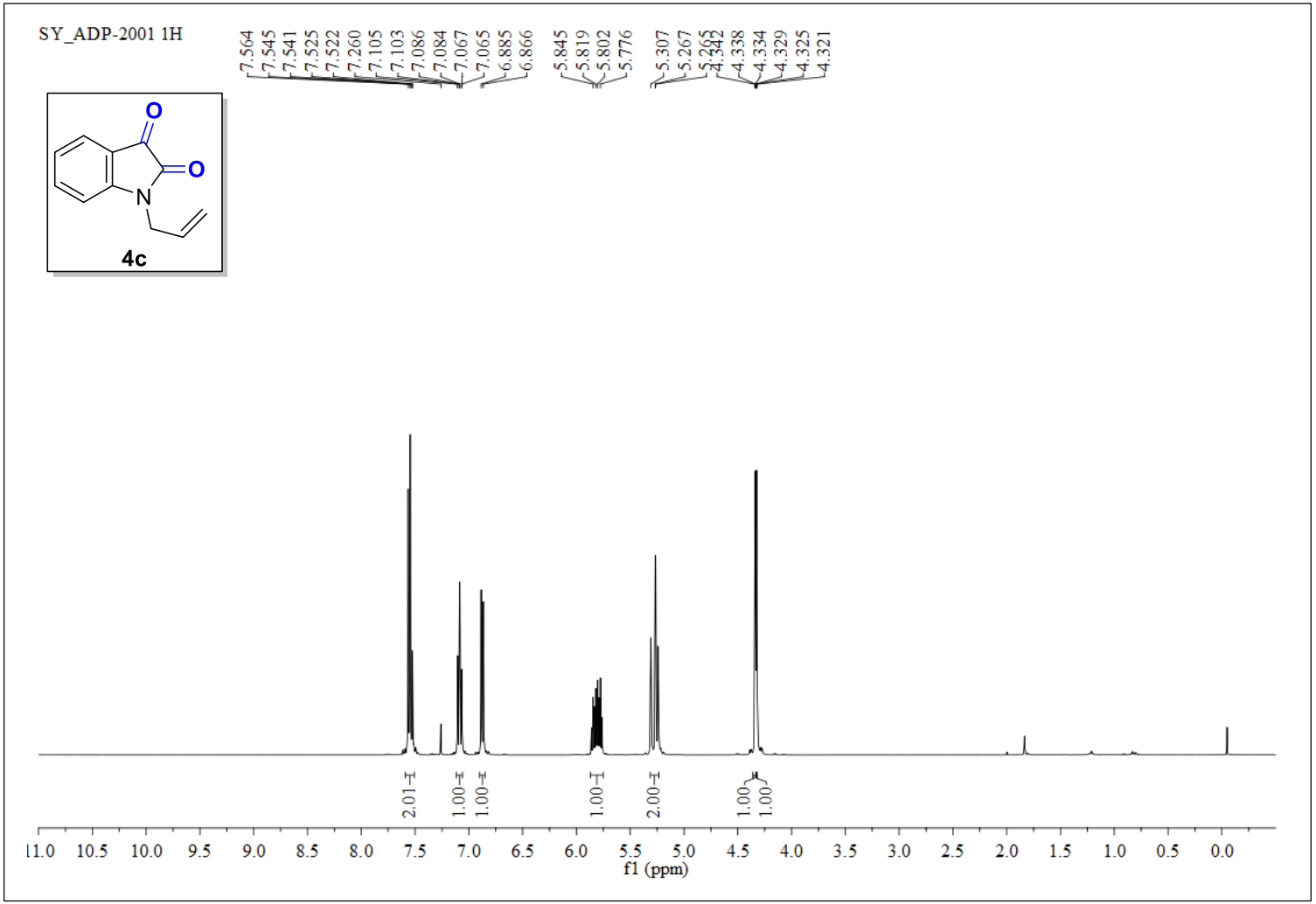

Figure S69. ^{1}H NMR (400 MHz, $CDCl_3$) of **4c**.

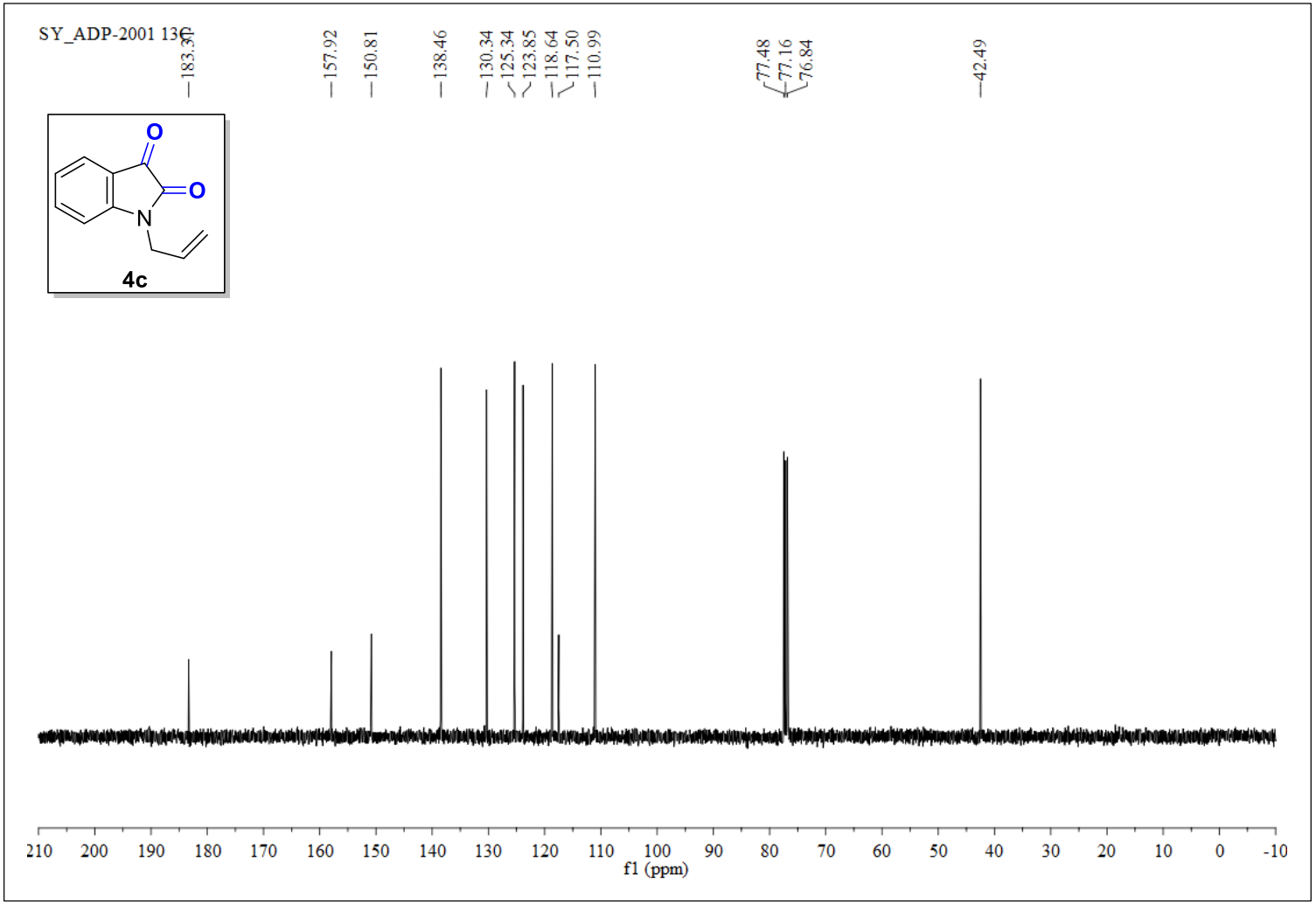

Figure S70. $^{13}C\{^{1}H\}$ NMR (100 MHz, $CDCl_3$) of **4c**.

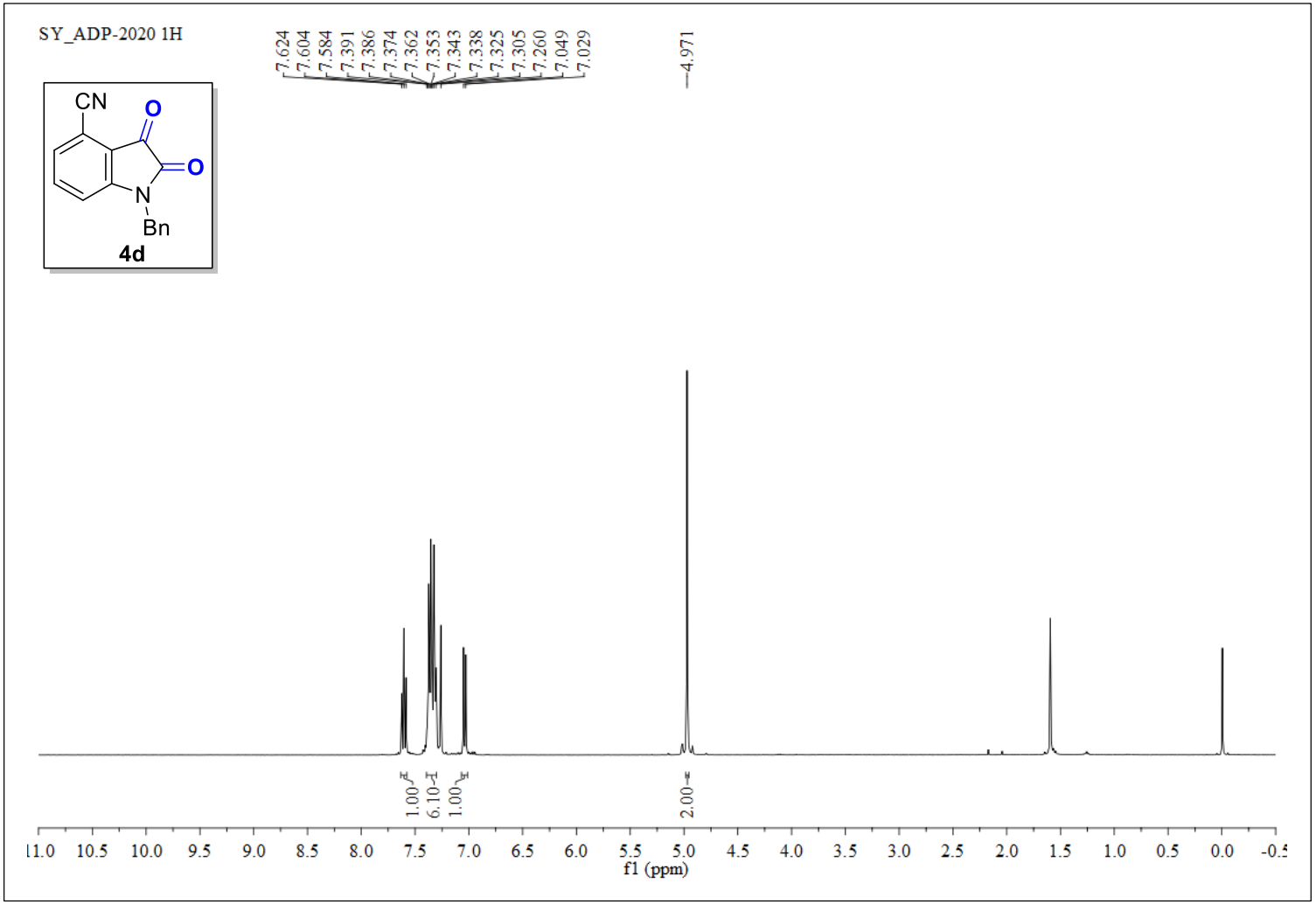

Figure S71. ^{1}H NMR (400 MHz, $CDCl_3$) of **4d**.

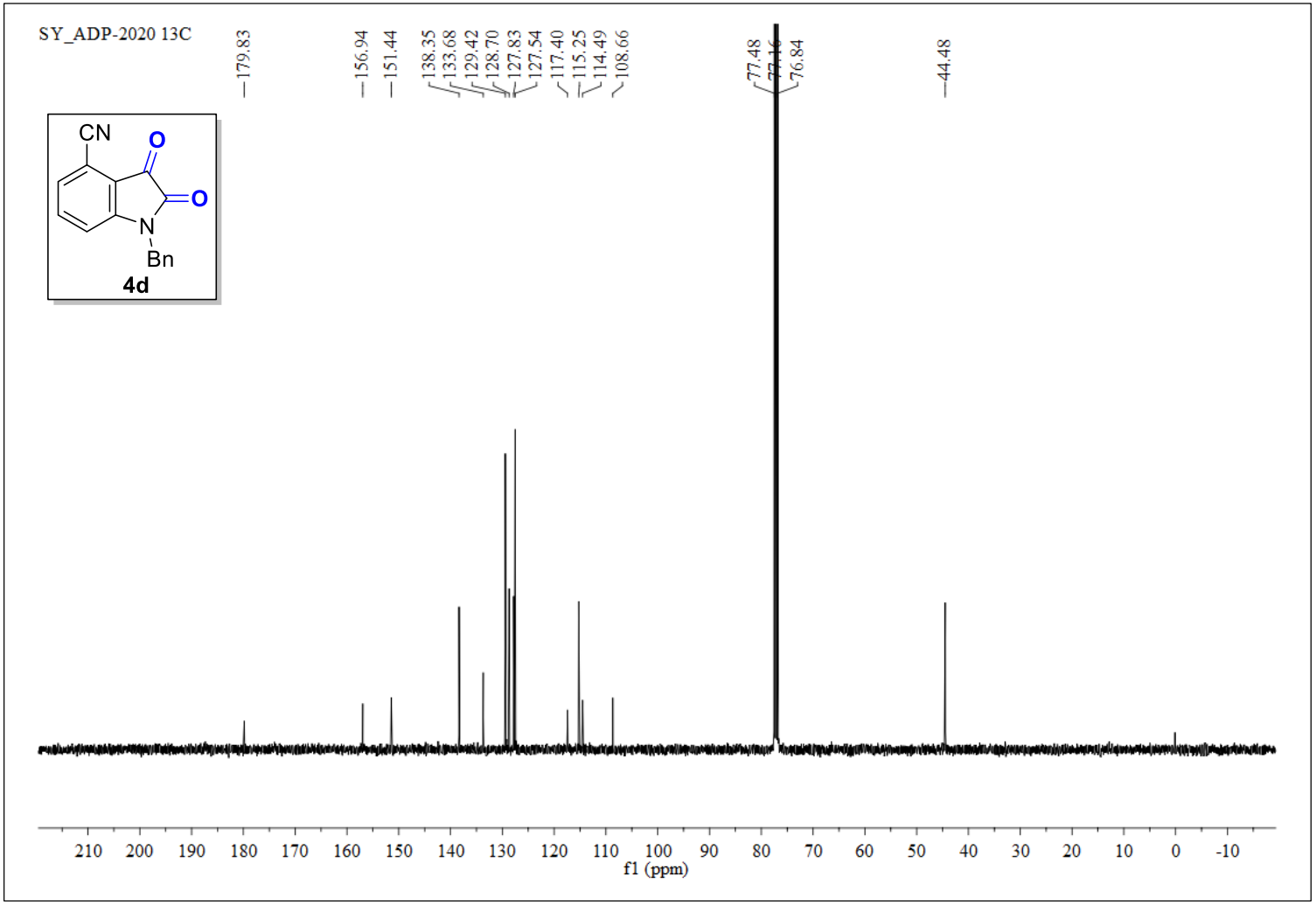

Figure S72. $^{13}C\{^{1}H\}$ NMR (100 MHz, $CDCl_3$) of **4d**.

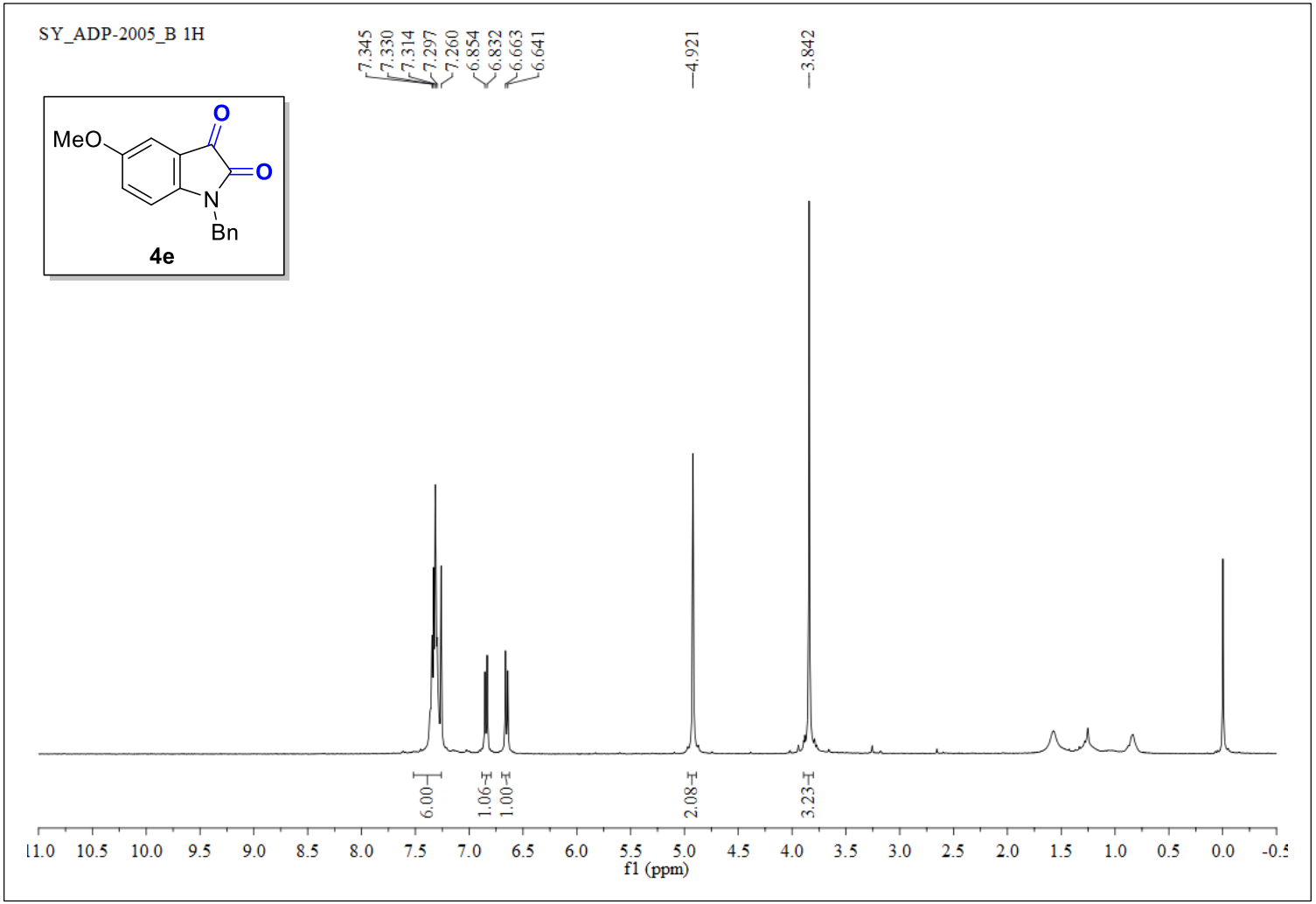

Figure S73. ^{1}H NMR (400 MHz, $CDCl_3$) of **4e**.

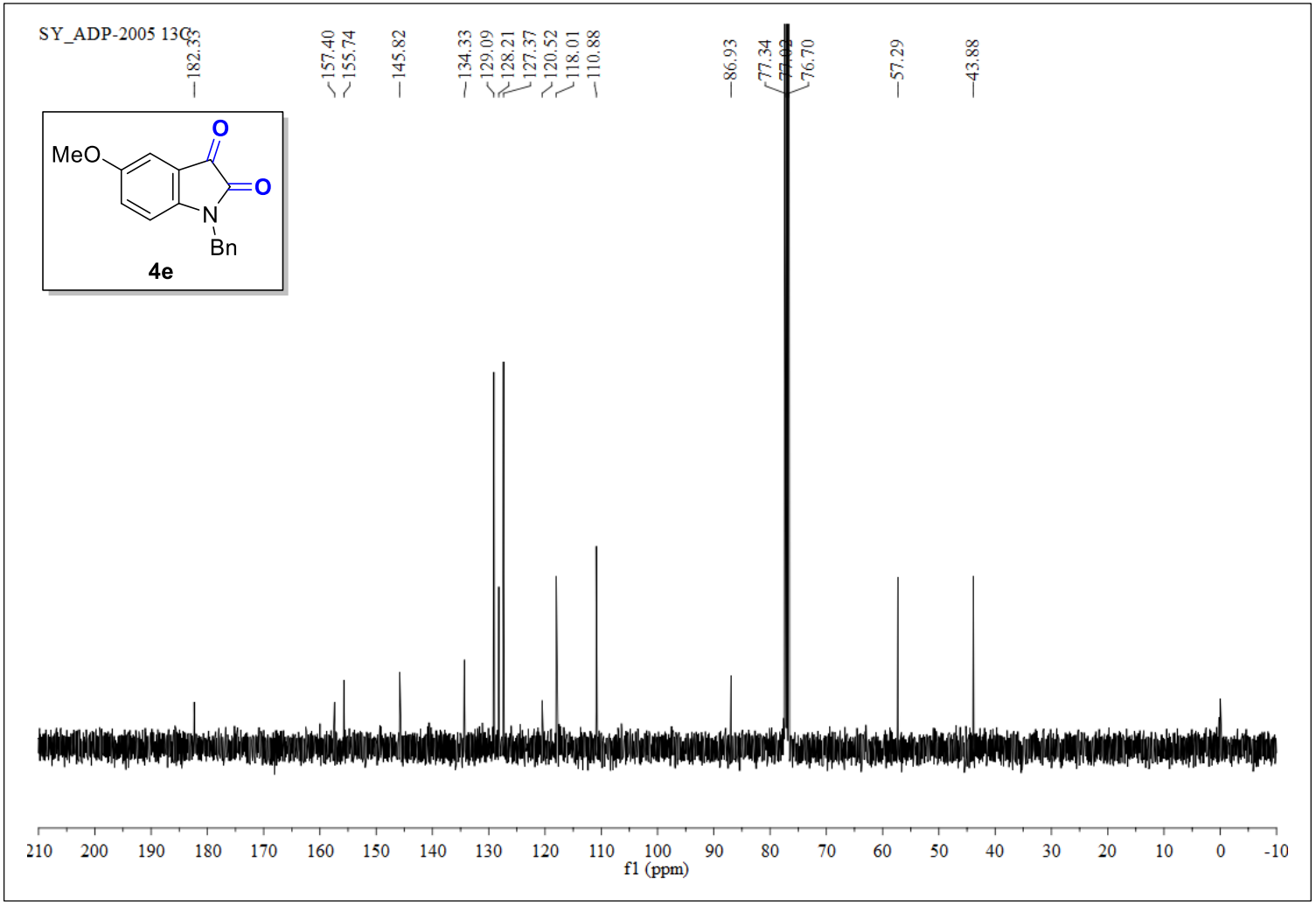

Figure S74. $^{13}C\{^{1}H\}$ NMR (100 MHz, $CDCl_3$) of **4e**.

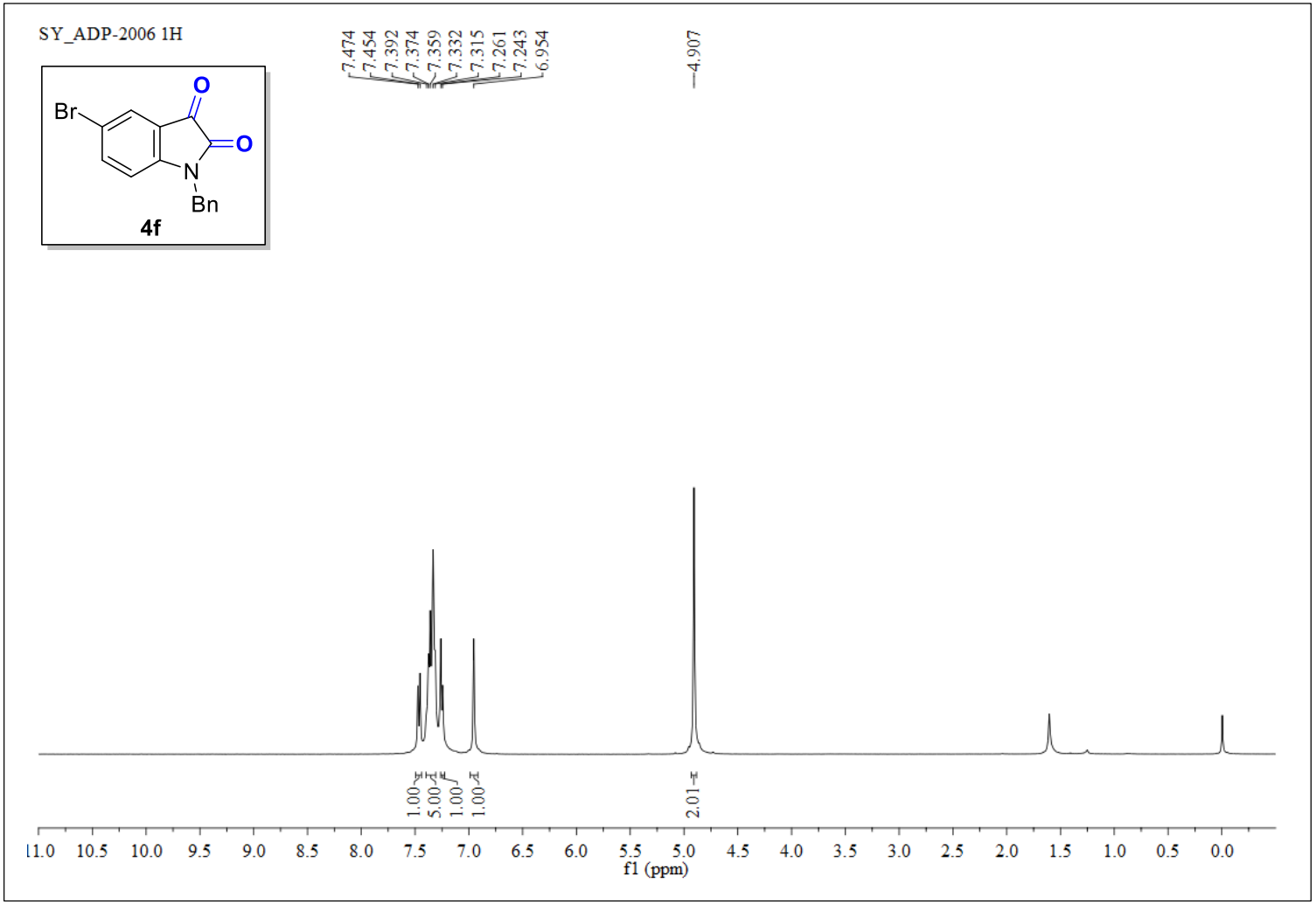

Figure S75. ^{1}H NMR (400 MHz, $CDCl_3$) of **4f**.

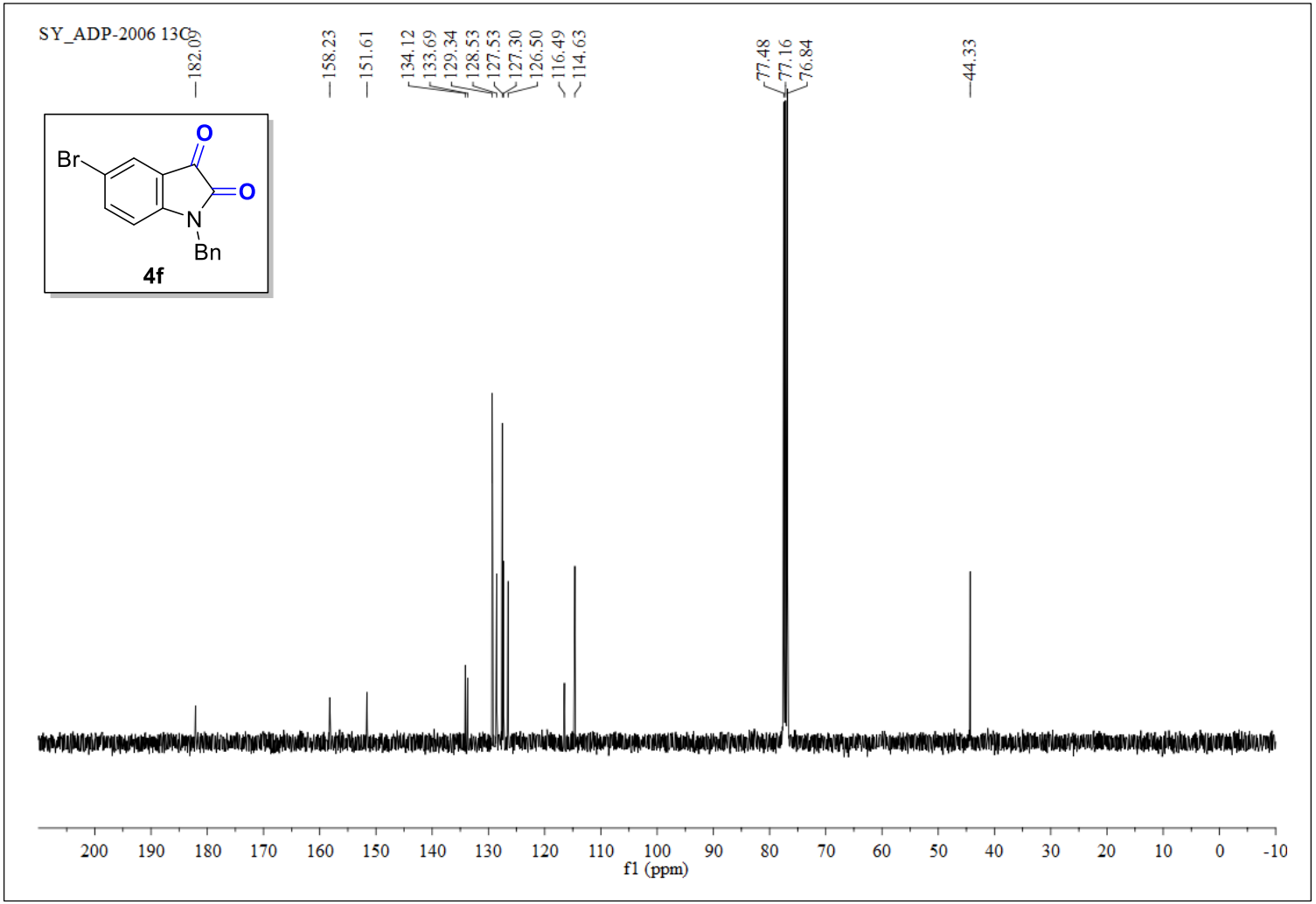

Figure S76. $^{13}C\{^{1}H\}$ NMR (100 MHz, $CDCl_3$) of **4f**.

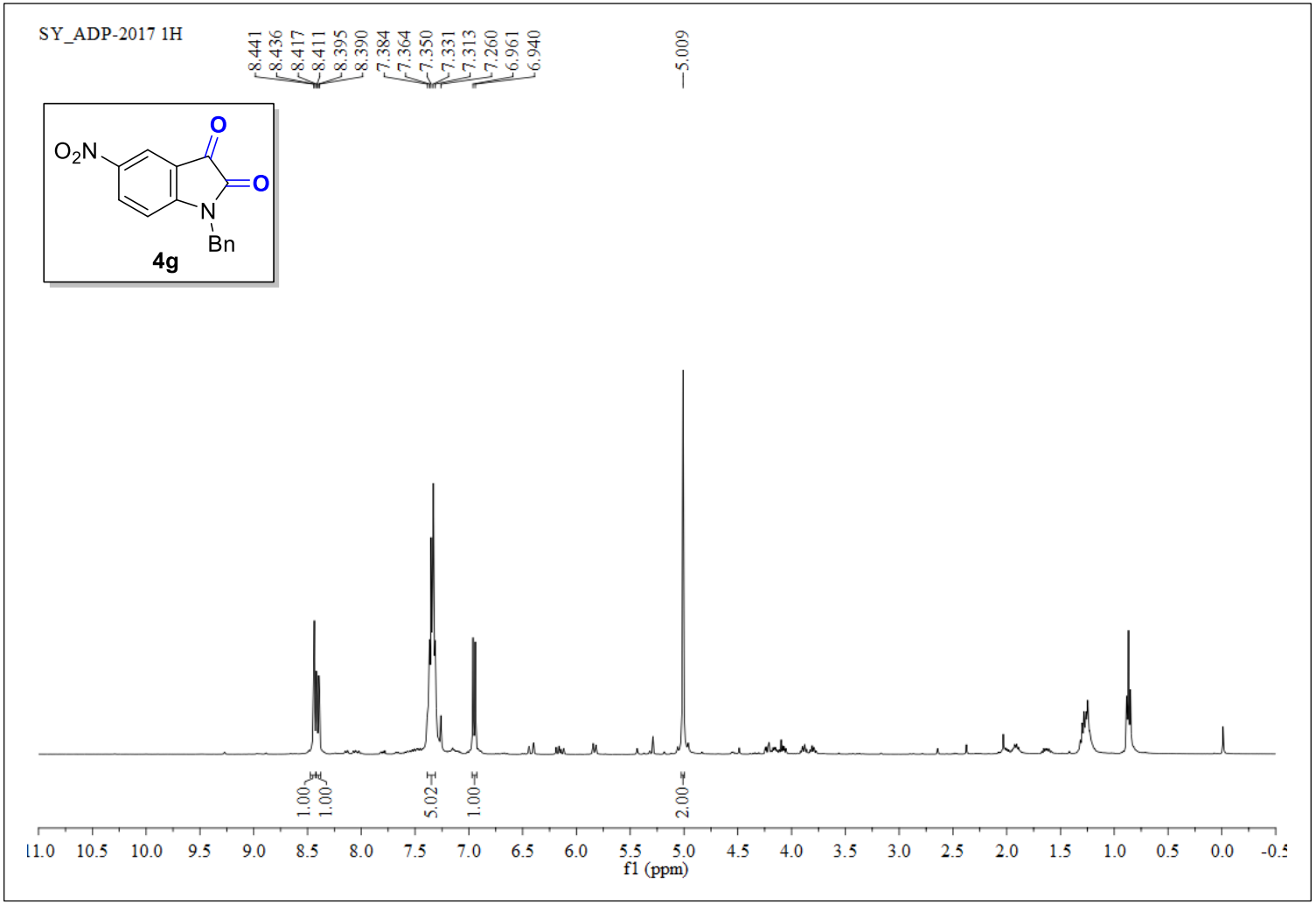

Figure S77. ^{1}H NMR (400 MHz, $CDCl_3$) of **4g**.

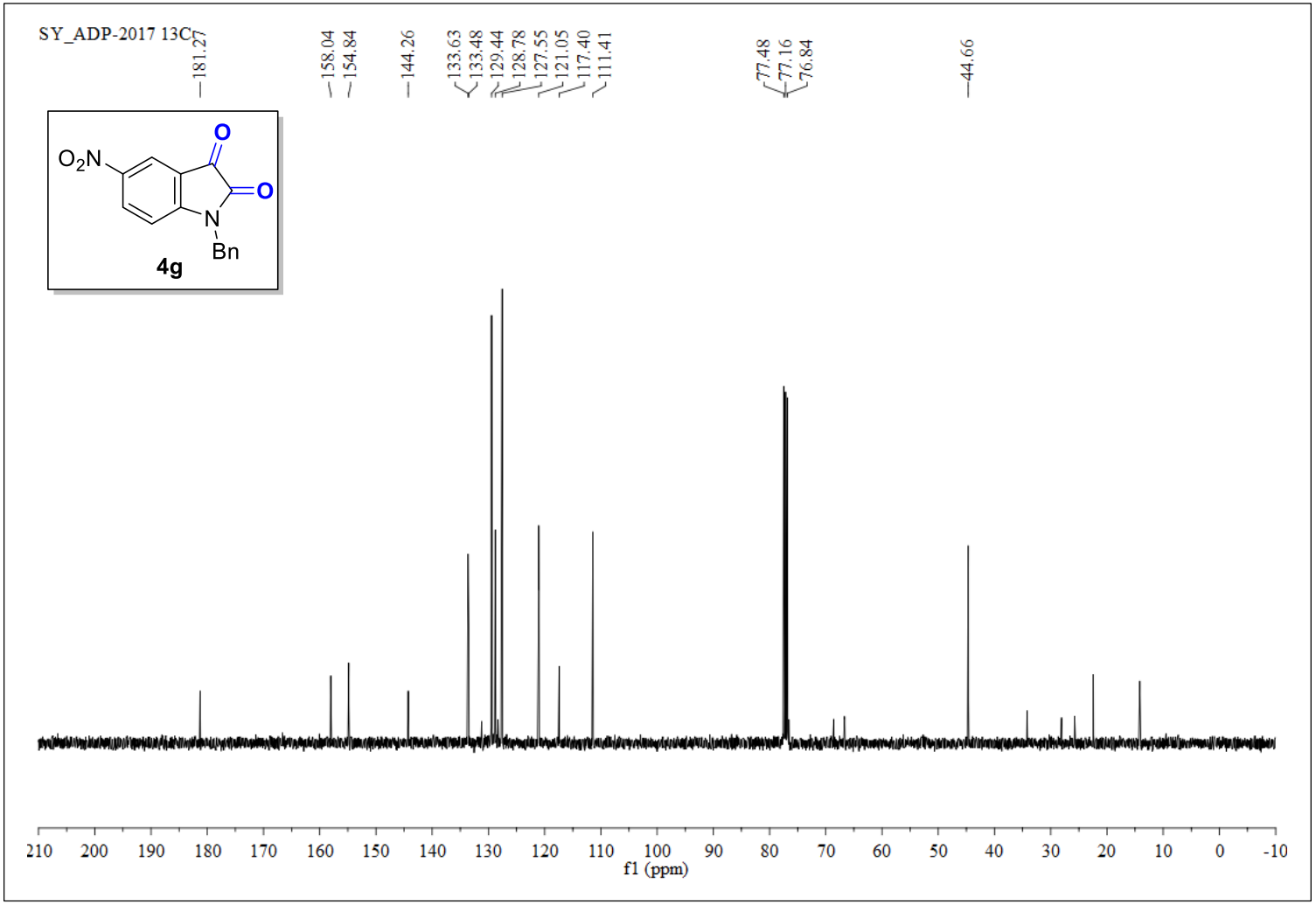

Figure S78. $^{13}C\{^{1}H\}$ NMR (100 MHz, $CDCl_3$) of **4g**.

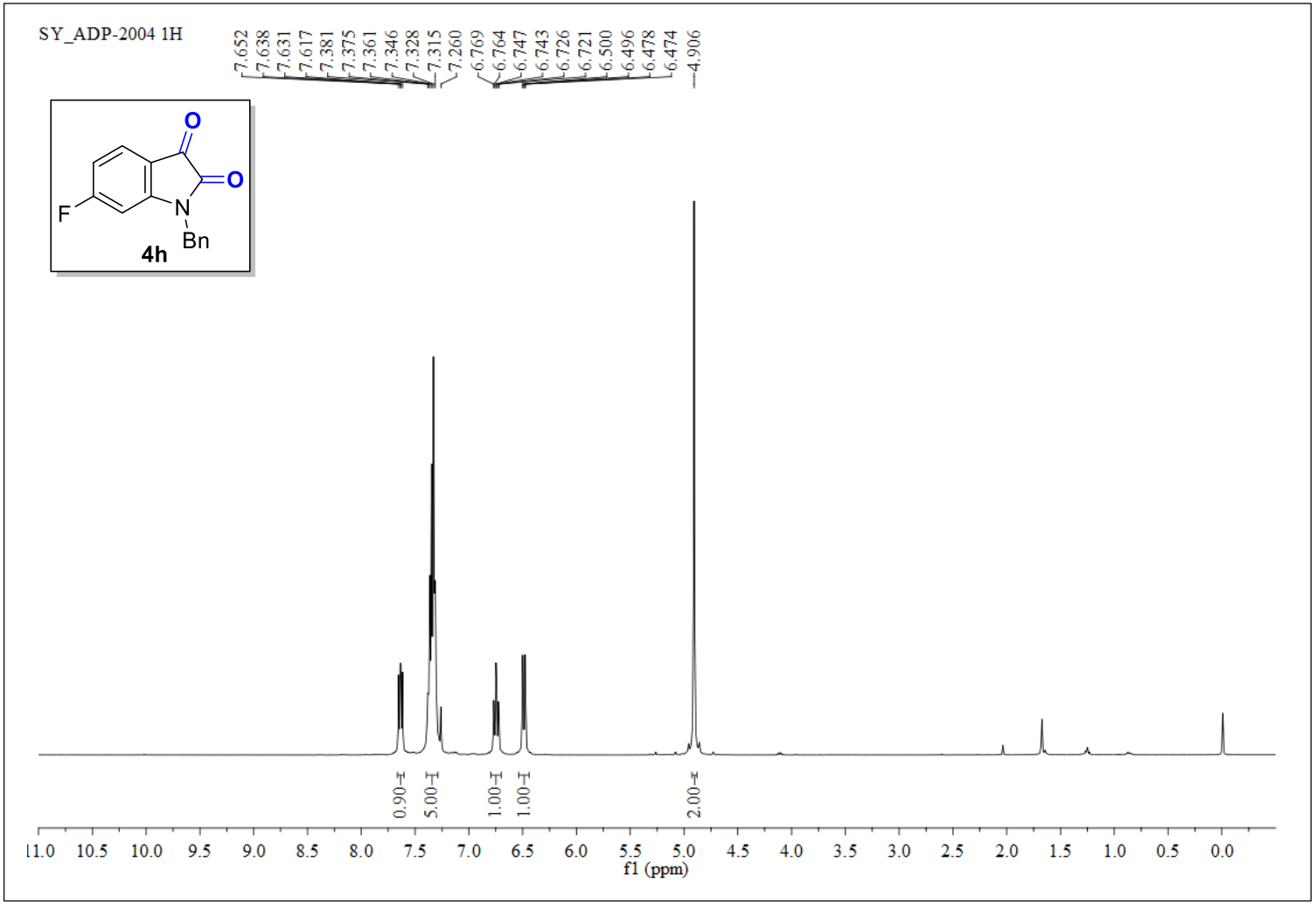

Figure S79. ^{1}H NMR (400 MHz, $CDCl_3$) of **4h**.

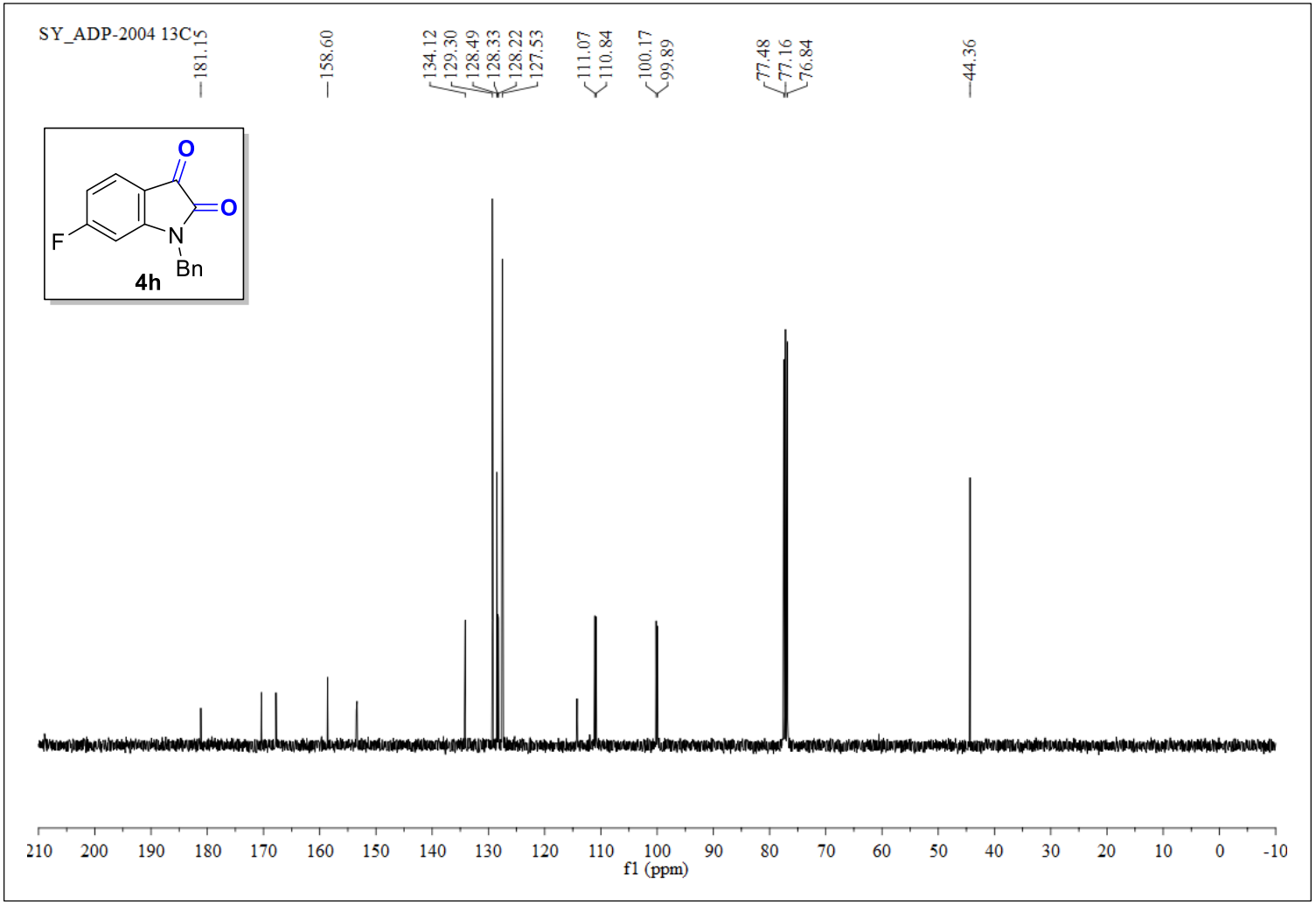

Figure S80. $^{13}C\{^{1}H\}$ NMR (100 MHz, $CDCl_3$) of **4h**.

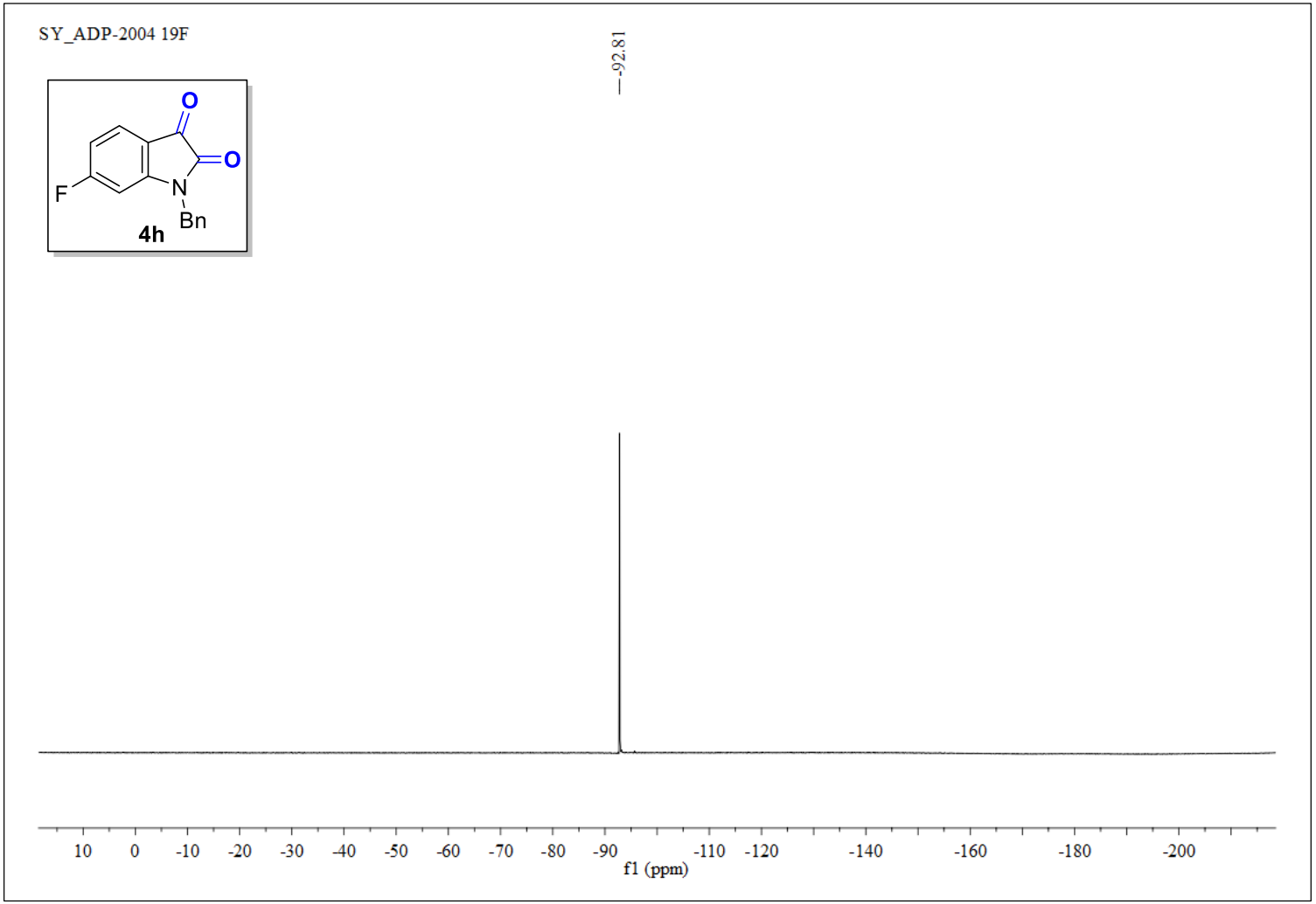

Figure S81. ^{19}F NMR (373 MHz, $CDCl_3$) of **4h**.

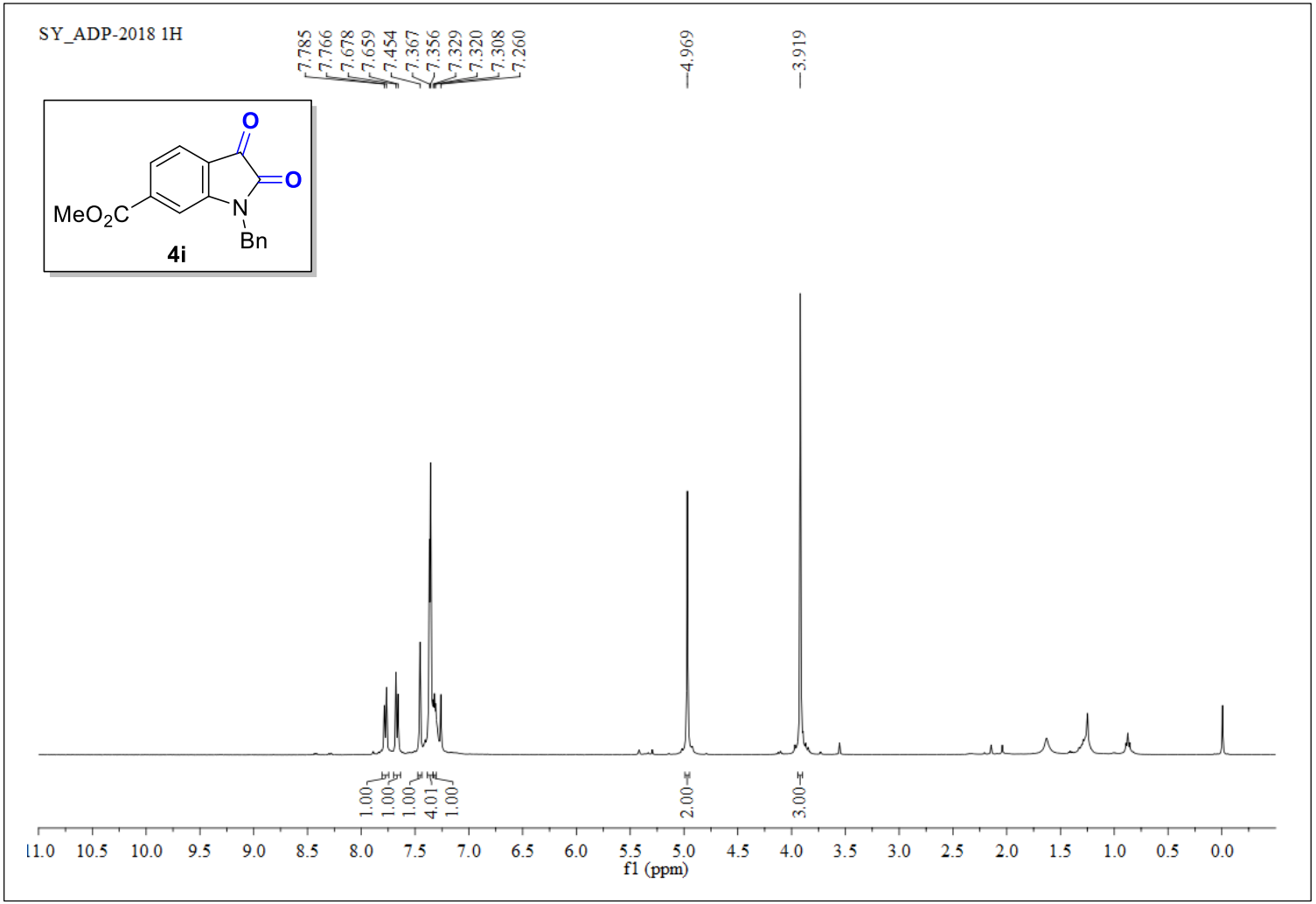

Figure S82. ^{1}H NMR (400 MHz, $CDCl_3$) of **4i**.

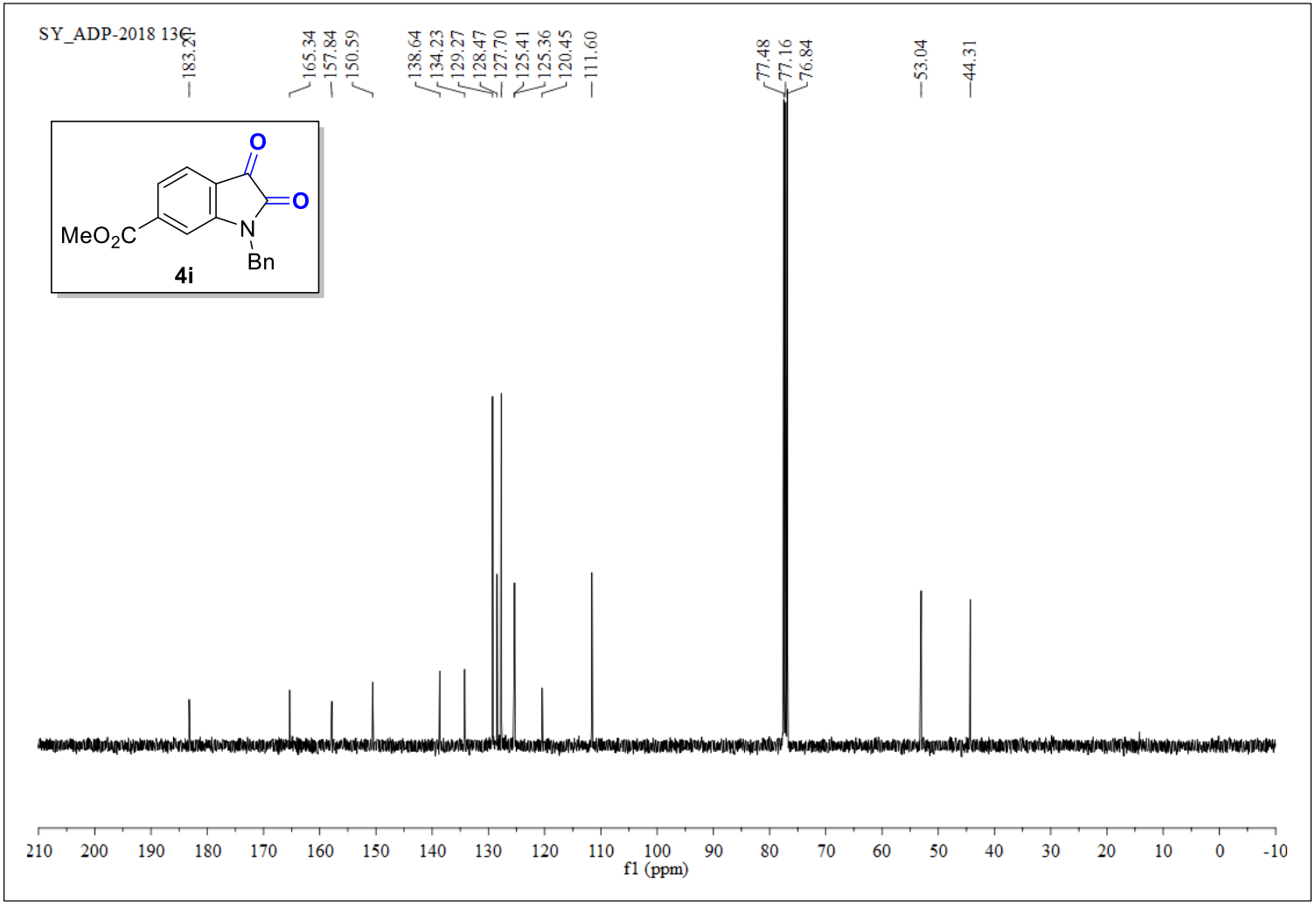

Figure S83. $^{13}C\{^{1}H\}$ NMR (100 MHz, $CDCl_3$) of **4i**.

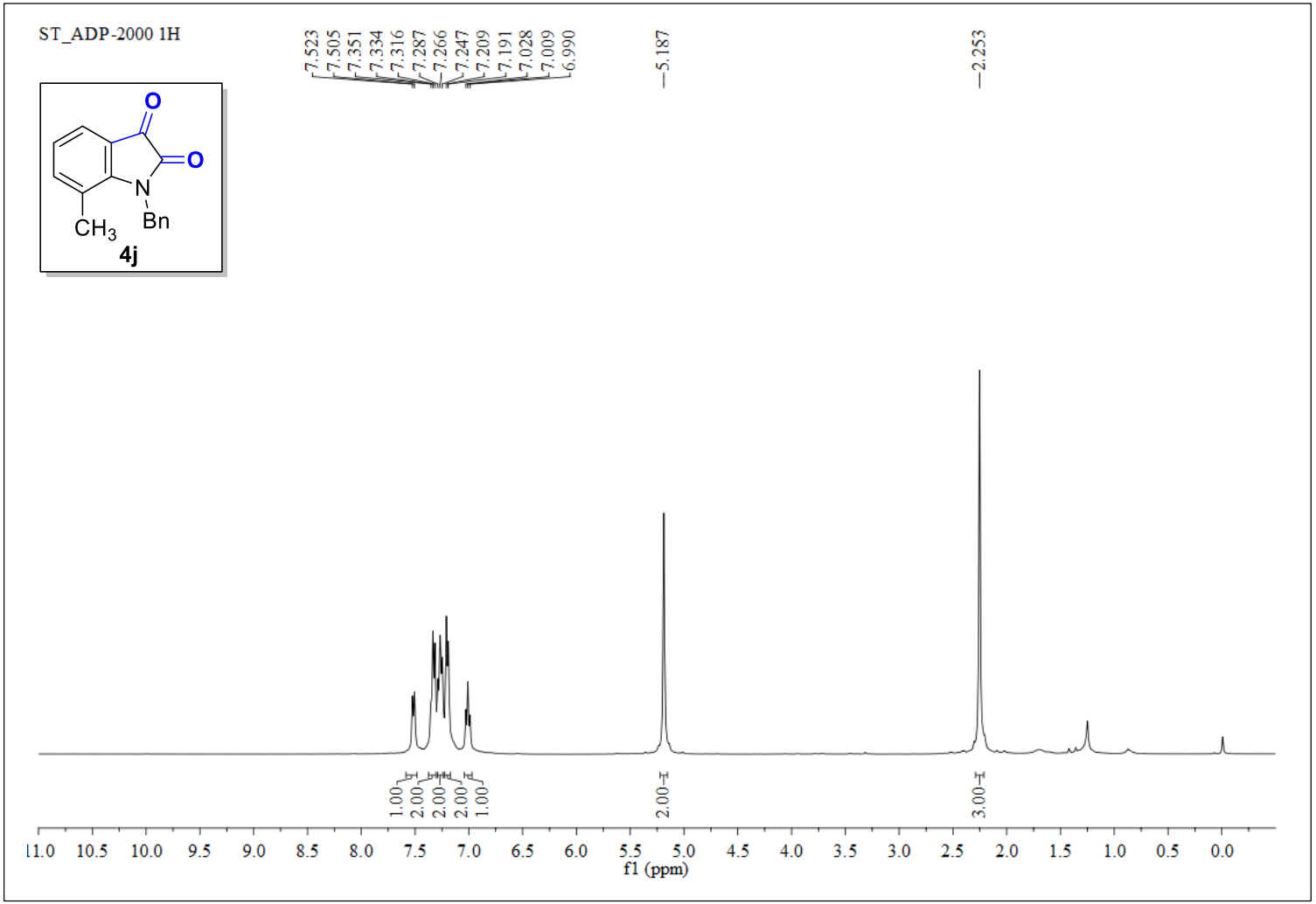

Figure S84. ^{1}H NMR (400 MHz, $CDCl_3$) of **4j**.

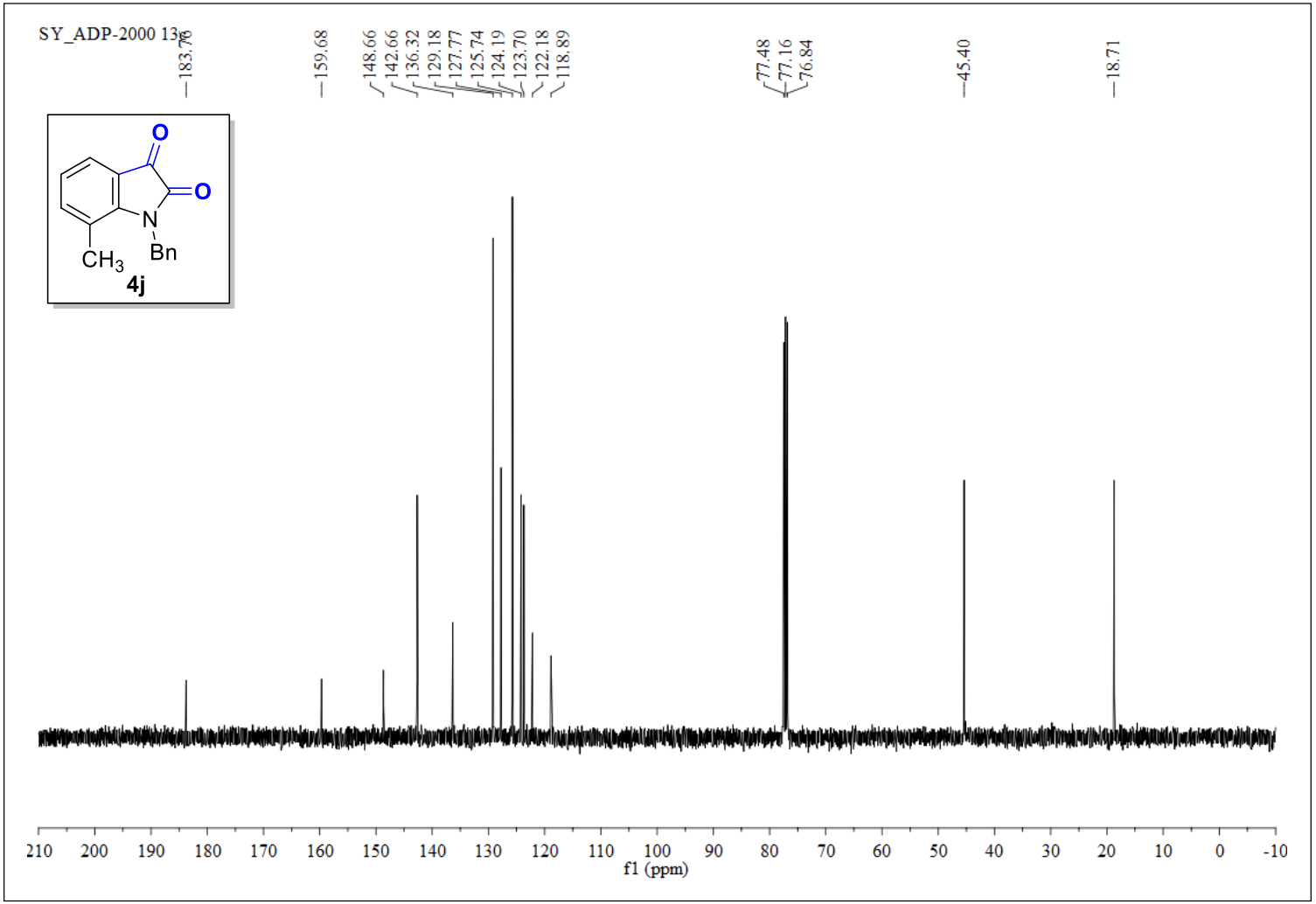

Figure S85. $^{13}C\{^{1}H\}$ NMR (100 MHz, $CDCl_3$) of **4j**.

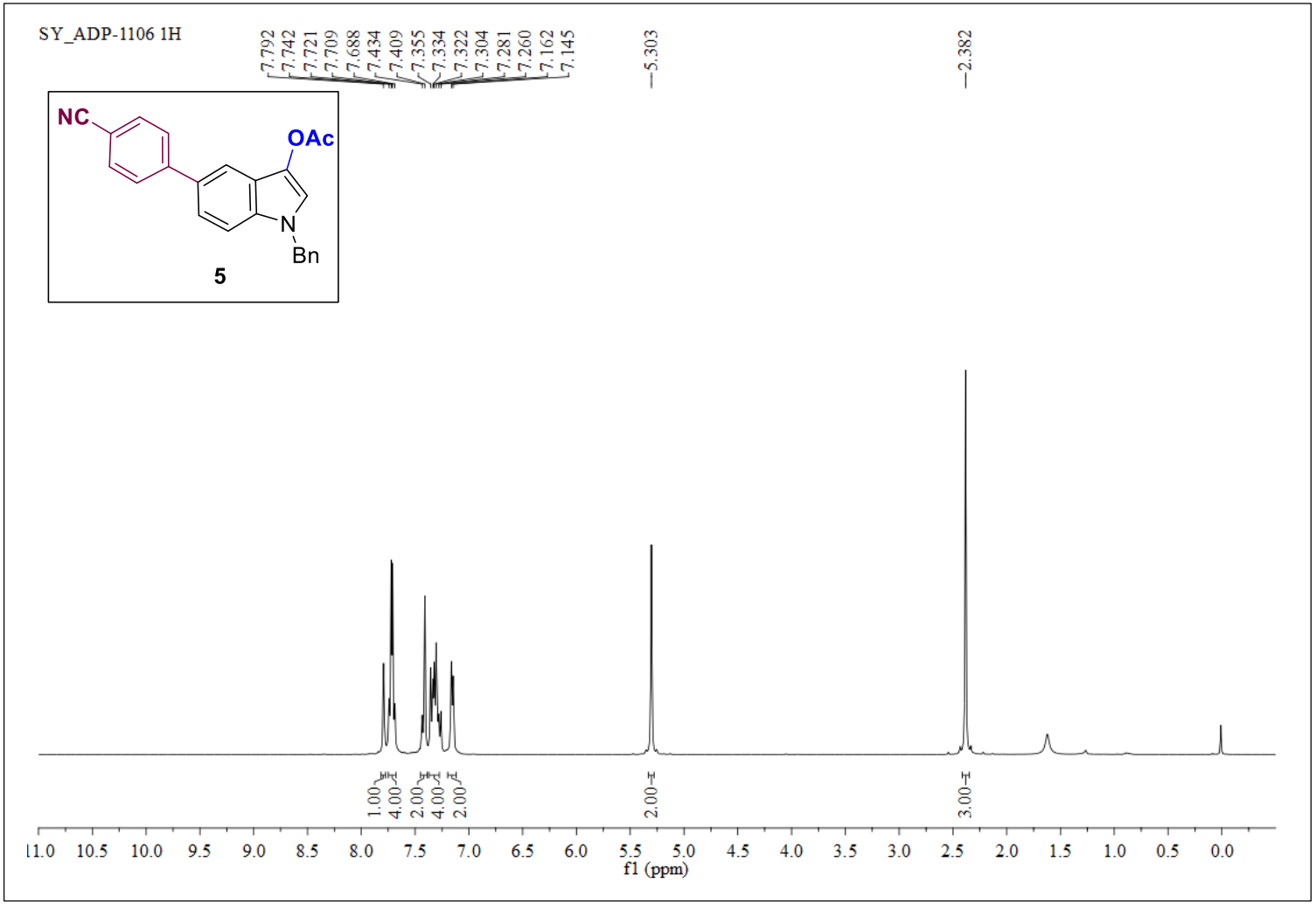

Figure S86. ^{1}H NMR (400 MHz, $CDCl_3$) of **5**.

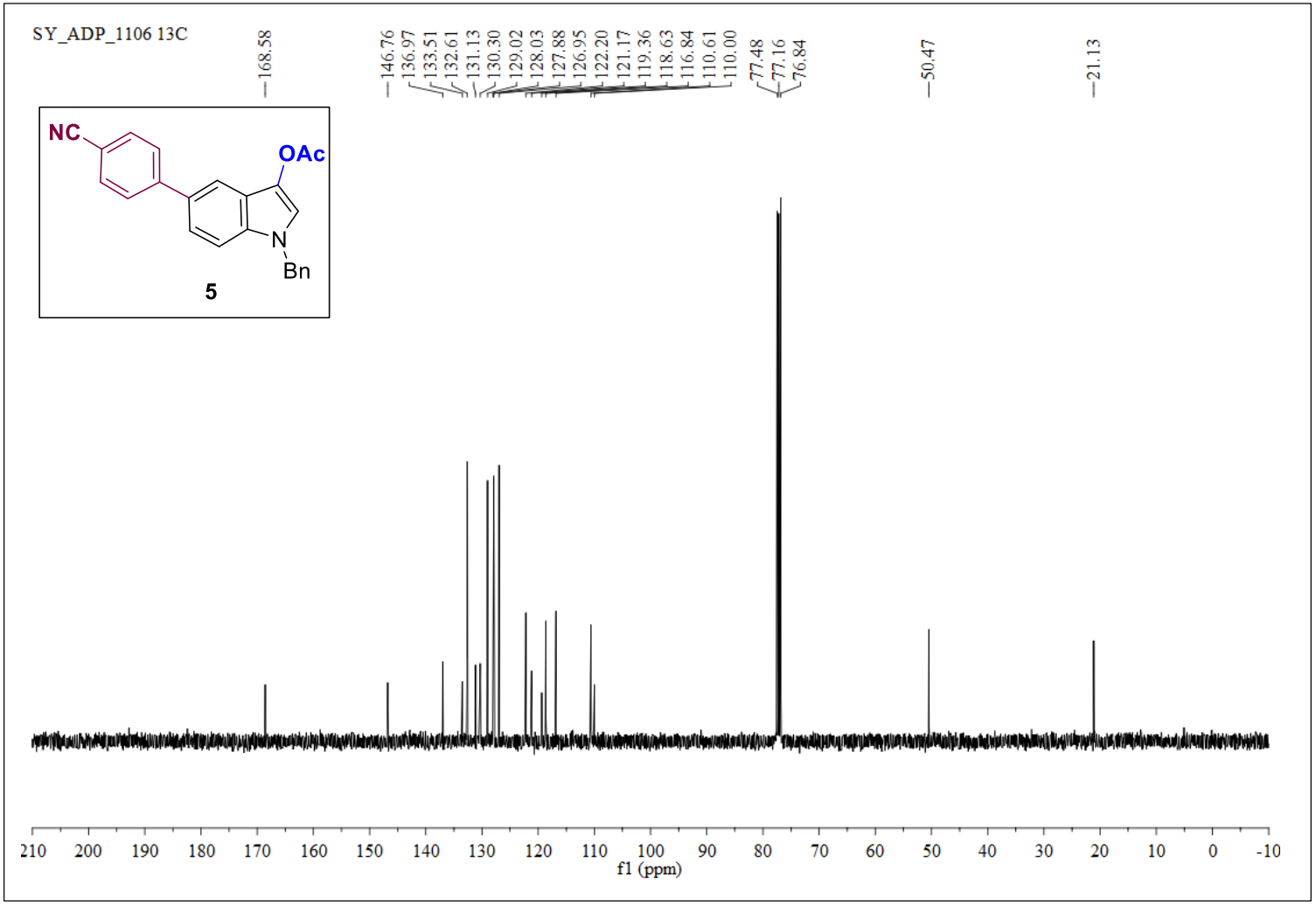

Figure S87. $^{13}C\{^{1}H\}$ NMR (100 MHz, $CDCl_3$) of **5**.

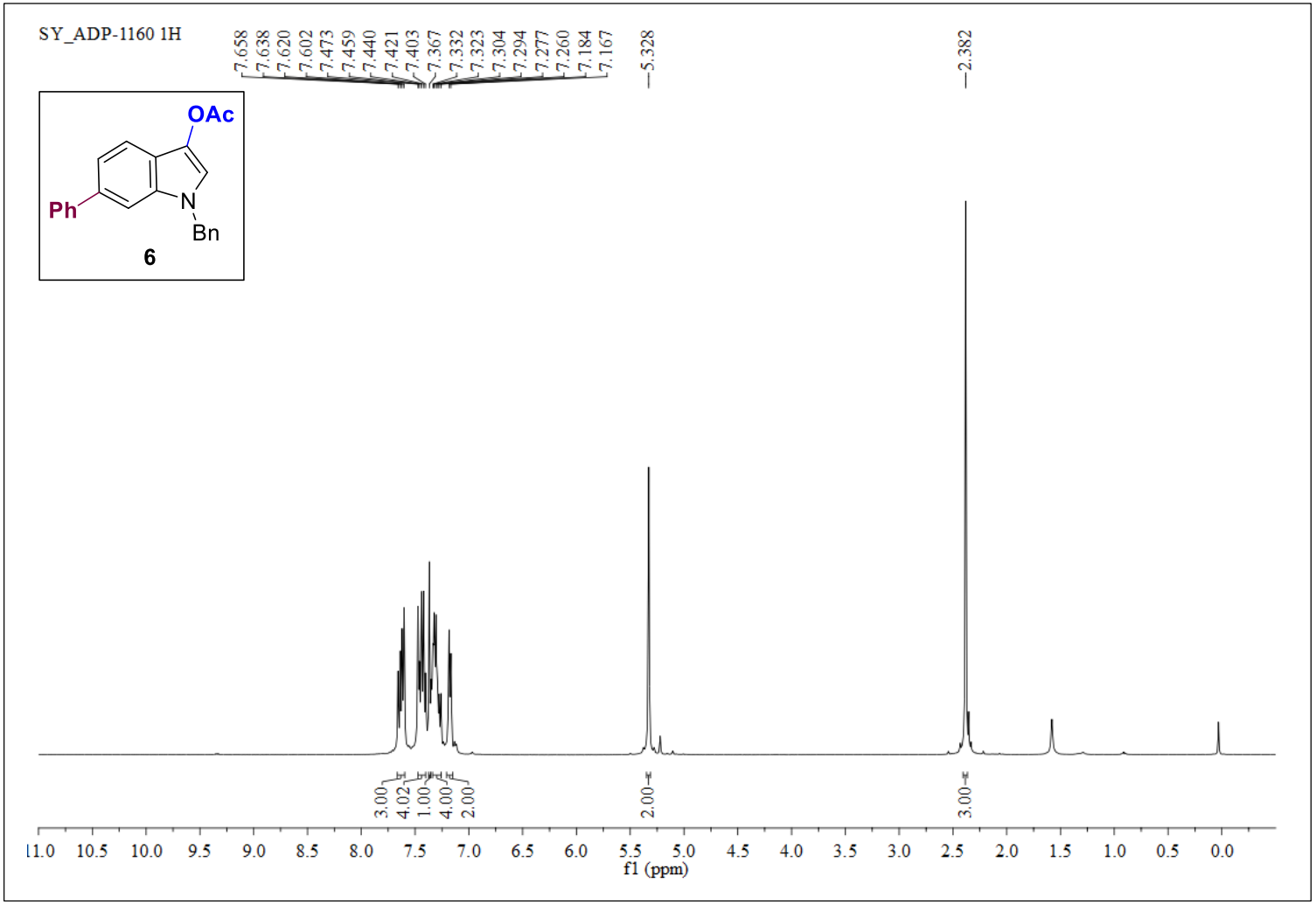

Figure S88. ^{1}H NMR (400 MHz, $CDCl_3$) of **6**.

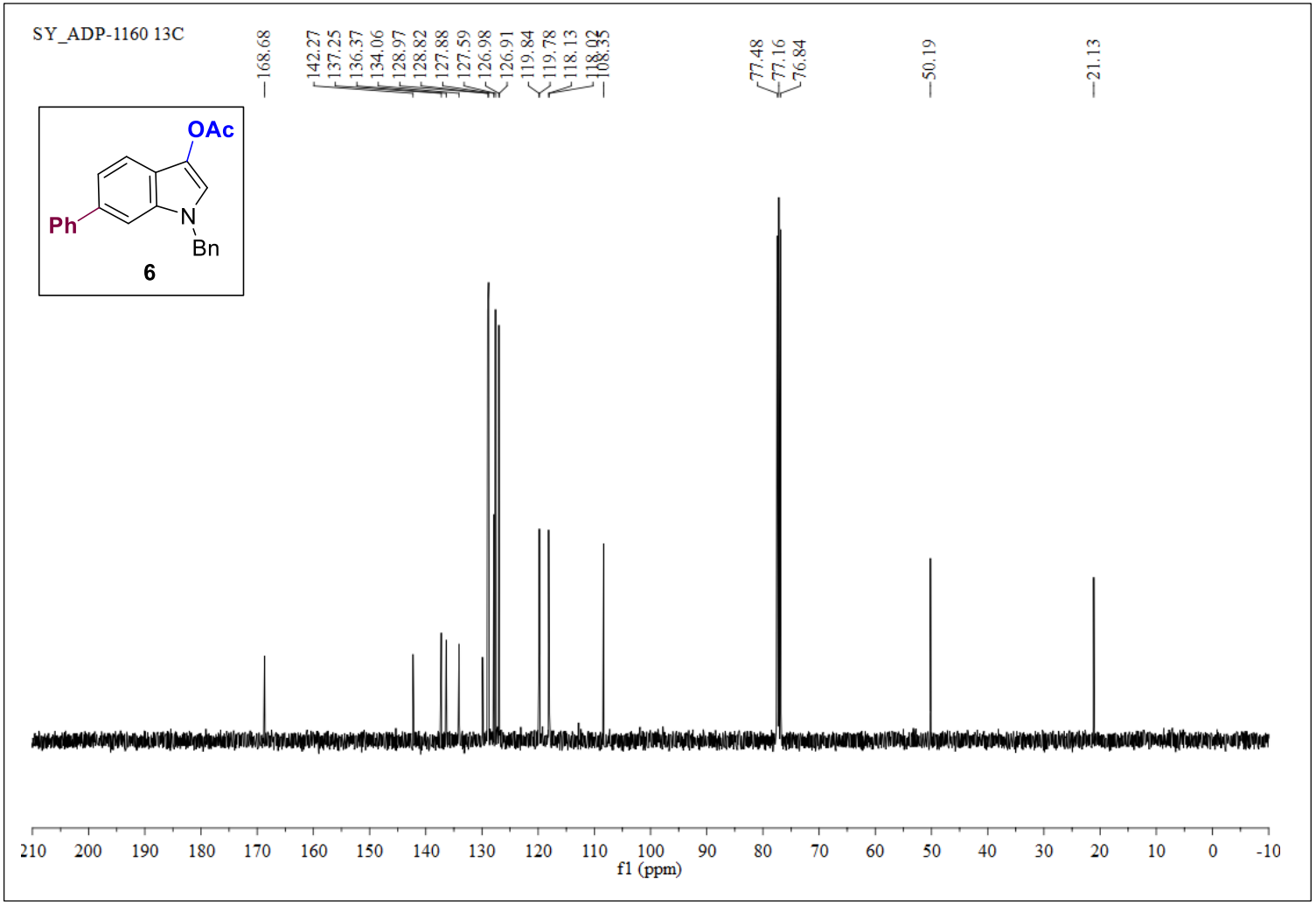

Figure S89. $^{13}C\{^{1}H\}$ NMR (100 MHz, $CDCl_3$) of **6**.

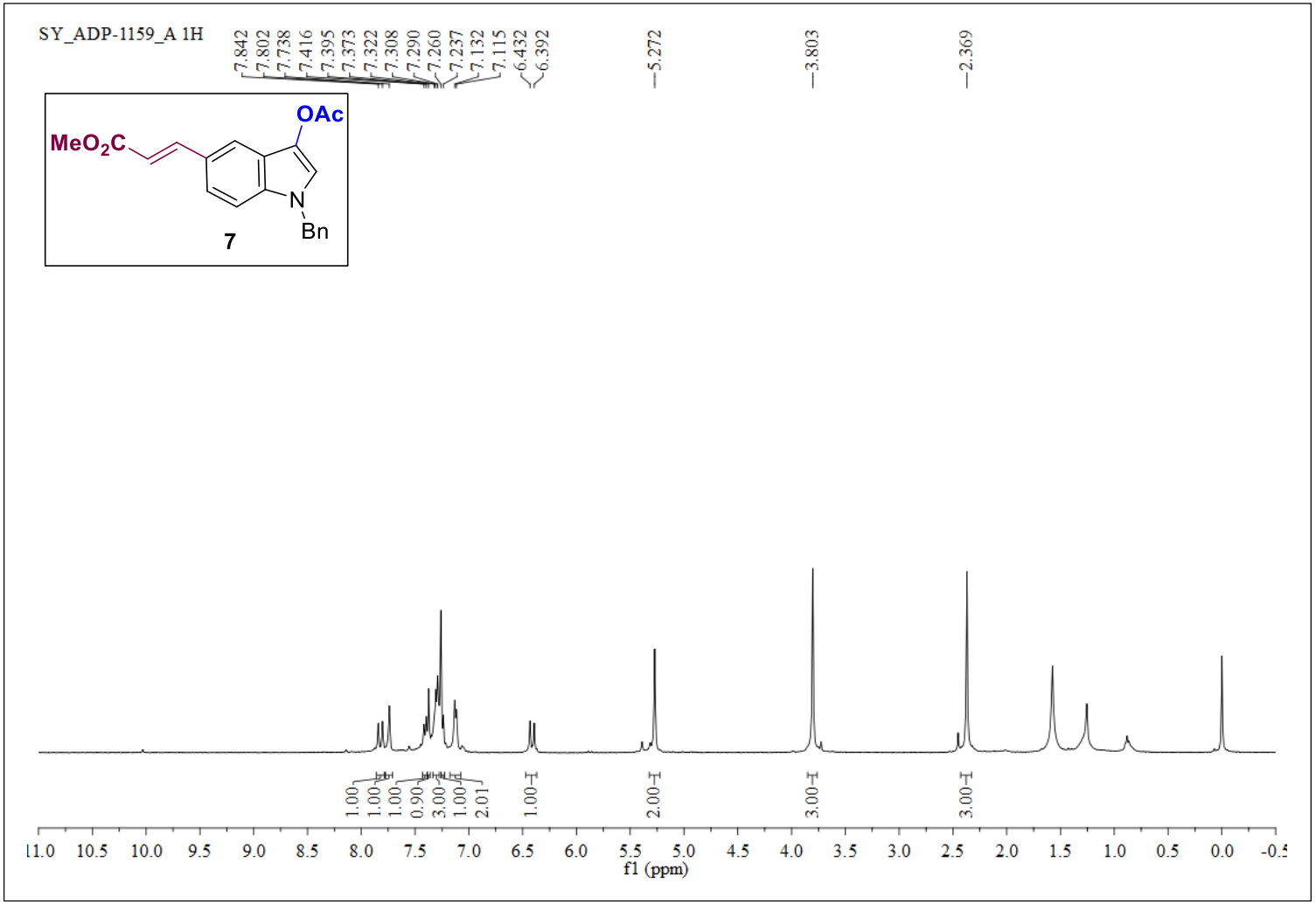

Figure S90. ^{1}H NMR (400 MHz, $CDCl_3$) of **7**.

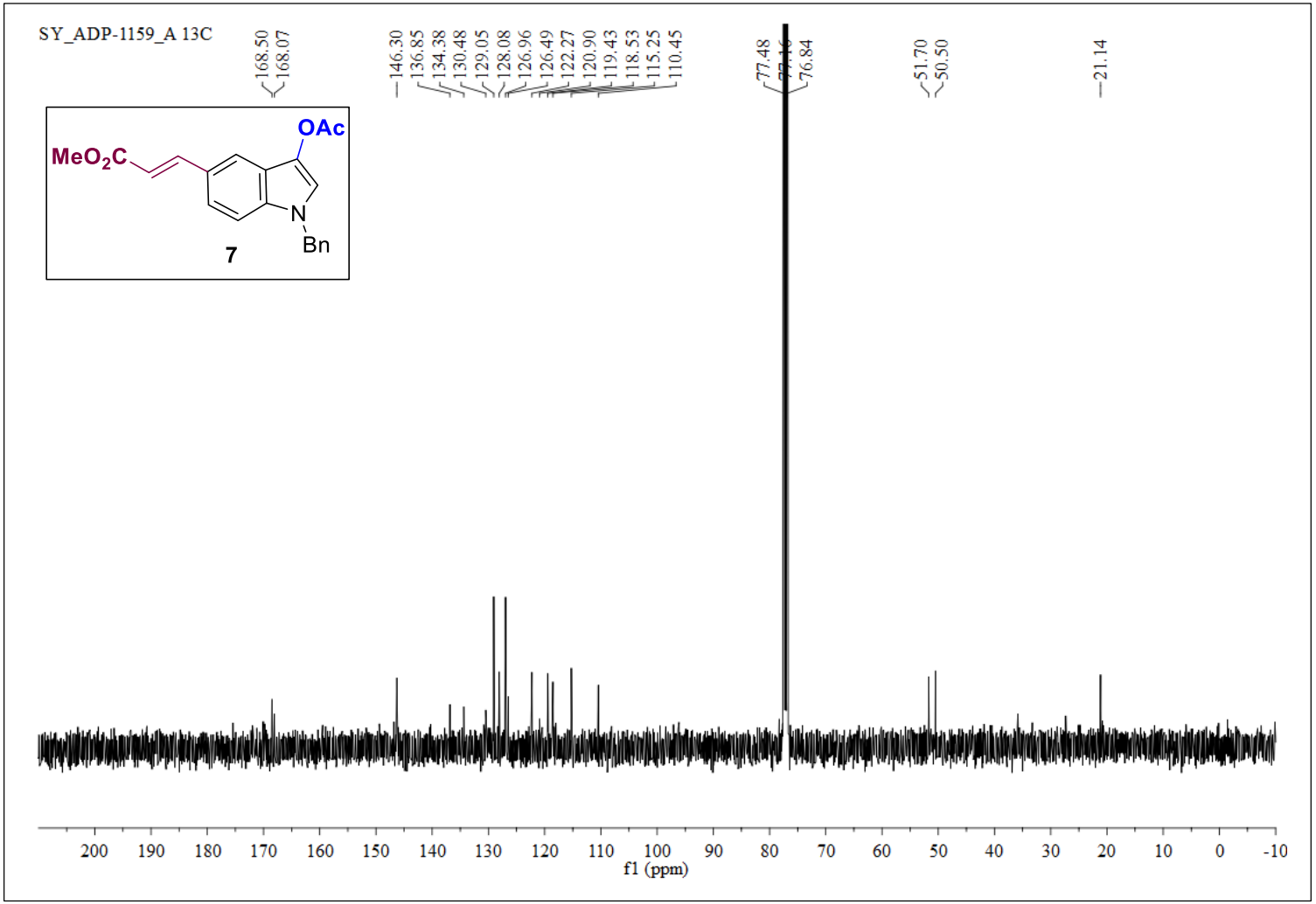

Figure S91. $^{13}C\{^{1}H\}$ NMR (100 MHz, $CDCl_3$) of **7**.

11.3 Refernces

1. P. Y. Choy, C. P. Lau and F. Y. Kwong, *J. Org. Chem.* 2011, **76**, 80–84.
2. Y. Zi, Z.-J. Cai, S.-Y. Wang and S.-J. Ji, *Org. Lett.*, 2014, **16**, 3094−3097.
3. G. Satish, A. Polu, T. Ramar and A. Ilangovan, *J. Org. Chem.*, 2015, **80**, 5167−5175.

12. Crystallographic details

12.1 X-ray Data collection, structure solution and refinement

Single crystals suitable for data collection were obtained by slow evaporation of dichloromethane-pet-ether (1:2 v/v) solution of **2k** and **3j** at 298 K. Diffraction intensities were collected on a single crystal with a SuperNova, Single source at offset/far, EosS2 diffractometer, with mirror-monochromated Mo-*K*α (λ = 0.71073 Å) radiation at 293(2) K. The 'CrysAlisPro 1.171.40.69a' program was used for data reduction. Data were corrected for Lorentz and polarization effects; empirical absorption correction using spherical harmonics and frame scaling, implemented in SCALE3 ABSPACK scaling algorithm. The structures were solved with SHELXT and refined with the SHELXL–2018/3 package[1-2], incorporated into the Olex2 1.5–alpha crystallographic collective package[3]. The position of the hydrogen atoms was calculated by assuming ideal geometries and included in the last cycle of the refinement. All non–hydrogen atoms were refined with anisotropic thermal parameters by full-matrix least-squares minimization procedures on F^2.

The Perspective view of **2k**, **3j** and their data collection and structure refinement details are in Figs. S92-S93 and Table S11 respectively.

CCDC-numbers 2253525 (**2k**) and 2253523 (**3j**) contain supplementary crystallographic data for this paper. These data can be obtained free of charge from The Cambridge Crystallographic Data Centre via www.ccdc.cam.ac.uk/data_request/cif, or by emailing data_request@ccdc.cam.ac.uk, or by contacting The Cambridge Crystallographic Data Centre, 12 Union Road, Cambridge CB2 1EZ, UK; fax: +44 1223 336033.

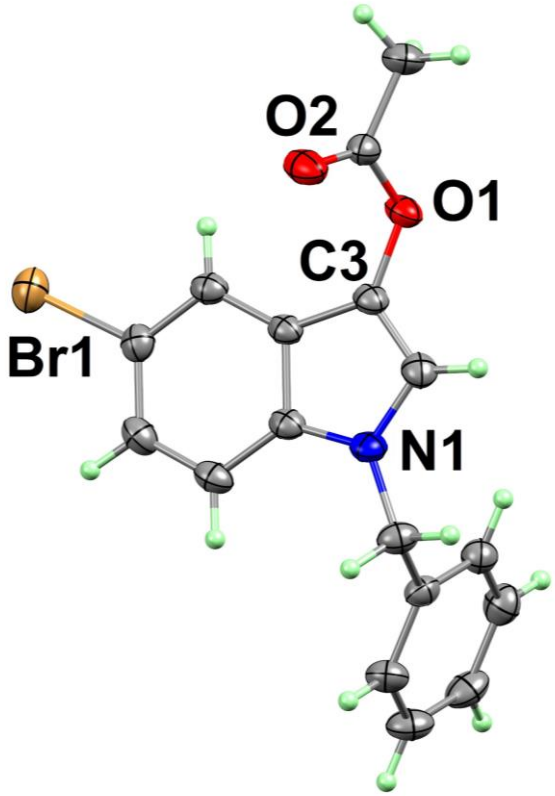

Figure S92. Perspective view (contour probability of 20%) of **2k**. Only, N1, C3, O1, O2 and Br1 atoms are labelled.

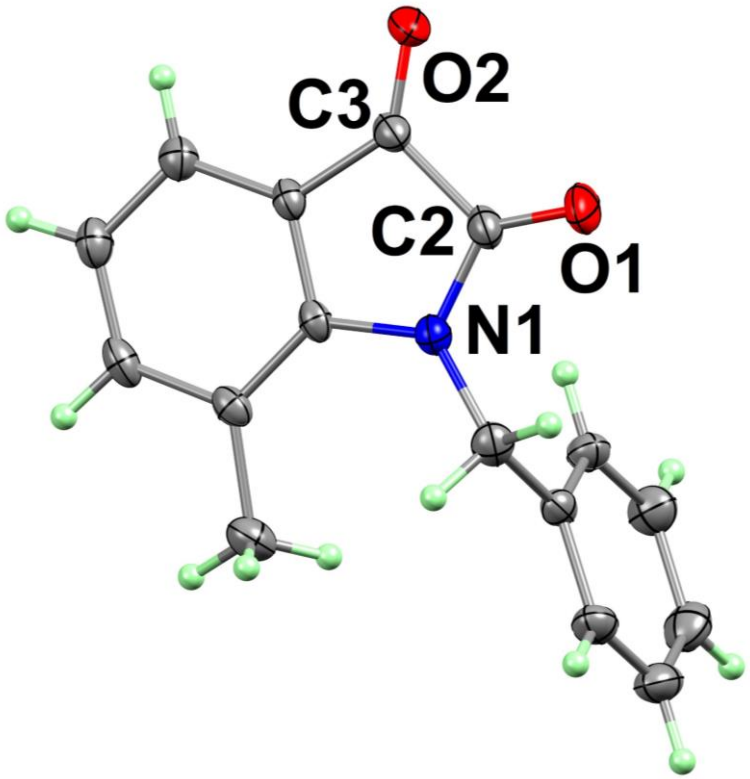

Figure S93. Perspective view (contour probability of 20%) of **3j**. Only, N1, C3, O1 and O2 atoms are labelled.

Table S11. Data collection and structure refinement parameters for **2k** and **3j.**

	2k	**3j**
Empirical formula	$C_{17}H_{14}BrNO_2$	$C_{16}H_{13}NO_2$
Formula weight	344.20	251.27
Crystal color, habit	White, block	Red, needle
Temperature (K)	293(2)	293(2)
Wavelength (Å)	0.71073	0.71073
Crystal system	Monoclinic	Orthorhombic
Space group	$P2_1/c$	$Pna2_1$
Crystal size (mm^3)	0.20 x 0.15 x 0.14	0.30 x 0.20 x 0.10
a (Å)	9.6226(8)	7.5072(8)
b (Å)	17.3895(10)	23.008(3)
c (Å)	9.3029(7)	7.4733(6)
α (^{o})	90.0	90.0
β (^{o})	106.767(9)	90.0
γ (^{o})	90.0	90.0
V ($Å^3$)	1490.5(2)	1290.8(2)
Z	4	4
D_{calc} ($g\ cm^{-3}$)	1.534	1.293
μ (mm^{-1})	2.761	0.086
no. reflections collected	7390	3374

no. unique reflection	3479 (R_{int} = 0.0229)	1746 (R_{int} = 0.0214)
no. reflections used [$I > 2\sigma(I)$]	2543	1259
R_1^a, wR_2^b	R_1 = 0.0382[a]	R_1 = 0.0359[a]
[$I > 2\sigma(I)$]	wR_2= 0.0976[b]	wR_2= 0.0657[b]
R_1^a, wR_2^b	R_1 = 0.0600[a]	R_1 = 0.0592[a]
(All data)	wR_2= 0.1086[b]	wR_2= 0.0731[b]
Goodness-of-fit on F^2	1.117	0.975

($^a R_1 = \Sigma||F_o| - |F_c||/\Sigma|F_o|$. $^b wR_2 = \{\Sigma[w\,(|F_o|^2 - |F_c|^2)^2]/\Sigma[w(|F_o|^2)^2]\}^{1/2}$)

12.2 References

1. G.M. Sheldrick, SHELXL–2016, Program for Crystal Structure Refinement University of Göttingen, Göttingen, Germany, 2014.
2. G.M. Sheldrick, Acta Crystallogr. Sect. C: Cryst. Struct. Commun. C71 (2015) 3–8.
3. O.V. Dolomanov, L.J. Bourhis, R.J. Gildea, J.A.K. Howard and H. Puschmann, *J. Appl. Cryst.*, 2009, **42**, 339–341.